11:11:40 OCA PAD INITIATION - PROJECT HEADER INFORMATION 05/11/89

Active

Project #: E-21-T21 Cost share #: E-21-329 Rev #: 0
Center # : R6583-T21 Center shr #: F6583-T21 OCA file #: 128
Work type : RES
Contract#: F30602-88-D-0025-0021 Mod #: Document : DO
Prime #: Contract entity: GTRC

Subprojects ? : N
Main project #:

Project unit: EE Unit code: 02.010.118
Project director(s):
PARIS D T EE (404)894-2902

Sponsor/division names: AIR FORCE / GRIFFISS AFB, NY
Sponsor/division codes: 104 / 023

Award period: 890417 to 890716 (performance) 890816 (reports)

Sponsor amount	New this change	Total to date
Contract value	25,000.00	25,000.00
Funded	25,000.00	25,000.00
Cost sharing amount		2,778.00

Does subcontracting plan apply ?: Y

Title: MICROWAVE MODULE HOUSING INTERNAL ELECTRICAL EFFECTS

PROJECT ADMINISTRATION DATA

OCA contact: Brian J. Lindberg 894-4820

Sponsor technical contact

WALTER A. KOZIARZ

DEPARTMENT OF THE AIR FORCE
ROME AIR DEVELOPMENT CENTER/RBRE
GRIFFISS AFB, NY 13441-5700

Sponsor issuing office

GERARD J. BROWN/PKRM
(315)330-2308
ROME AIR DEVELOPMENT CENTER
DIRECTORATE OF CONTRACTING (PKRM)
GRIFFISS AFB, NY 13441-5700

Security class (U,C,S,TS) : U
Defense priority rating : DO-A7
Equipment title vests with: Sponsor
NONE PROPOSED OR ANTICIPATED.

CNR resident rep. is ACO (Y/N): Y
GOV'T supplemental sheet
GIT

Administrative comments -
DELIVERY ORDER FULLY FUNDS TASK N-9-5732 (DR. DONALD W. GRIFFIN, A VISITING PROFESSOR AT GEORGIA TECH).

GEORGIA INSTITUTE OF TECHNOLOGY
OFFICE OF CONTRACT ADMINISTRATION

NOTICE OF PROJECT CLOSEOUT

Closeout Notice Date 01/22/90
Original Closeout Started *********

Project No. E-21-T21_____ Center No. R6583-T21_____

Project Director JOY E B_____ School/Lab EE_____

Sponsor AIR FORCE/GRIFFISS AFB, NY_____

Contract/Grant No. F30602-88-D-0025-0021_____ Contract Entity GTRC

Prime Contract No. _____

Title MICROWAVE MODULE HOUSING INTERNAL ELECTRICAL EFFECTS_____

Effective Completion Date 890930 (Performance) 891030 (Reports)

Closeout Actions Required:	Y/N	Date Submitted
Final Invoice or Copy of Final Invoice	Y	_____
Final Report of Inventions and/or Subcontracts	Y	_____
Government Property Inventory & Related Certificate	Y	_____
Classified Material Certificate	Y	_____
Release and Assignment	Y	_____
Other _____	N	_____

Subproject Under Main Project No. _____

Continues Project No. _____

Distribution Required:

Project Director	Y
Administrative Network Representative	Y
GTRI Accounting/Grants and Contracts	Y
Procurement/Supply Services	Y
Research Property Managment	Y
Research Security Services	Y
Reports Coordinator (OCA)	Y
GTRC	Y
Project File	Y
OCA/CSD	N
Other _____	N
_____	N

NOTE: Final Questionnaire sent to PDPI.

ROME AIR DEVELOPMENT CENTER
EXPERT SCIENCE AND ENGINEERING PROGRAM
CONTRACT NO. F30602-88-D-0025

R & D STATUS REPORT

PERIOD COVERED: April 17, 1989 to May 19, 1989

TASK NUMBER: N-9-5732

TITLE: Microwave module housing internal electrical effects

PRINCIPAL INVESTIGATOR: Dr. Donald W. Griffin

INSTITUTION: Georgie Institute of Technology

OTHER PARTICIPANTS AND TITLES:

None

A. TECHNICAL PROGRESS ACHIEVED ON EFFORT:

After detailed examination of the statement of work exploratory experiments were conducted to observe the internal electrical effects within an existing microwave transmit/receive (T/R) module housing provided as an example of a housing that has a known in-band oscillation. Resonances associated with the electromagnetic cavity formed by the housing when it is enclosed with a lid were identified using a novel method and relatively simple and inexpensive microwave test instrumentation.

Further experiments have been conducted to develop this novel method of measurement so that at each measured electromagnetic resonance a detailed recording of the electric field distribution over the inside surface of the housing lid may be made. It is anticipated that the electromagnetic cavity resonances will have field distributions that are complicated as a result of various projections from the cavity walls but that they are derived from TE modes with electric fields normal to the inner surface of the housing's flat lid.

These experiments have been successful and work has commenced on the construction of a prototype instrument with which accurate recordings of the resonant electric field distributions will be possible. From these recordings it should be possible to derive magnetic field distributions and identify the main coupling positions with the monolithic microwave integrated circuits mounted on the floor of the module housings. Design rules may be developed and tested with such an instrument.

B. TRAVEL:

Georgia Institute of Technology, Atlanta, GA, to Rome Air Development Center, Rome, N.Y., for initial discussions of the task and explanation of the effects that may be present in typical housings, possible methods of investigation and their relevance to the eventual development of design rules.

C. PRESENTATIONS AND PUBLICATIONS:

Nil apart from discussions at RADC explained in B.

D. LEVEL OF EFFORT BY EACH CONTRIBUTOR (IN MAN-MONTHS OR MAN-HOURS)

200 man-hours by D.W. Griffin.

ROME AIR DEVELOPMENT CENTER
EXPERT SCIENCE AND ENGINEERING PROGRAM
CONTRACT NO. F30602-88-D-0025

R & D STATUS REPORT

PERIOD COVERED: May 22, 1989 to June 23, 1989

TASK NUMBER: N-9-5732

TITLE: Microwave module housing internal electrical effects

PRINCIPAL INVESTIGATOR: Dr. Donald W. Griffin

INSTITUTION: George Institute of Technology

OTHER PARTICIPANTS AND TITLES:

None

A. TECHNICAL PROGRESS ACHIEVED ON EFFORT:

The prototype instrument for recording the electric field distribution over the inner surface of the lid on a microwave module housing has been completed and used successfully to measure distributions for three in-band resonances in a typical microwave transmit/receive (T/R) module housing.

The accuracy of the instrument is dependent upon certain special fabrication steps devised and implemented by the principal investigator. These steps ensure that as the measuring probe is mechanically scanned over the surface where electric field measurements are made the internal characteristics of the housing acting as a resonator do not change.

The research has included three main stages of learning, namely, how to construct an accurate probing and scanning assembly, how to operate the associated microwave assembly to yield repeatable results and how to record and interpret the characteristic field distribution for each resonance that may be present. By using standard resonators, for which an analytical field distribution can be obtained, empirical relations have been deduced for deriving actual fields from measured distributions. An extension of time appears necessary for deriving analytically more general relationships to replace the empirical ones. This will supplement a report that details the instrument, results obtained and the way design rules may be evolved and future designs checked on either complete or partially assembled module housings.

B. TRAVEL:

Georgia Institute of Technology, Atlanta, GA, to Rome Air Development Center, Rome, N.Y. to present research results and demonstrate the operation of the prototype instrument for measuring electric field distributions associated with electromagnetic resonances inside housings.

Georgia Institute of Technology to Raytheon, Wayland MA for the same purposes as the RADC visit.

C. PRESENTATIONS AND PUBLICATIONS:

Griffin, D.W., "A new method of measuring standing wave distributions on electromagnetic waveguiding structures", IEEE/IMTC Instrumentation and Measurement Technology Conference, Washington, DC, April 25-27, 1989.

D. LEVEL OF EFFORT BY EACH CONTRIBUTOR (IN MAN-MONTHS OR MAN-HOURS)

200 man-hours by D.W. Griffin.

CONTRACT FUNDS STATUS REPORT (DD FORM 1586)
CONTRACT NUMBER F30602-88-D-0025
QUARTER: MAY-JUN '88

	CURRENT QUARTER FUNDING		$0.00
	CURRENT QUARTER EXPENDITURES		$0.00
	CONTRACT CEILING		$4,200,000.00
	FUNDING TO DATE	-	$0.00
*	PENDING COMMITMENTS	-	$766,000.00
	AVAILABLE FUNDING		$3,434,000.00
	FUNDING TO DATE		$0.00
	YTD EXPENDITURES	-	$0.00
	OUTSTANDING EXPENDITURES		$0.00

*	C-8-2120	WESTINGHOUSE/BEAUDET	$56,000.00
	C-8-2129	RENSSELAER/DAS	$100,000.00
	E-8-7066	UNIV OF PENN/STEINBERG	$100,000.00
	E-8-7124	BOSTON COLLEGE/McFADDEN	$35,000.00
	E-8-7125	BRANDEIS UNIV/HENCHMAN	$23,000.00
	E-8-7126	PENN STATE/CASTLEMAN	$22,000.00
	A-8-1631	UNIV OF PENN/STEINBERG	$100,000.00
	B-8-3617	GA WASHINGTON UNIV/MELTZER	$100,000.00
	B-8-3618	GA WASHINGTON UNIV/BERKOVICH	$100,000.00
	C-8-2492	GA TECH/SMITH	$50,000.00
	A-8-1203	GA TECH/HUGHES	$80,000.00
		TOTAL PENDING	$766,000.00

CONTRACT FUNDS STATUS REPORT (DD FORM 1586)
CONTRACT NUMBER F30602-88-D-0025
QUARTER: JUL-SEPT '88

CURRENT QUARTER FUNDING			$698,034.00
DO # 0001	$56,000		
0002	$95,141		
0003	$78,854		
0004	$230,000		
0005	$45,561		
0006	$25,000		
0007	$20,000		
0008	$98,374		
0009	$29,403		
0010	$19,701		
	$698,034		
CURRENT QUARTER EXPENDITURES			$0.00
CONTRACT CEILING			$4,200,000.00
FUNDING TO DATE		-	$698,034.00
* PENDING COMMITMENTS		-	$426,563.00
AVAILABLE FUNDING			$3,075,403.00
FUNDING TO DATE			$698,034.00
YTD EXPENDITURES		-	$0.00
OUTSTANDING EXPENDITURES			$698,034.00

* DO # 0001	INCREMENTAL FUNDING		$90,729.00
0002	INCREMENTAL FUNDING		$66,680.00
0003	INCREMENTAL FUNDING		$54,154.00
0004	INCREMENTAL FUNDING		$20,000.00
C-8-2400	STATE UNIV OF NY/FAM		$95,000.00
C-8-2402	RENSSELAER/SAULNER		$100,000.00
TOTAL PENDING			$426,563.00

CONTRACT FUNDS STATUS REPORT (DD FORM 1586)
CONTRACT NUMBER F30602-88-D-0025
QUARTER: JAN-MAR '89

CURRENT QUARTER FUNDING			$574,457.00
DO #	0001	$90,729	
	0011	$75,000	
	0012	$75,000	
	0013	$59,989	
	0014	$49,989	
	0015	$70,000	
	0016	$43,750	
	0017	$30,000	
	0018	$22,000	
	0019	$38,000	
	0020	$20,000	
		$574,457	

CURRENT QUARTER EXPENDITURES		$86,324.15
CONTRACT CEILING		$4,200,000.00
FUNDING TO DATE	-	$1,393,325.00
* PENDING COMMITMENTS	-	$594,651.00
AVAILABLE FUNDING		$2,212,024.00
FUNDING TO DATE		$1,393,325.00
YTD EXPENDITURES	-	$115,064.97
OUTSTANDING EXPENDITURES		$1,278,260.03

*	DO # 0007	INCREMENTAL FUNDING	$20,000.00
	0011	INCREMENTAL FUNDING	$19,568.00
	0012	INCREMENTAL FUNDING	$24,700.00
	0015	INCREMENTAL FUNDING	$29,783.00
	0016	INCREMENTAL FUNDING	$31,250.00
	0017	INCREMENTAL FUNDING	$10,000.00
	0018	INCREMENTAL FUNDING	$12,000.00
	0019	INCREMENTAL FUNDING	$12,000.00
	C-8-2404	STANFORD UNIV/WIDROW	$100,000.00
	N-9-5732	GRIFFIN	$25,000.00
	A-9-1476	BOWDOIN COLLEGE/CHONACKY	$20,350.00
	E-9-7110	UNIV OF LOWELL/SALES	$50,000.00
	S-9-7559	UNIV OF MICHIGAN/ROBINSON	$20,000.00
	B-9-3621	SRI/LUNT	$20,000.00
	N-9-5308	KAMAN SCIENCES	$100,000.00
	E-9-7119	DARTMOUTH COLLEGE/CRANE	$100,000.00
		TOTAL PENDING	$594,651.00

CONTRACT FUNDS STATUS REPORT (DD FORM 1586)
CONTRACT NUMBER F30602-88-D-0025
QUARTER: APR-JUN '89

	CURRENT QUARTER FUNDING		$160,350.00
	DO # 0021	$25,000	
	0022	$45,000	
	0023	$20,350	
	0024	$50,000	
	0025	$20,000	
		$160,350	
	CURRENT QUARTER EXPENDITURES		$318,963.82
	CONTRACT CEILING		$4,200,000.00
	FUNDING TO DATE	-	$1,553,675.00
*	PENDING COMMITMENTS	-	$718,994.00
	AVAILABLE FUNDING		$1,927,331.00
	FUNDING TO DATE		$1,553,675.00
	YTD EXPENDITURES	-	$434,028.79
	OUTSTANDING EXPENDITURES		$1,119,646.21

*	DO # 0007	INCREMENTAL FUNDING	$20,000.00
	0011	INCREMENTAL FUNDING	$19,568.00
	0012	INCREMENTAL FUNDING	$24,700.00
	0015	INCREMENTAL FUNDING	$29,783.00
	0016	INCREMENTAL FUNDING	$31,250.00
	0017	INCREMENTAL FUNDING	$10,000.00
	0018	INCREMENTAL FUNDING	$12,000.00
	0019	INCREMENTAL FUNDING	$12,000.00
	0022	INCREMENTAL FUNDING	$54,693.00
	B-9-3621	SRI/LUNT	$20,000.00
	N-9-5308	KAMAN SCIENCES	$100,000.00
	E-9-7119	DARTMOUTH COLLEGE/CRANE	$100,000.00
	N-9-5740	CHRISTIANSON	$15,000.00
	N-9-5317	UNIV OF CO/NORGARD	$50,000.00
	S-9-7625	UNIV OF CA/DAVIS/KOWELL	$20,000.00
	N-9-5314	KAMAN SCIENCES	$100,000.00
	N-9-5315	KAMAN SCIENCES	$100,000.00
		TOTAL PENDING	$718,994.00

E-2/T 2

CONTRACT FUNDS STATUS REPORT (DD FORM 1586)
CONTRACT NUMBER F30602-88-D-0025
QUARTER: JUL-SEP '89

CURRENT QUARTER FUNDING			$476,000.00
DO #	0017	$10,000	
	0026	$15,000	
	0027	$20,000	
	0028	$50,000	
	0029	$40,000	
	0030	$30,000	
	0031	$20,000	
	0032	$66,000	
	0033	$70,000	
	0034	$85,000	
	0035	$70,000	
		$476,000	
CURRENT QUARTER EXPENDITURES			$415,422.69
CONTRACT CEILING			$4,200,000.00
FUNDING TO DATE		-	$2,029,675.00
* PENDING COMMITMENTS		-	$253,994.00
AVAILABLE FUNDING			$1,916,331.00
FUNDING TO DATE			$2,029,675.00
YTD EXPENDITURES		-	$849,451.48
OUTSTANDING EXPENDITURES			$1,180,223.52

* DO #	0007	INCREMENTAL FUNDING	$20,000.00
	0011	INCREMENTAL FUNDING	$19,568.00
	0012	INCREMENTAL FUNDING	$24,700.00
	0015	INCREMENTAL FUNDING	$29,783.00
	0016	INCREMENTAL FUNDING	$31,250.00
	0018	INCREMENTAL FUNDING	$12,000.00
	0019	INCREMENTAL FUNDING	$12,000.00
	0022	INCREMENTAL FUNDING	$54,693.00
	N-0-5703	UNIV OF SOUTHERN FLA/WILSON	$50,000.00
		TOTAL PENDING	$253,994.00

CONTRACT FUNDS STATUS REPORT (DD FORM 1586)
CONTRACT NUMBER F30602-88-D-0025
QUARTER: OCT-DEC '88

	CURRENT QUARTER FUNDING		$120,834.00
	DO # 0004	$66,680	
	0006	$54,154	
		$120,834	
	CURRENT QUARTER EXPENDITURES		$28,740.82
	CONTRACT CEILING		$4,200,000.00
	FUNDING TO DATE	-	$818,868.00
*	PENDING COMMITMENTS	-	$784,729.00
	AVAILABLE FUNDING		$2,596,403.00
	FUNDING TO DATE		$818,868.00
	YTD EXPENDITURES	-	$28,740.82
	OUTSTANDING EXPENDITURES		$790,127.18

*	DO # 0001	INCREMENTAL FUNDING	$90,729.00
	0007	INCREMENTAL FUNDING	$20,000.00
	C-8-2400	STATE UNIV OF NY/FAM	$95,000.00
	C-8-2402	RENSSELAER/SAULNER	$100,000.00
	B-9-3592	UNIV OF CA/DAVIS/LEVITT	$60,000.00
	N-9-5514	SOHAR INC./HECHT	$50,000.00
	C-9-2015	NCS/O'NEAL	$100,000.00
	A-9-1120	HITEC, INC./KAZAKOS	$75,000.00
	E-9-7057	UNIV OF TX/ARLINGTON/FUNG	$40,000.00
	E-9-7093	MONTANA STATE/JOHNSON	$34,000.00
	S-9-7552	ALFRED UNIV/SYNDER	$20,000.00
	C-9-2404	STANFORD UNIV/WIDROW	$100,000.00
		TOTAL PENDING	$784,729.00

F-21-T21

MICROWAVE MODULE HOUSING

INTERNAL ELECTRICAL EFFECTS

Donald W. Griffin

Georgia Tech Research Institute,
Georgia Institute of Technology,
Atlanta, GA, 30332.

TABLE OF CONTENTS

ABSTRACT

A special purpose two-dimensional standing wave detector for measuring resonant electric field distributions at the flat lid on microwave housings and packages is described and its use as a diagnostic and design development tool for module housings is demonstrated. Empirical and analytical relationships between measurables and the electric field are presented.

SUMMARY

Microwave housings and packages designed to provide precise physical support, good heat removal and excellent electromagnetic shielding for such components as monolithic microwave integrated circuits (MMICs), are usually broad-based, low profile rectangular, metal box-shaped structures. Most components, particularly semiconducting chips, are mounted on the broad floor of the housing while signal and bias connections are made via the narrow side walls. Assembly is usually completed by a flat metal lid fastened around the perimeter at the top edge of the side walls.

Such housings and packages will act as resonant electromagnetic cavities if it is not possible to include sufficient microwave absorbent material within the enclosure to prevent them being energised as such. Potentially resonant enclosures must be designed in such a way that the microwave performance of the assembly within the enclosure is not degraded in any way by either in-band or out-of-band resonances. Such resonances can cause undesirable electromagnetic coupling that may affect passive as well as active components in the assembly. The box shape favours TE followed at higher frequencies by TM mode resonances.

There appear to be few, if any, design aids specific to the problem of housing and package design. The wide range of geometric detail due to internal wall projections, component materials and dimensions, etc., adds complexity to any design analysis that aims to predict, (a) electromagnetic resonances, (b) details of associated electric and magnetic field distributions, (c) couplings between parts of the enclosed assembly due to resonances and (d) the resultant effect on performance characteristics.

With the aim of testing housings and packages and developing design improvements a method of measuring the frequencies at which resonances occur and the distribution of the associated electric field intensity at the inside face of the housing lid has been developed and tested. The method does not require modification of the housing or package in any way nor does it need to use any of the connections to the microwave assembly within the housing. It is only

necessary that the housing have a flat lid and that it be left off so that the housing can be mounted on an equivalent flat plate on the test instrument. The microwave assembly in the housing or package may be operated normally while resonant field distributions are being measured.

An electric field probe extends from a small aperture at the centre of the instrument plate that takes the place of the housing or package lid. The probe can be scanned across the whole area normally covered by the lid by movement of the housing or package on the instrument plate in two dimensions. The instrument is effectively a special purpose two-dimensional standing wave detector. It is special purpose because instead of measuring standing wave patterns in a uniform waveguide terminated in a load it measures patterns associated with resonances in cavities that are usually of uniform depth but may contain a wide selection of projections from the floor and side walls as well as a wide variety of materials. The constraints of this special purpose impose both excitation and detection functions on the probe in contrast to the simple detection function of the probe in a conventional standing wave detector.

The simplest way to do this is to connect a microwave signal source and reflectometer to the coaxial electric field probe. At the resonance selected for study probe penetration is adjusted to give critical coupling to the housing cavity at the position in the cavity where the electric field intensity at the inside surface of the lid is a maximum. This appears as near zero reflected signal in the reflectometer. Thus absorbed power can be used as a qualitative measure of the relative electric field in the housing as the probe is scanned in two dimensions.

Measurements on known resonant field distributions in regular cavities may be used to derive an empirical relation between the recorded quantity and the electric field intensity at the probe. Also equivalent circuit analysis at arbitrarily chosen positions of the measuring probe in a uniform cavity can be used to derive an analytical relationship between the electric field and measurements. However detuning of the cavity from the test frequency as the probe is scanned complicates the derivation of an analytical relationship. A scheme of frequency scanning and peak absorption detection is a practical way

of eliminating detuning effects in which case analytical derivation of the electric field from absorption measurements is a simpler procedure if it is needed.

The prototype instrument yields results that demonstrate the practical application of this new measurement assembly as a diagnostic and design development tool for microwave housings and packages of rectangular metal box basic shape. Resonances in the 8 to 12 GHz range have been accurately measured and indicate that by scaling dimensions an assembly for use at millimetre wavelengths is feasible.

1. INTRODUCTION

The development of integrated microwave systems has been progressing for the past two decades and has reached the stage where monolithic microwave integrated circuits (MMICs) on gallium arsenide (GaAs) can be designed and fabricated to perform as power amplifiers for transmitters, low noise amplifiers for receivers, switches for use in digital phase shifters and so forth. In combination, complex modules can be produced for various systems applications, such as transmit-receive (T/R) modules for use in large phased array radar assemblies comprised of thousands of such modules.

A serious problem that has been commonly encountered throughout this period of development is the unsatisfactory performance of otherwise well-designed units when they are enclosed in a metal housing (module package) essential for prevention of interactions amongst modules in an assembly. The design of the housing is a classical microwave problem of significant complexity because of the range of component parts, shapes, sizes, materials, etc. to be accommodated.

Ideally a set of design rules that yield a housing within which there are no undesirable interactions amongst the functional components inside the housing is required. In addition, laboratory techniques for providing data that may be needed in the implementation of the design rules and for testing the behaviour of housings throughout the entire relevant frequency range are needed. There appears to have been little systematic work published on either of these aspects of microwave housings for integrated systems.

A novel measurement method for identifying electromagnetic resonances and determining an outline of the field distribution associated with the resonances will be described and illustrated by reference to a T/R system housing that has been found to exhibit unacceptable features during pre-production development.

Development trends provide simple starting points for design rules. Thus, assemblies that include MMIC chips are invariably planar and the

housing is therefore invariably rectangular box-shaped with the components fastened or attached to a broad, long face of the box. The box is usually of minimum height consistent with providing a large enough dimension to accommodate microwave and supply connectors on the end and/or side walls. The top wall is usually a planar lid without any attached components. The shape of the empty box favours excitation of TE waveguide modes followed by TM modes at higher frequencies.

The function of the system to be housed introduces further order in the development of design rules. This will be illustrated by reference to T/R systems.

2. BASIC FEATURES OF MODULE HOUSINGS

2.1 The three basic functions

The housing for the typical microwave solid state module used in modern communication and radar assemblies performs at least three basic functions. First and foremost, it is a physical support structure for all of the components that go to make up the module and because the microwave parts must be precisely located relative to each other, the housing must meet stringent mechanical tolerance specifications. Secondly, it provides the means for heat removal. The need to transfer the heat generated in microwave devices fabricated in GaAs or Si to a heat sink with minimum thermal resistance involves special technology and it is important that the module housing not degrade this critical part of the entire process of heat removal. Thirdly, it acts as an electromagnetic shield. The microwave performance of the module should not be degraded beyond certain specified limits by extraneous electromagnetic signals, and conversely, the module should not create uncontrolled electromagnetic fields that may couple to adjacent modules or other electrical subassemblies and assemblies.

Thus, creation of the housing for an advanced multifunction microwave module involves precision mechanical engineering, careful thermal design and also electromagnetic shielding design that limits both interference from outside and leakage from inside.

The second and third basic functions require material that has both high thermal and electrical conductivity and the obvious choice is metallic material, except where electrical power and signal paths must be provided through, and therefore insulated from, the housing. The provision of these paths may also impose additional requirements on the thermal design if, for example, the enclosed space must remain hermetically sealed over a range of temperature. The thermal expansion coefficients of the insulating material and the metal must then be matched over the specified range and this imposes restrictions on the choice of materials. For example, kovar may be needed for those parts of the housing where power and signal connectors are positioned so that high integrity glass-to-metal hermetic seals can be used. In other parts of the housing kovar may not be suitable

in which case a transition to a more suitable conducting material for either thermal or electrical reasons may be necessary. The need to transfer the heat generated in microwave devices fabricated in GaAs or Si to a heat sink with minimum thermal resistance involves special technology and it is important that the module housing should not degrade this critical part of the entire process of heat removal.

2.2 Module housing basic shape.

There are certain basic features of module housings that arise from the component fabrication technologies. Components of prime importance in new and future modules are planar in form, e.g. MMICs, and so the physical support structure for them needs to be planar also. To shield the assembly it is usual for this planar support to be the floor of a rectangular box shaped metallic housing. The side walls must be made high enough to provide room for microwave signal connectors and also power supply and control signal connectors. It follows that the roof or lid that completes the enclosure may be a simple planar sheet fastened to the top edge of the side walls around the perimeter of the box.

In assemblies that involve a large number of identical modules, such as phased array radar systems, each module is restricted in two of its dimensions by the aperture area occupied by each array element, often one quarter of a wavelength squared ($\lambda^2/4$). Thus the cross-sectional area of the rectangular box housing is subject to an upper limit and if it is set equal to that limit then the aspect ratio of that rectangular cross-section will depend upon the geometrical layout of the array of elements used to fill the overall antenna aperture. Input and output connections to each module are then most conveniently located in those end walls of the housings that are parallel to the antenna aperture plane, although connections can be made through other walls provided they do not touch each other or, alternatively, clearances or recesses are provided that are accessible from one or both ends of the overall assembly. Implicit in this line of reasoning is the assumption that the planes upon which the microwave module components are assembled are at right angles to the antenna array aperture. This type of assembly can be regarded as one in which integration occurs within the modules in what is the longitudinal

plane and assembly occurs in the transverse or aperture plane by stacking the modules alongside each other until the entire aperture is filled.

2.3 Housing dimensions and inherent electromagnetic cavity resonances.

With the trend towards integrating several functions within a module the floor area of module housings can easily approach a square wavelength or more while the height of the side walls can be kept to a small fraction of a wavelength using modern miniature connectors. The width to height ratios of the rectangular cavities that are created are therefore large and the lowest frequencies at which resonances occur have field configurations like TE waveguide modes with electric fields orientated normal to the inside surfaces of the lid and floor of the box. The field distributions and resonant frequencies will be modified to a greater or lesser extent by metallic projections from the floor of the box, such as septa, posts, component packages, etc., and design is often attempted with the aim of making the lowest resonance well above the operating frequency range of the microwave module.

Figure 1 shows the dimensions of a representative example of a housing for accommodating an assembly of X-band monolithic integrated circuits that provide amplified power at about 10 GHz via a circulator to drive one element of a phased array antenna and also amplify return signals that emerge from the circulator. This transmit-receive function also involves microwave diode switches, delay line type phase shifting as well as circuits for the necessary bias supplies and control signals. Note that there are septa at positions A and B in the simplified drawing of Figure 1(a) and that the circulator shell C projects well above the floor of the housing in the side view in Figure 1(b). Figure 1(c) is a plan view of components within the housing and Figure 1(d) is a detailed drawing of the housing.

2.4 What needs to be known about electromagnetic resonances - the problems that require solution.

Given the details of a typical module like that shown in Figure 1 there appear to be no simple analytical methods or computer-aided design tools that may be used to calculate,

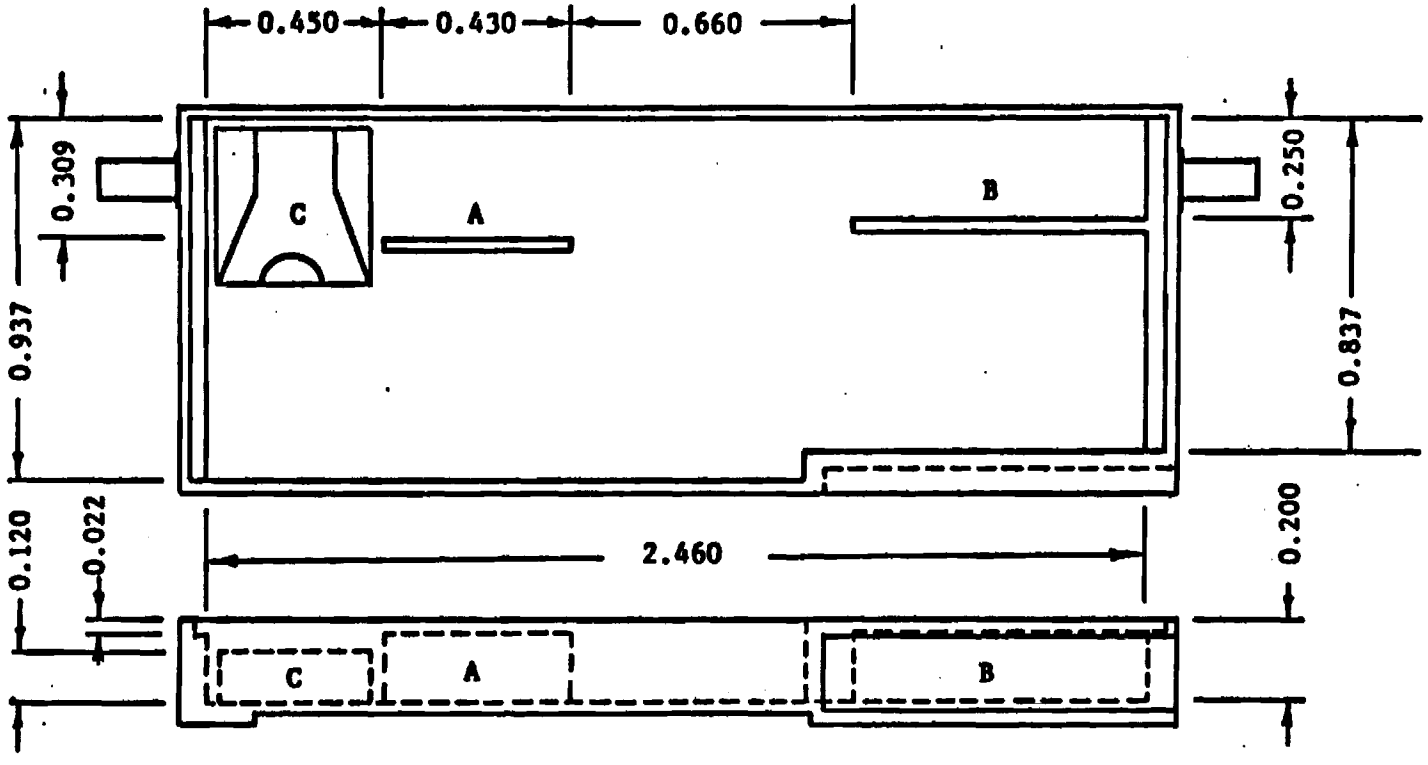

All dimensions nominal and in US inches.

igure 1(a) An example of a housing for a microwave phase array radar transmit-receive (T/R) module. (a) Outline and salient dimensions.

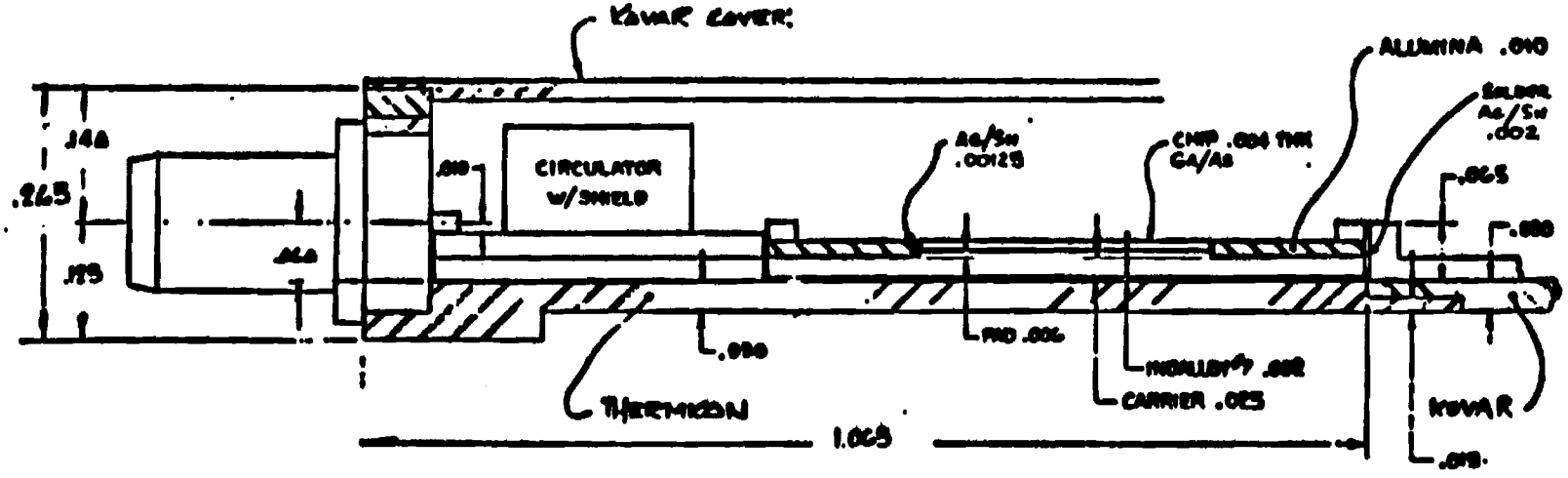

Figure 1(b) T/R module axial cross-section showing some components.

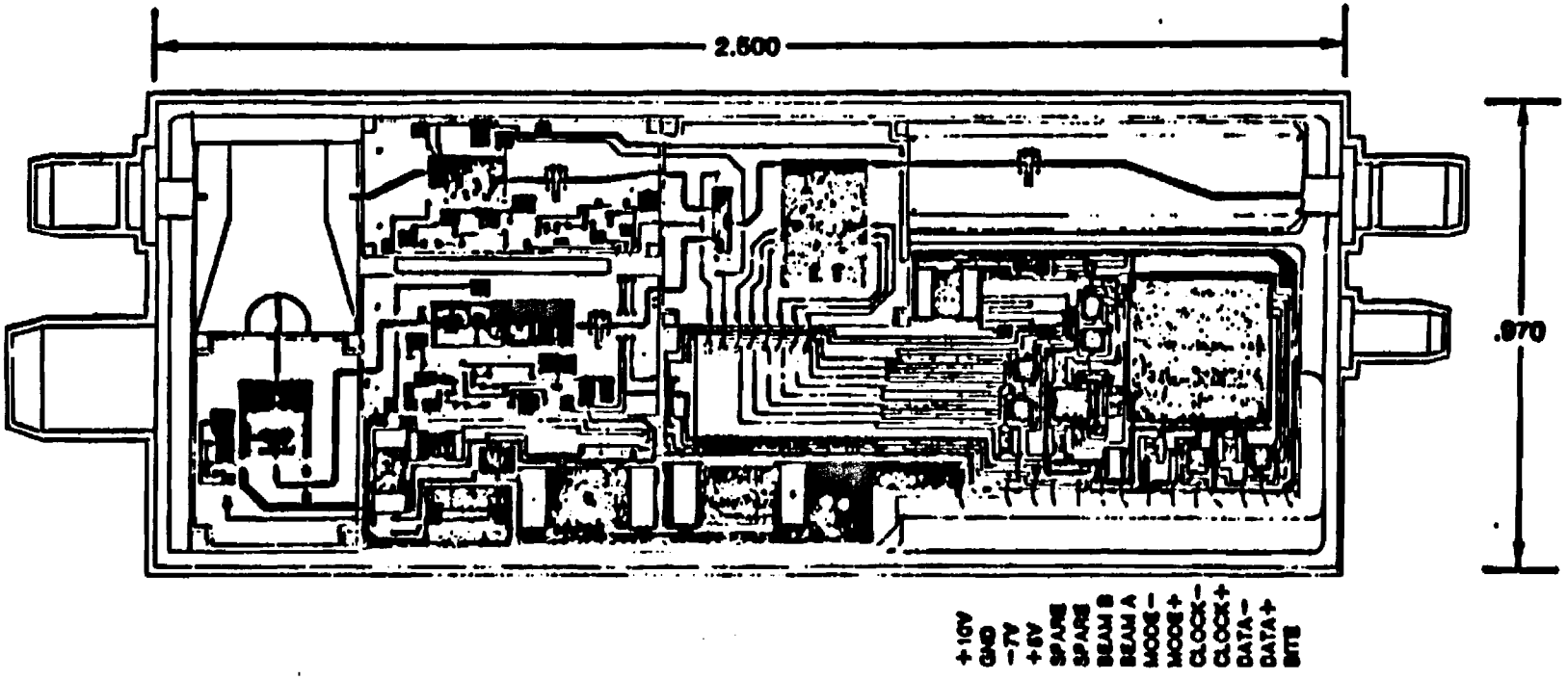

Figure 1(c) T/R module top view with lid off showing MMIC and discrete component layout.

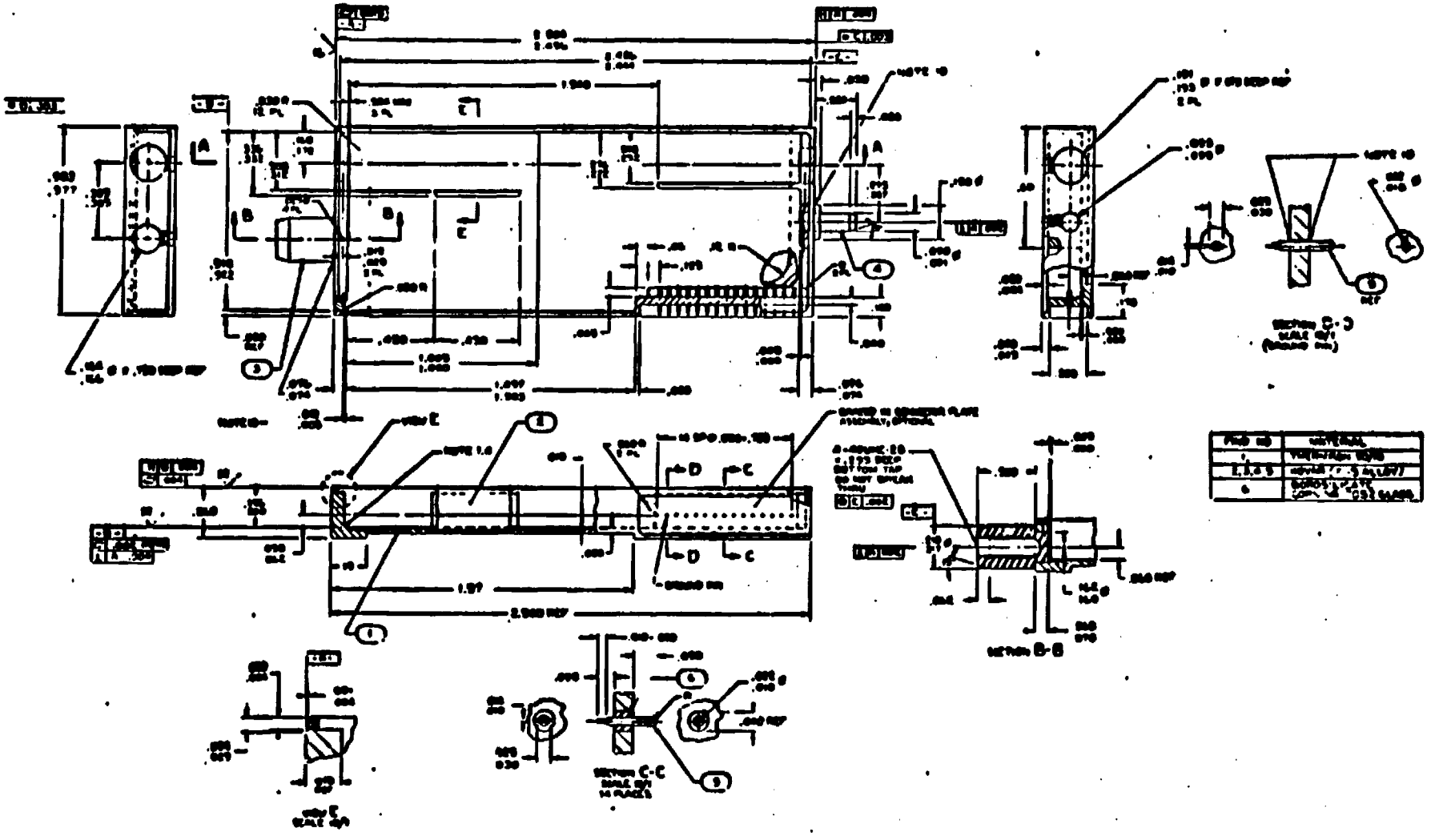

Figure 1(d) T/R module–housing dimensioned drawing.

(a) the microwave (or millimeter-wave) frequencies at which electromagnetic cavity resonances will occur inside this module housing,

(b) the details of the electric and magnetic field distributions associated with each resonance that may occur within the specified operating-frequency band of the T/R module,

(c) the coupling between each of the electromagnetic resonances and the microwave circuits enclosed by the module housing, and,

(d) the effects that couplings due to cavity resonances may have on the performance characteristics of the module compared with specifications.

Indeed, the development of analytical methods and/or design tools capable of yielding accurate information on resonant frequencies, field distributions, coupling points and effects on performance must be regarded as a particularly difficult problem because of the wide range of geometrical detail that must be used as the starting point. In addition, the calculations must accurately take account of microwave losses if amplitudes of field components and hence coupling effects are to be determined. To do this the contributions of all of the conductors, dielectrics and magnetic materials inside the housing must be combined in the correct way to determine the quality factor of each resonance.

2.5 Remedies for electromagnetic resonances.

A basic point that must not be overlooked is that the only way to prevent electromagnetic cavity resonances is to introduce sufficient microwave loss for all cavity modes that may cause unwanted module characteristics. If that is not acceptable then the only other design remedies involve controlling the frequencies at which resonances can occur, and/or the field distributions associated with them and/or the coupling between the resonances and the microwave circuit. These remarks apply to resonances both within and outside the operating frequency band of the

module in the housing, because malfunction is not restricted by specification of an operating frequency range. For example, oscillation of an amplifier may occur due to cavity resonance induced positive feedback at a frequency outside the specified band of operation.

2.6 Is malfunction likely with the module housing lid closed and no microwave cavity resonance present?

Unwanted oscillations and deviations from desired operation over frequency intervals within the required overall bandwidth, so called "resonances" or "glitches", may occur in T/R microwave modules due to a number of causes either acting together or in isolation. Because each module in general is a combination of a large signal power amplifier and a small signal low noise receiver amplifier, both designed to respond to the same range of microwave frequencies, the primary cause of unwanted features in the performance of the module is bound to be due to unwanted feedback effects within the several circuits that form the module.

Feedback effects can be visualised as occurring in a number of ways within microwave T/R modules including the following:

(a) within active devices due to the finite value of s_{12}, the reverse transmission coefficient from output to input, and the operating conditions of those devices,

(b) within individual stages of amplification due to the introduction of feedback circuit components, either by design or accident,

(c) within a subassembly of several stages of amplification as a result of part of the relatively high level output signal being coupled back to the input of the amplifier,

(d) within the overall assembly of power amplifier, circulator, transmit-receive switches and low noise receiver amplifier due to somewhat less than adequate isolation of the transmit-receive sections during the transmit mode of operation,

(e) between various parts of the overall assembly via electromagnetic coupling arising from excitation of waveguide-type cavity resonances in the space enclosed by the module housing,

(f) due to the particular test conditions set up external to the module especially with regard to the load presented to the module at its output port and the shielding or isolation provided between the output and the input to the module.

When the lid is put in place on a microwave module housing it may be argued that the circuit components will be altered in value by the introduction of that highly conducting plane due to the confinement and alteration of electric and magnetic fields in the immediate vicinity of each component. Close examination of a typical module like that illustrated in Figure 1 reveals that malfunction is not likely to occur due to effects of this type if there is no electromagnetic cavity resonance. The explanation follows from the high degree of field confinement caused by the GaAs substrate within which most of the module components and all of the active components are formed.

The substrate thickness is a mere few percent of the total distance between the floor and the lid of the housing and being in contact with the floor it means that magnetic fields associated with microwave currents on conductors on the top surface of the substrate are not affected by the more distant lid except in a very minor way. Furthermore, electric field effects associated with charges on the conducting and semi-conducting parts of the wafer are affected much more by the floor of the housing rather than the lid, because GaAs, the substrate material, has a dielectric constant of about 13. This is large and leads to close confinement of electric field effects within the GaAs between conducting paths on the top surface and the highly conducting floor of the housing.

Thus it can be argued that as long as the substrate is thin compared with the housing height, the MMIC components per se will not be altered by the lid being fastened in place. Thus malfunction due to feedback effects corresponding to categories (a), (b), (c) and (d) set out above are

not likely to be affected by placing the lid on the housing. Their presence will be evident when the MMICs are energised with the housing lid removed and their solution will probably require modifications being made to the MMICs.

The only items that do not form part of the MMICs are the larger lumped components at or near points of entry and exit and special items that for various reasons may not have been integrated into the MMICs. The components that have imposed the height requirement on the housing are the ones most likely to be affected when the lid is put in place. They include ferrite circulators, coaxial connectors and bias components that are immediately adjacent to the edges of MMICs and connected to them. However these components may be relatively distant from each other and it is difficult to see how deleterious feedback effects could be set up due to changes in circuit components that are widely separated. At most, a perturbation of the load impedance presented to the power output stage of the transmitter may occur, but this is likely to be too small to cause instability compared with the possible effect of test conditions set out as category (f).

The means of coupling widely separated parts of a module is through the electromagentic fields of a cavity resonance as identified above as category (e). Thus it is concluded that this is the major problem to be addressed when the lid of a housing is put in place particularly so if resonances cannot be prevented by the simple expedient of placing sufficient microwave loss material inside the cavity that is formed.

3. THE NEED FOR AN EXPERIMENTAL METHOD OF MEASURING RESONANCES IN HOUSINGS AND THE ASSOCIATED FIELD DISTRIBUTIONS.

A method of measuring cavity resonances in housings is needed for at least two important reasons,

(i) to provide a means of testing housings that may have been designed adequately from the mechanical and thermal point of view but rather empirically for the electromagnetic functions that they must serve, and,

(ii) as a means of gathering data on the effects of structural details that may be incorporated in housings, so that design rules, analytical models and possibly computer aided design tools may be developed to provide accurate procedures for designing housings that meet detailed electromagnetic specifications for reliable performance.

A method is needed that can be applied to any microwave housing with a flat metal lid that also satisfies the following constraints,

(a) the module housing may or may not have all components installed ready for normal operation, except that,

(b) the flat metal lid of the housing may not necessarily be fastened in place and consequently may be replaced by a flat metal plate that forms part of a test instrument,

(c) the input and output connectors on the module housing should be available for normal microwave signal operation and measurements, if necessary, and,

(d) the housing is not to be modified in any way, apart from (b) above, to accommodate resonance and field distribution measuring items.

Notwithstanding the long history of development of microwave measurements none of the methods and instruments that have been

developed in the past provide a solution to these requirements. A new instrument has been invented, a prototype has been built and its use has been demonstrated in an experimental investigation of the housing detailed in Figure 1. That study has revealed the existence of three resonances in the frequency range up to 12 GHz and recordings of the electric field distribution over the inside surface of the housing lid have been obtained.

An explanation of the method of measurement, the principles that underly the method, details of construction of critical components, the technique used for obtaining results and the way in which the results can be interpreted and used for developing the design of the module housing being studied are set out in the sections that follow.

4. A NEW METHOD OF MEASURING MICROWAVE CAVITY RESONANCES AND THEIR ASSOCIATED ELECTRIC FIELD DISTRIBUTIONS OVER CAVITY WALLS THAT ARE FLAT.

4.1 The guiding principles for the new method.

The standing wave detector assembly, shown in Figure 2(a), with its two main parts in the form of a length of rectangular section waveguide with a slot on the longitudinal centre-line of the broadface and an electric field probe and carriage assembly that can be positioned anywhere along the centre-line, is arguably the most accurate and highly developed instrument for measuring electric field distributions continuously along a path in a uniform waveguide. Careful design and development of the slot in the wall of the waveguide and the probe structure that is moved along that slot have been necessary pre-requisites for accuracy. The choice of an electric field probe, in the form of a thin straight wire, rather than a magnetic field probe, in the form of a small loop, has been essential also for accurate measurement of the electric field only rather than the magnetic field together with a residual component of electric field if the loop is used.

The electric field probe is simply an extension of the inner conductor of a coaxial line. The outer conductor is usually extended into the slot also, as shown in Figure 2(a) and labelled spline, so that the capacitance between the probe and slot remains constant as the probe and carriage are moved along the slot. This detail is mentioned because of its relevance to the development of the new method for use over the area covered by flat cavity walls.

The slot could be avoided if the top wall could be separated from the side walls of the waveguide and allowed to move in the direction of the axis of the waveguide with a sliding action on the top edge of the side walls. The waveguide would have to curve away from the top wall near the input and output end of the guide and therefore there would have to be a sliding action at edges transverse to the centre-line of the top face near the commencement of curvature. For accuracy of field measurement with a probe extending through a small hole on the centre-line of this

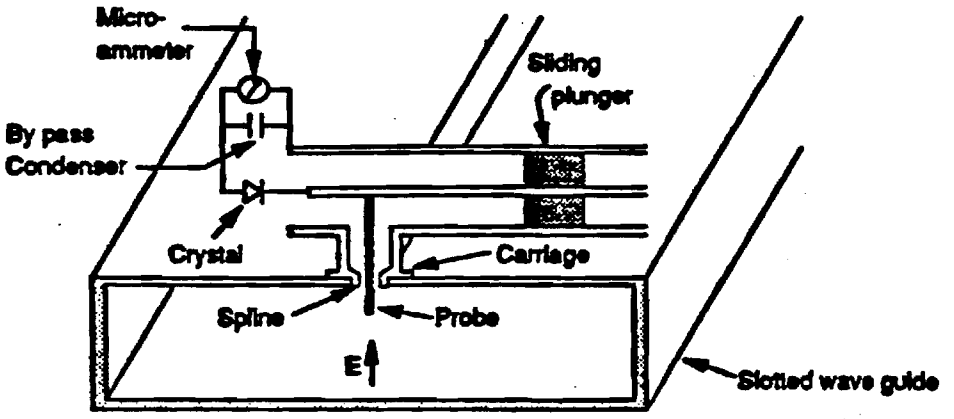

DIAGRAMMATIC REPRESENTATION OF STANDING-WAVE INDICATOR

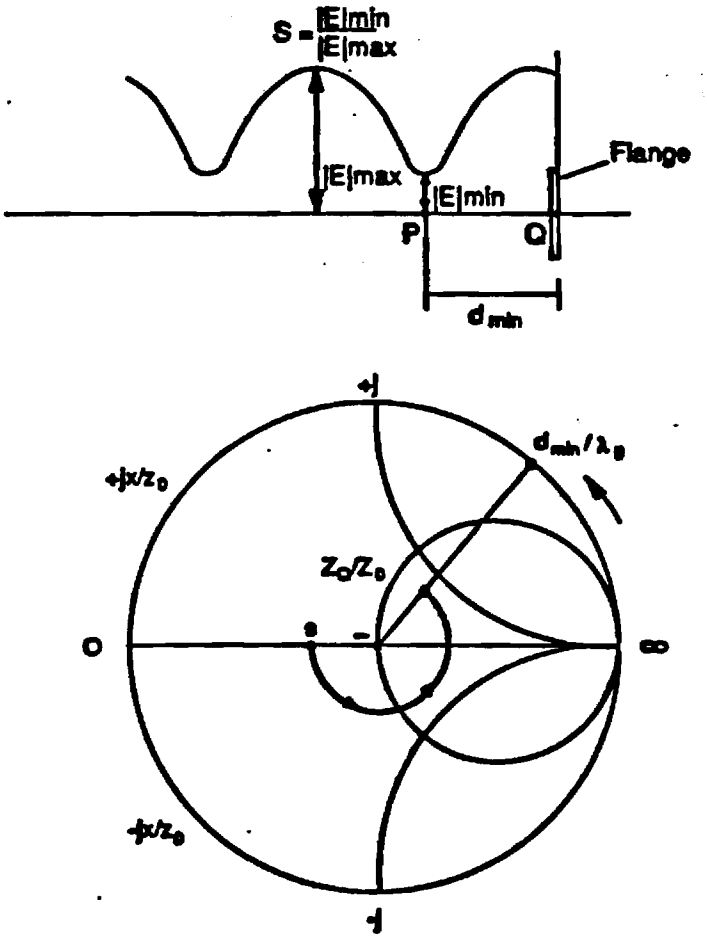

CALCULATION OF IMPEDANCE Z_Q AT FLANGE Q

Figure 2: Slotted waveguide assembly used for measuring the relative electric field distribution along the centre-line of one wall of a waveguide.

sliding top wall the impedance presented to wall currents at edges where sliding action occurs, would have to remain constant as movement occurred and preferably be negligibly small. On page 511 of Montgomery's book [1] Purcell describes a high power standing wave detector developed by Nordsiek of Columbia Radiation Laboratory. The contact between the movable top wall and the edges of the waveguide displayed no sparking at powers up to 100 kw and was judged to be "a perfect electrical contact". To avoid sparking a coupling hole in the sliding top wall was used instead of a coaxial probe.

While this alternative mechanical arrangement obviously has not been favoured as a basis for the development of a commercially available standing wave detector, it has one great advantage not mentioned in Montgomery [1] that makes it worthy of serious study for special applications. In principle it is not restricted to movement in one direction in the way that the slot in the waveguide restricts the movement of the probe and carriage in standing wave detectors. In fact, provided the flat plate that forms the top wall is large enough, it may be moved laterally as well as longitudinally so that the electric field probe and the small circular aperture that it passes through may be positioned anywhere in the area defined by the part of the top wall of the waveguide that has been removed and replaced by the movable flat plate. Thus, in principle, this alternative mechanical arrangement is a new more versatile instrument and could be called a two-dimensional standing wave detector.

Such an instrument would offer little or no advantage over the conventional standing wave detector as long as the fixed waveguide is simply uniform throughout its length and operated with the dominant TE_{10} mode of propagation for rectangular section waveguides. However, interesting possibilities arise for consideration if the application of this type of instrument is not restricted to the concepts of standing wave detection and derivation of the normalised impedance of a test component connected to the output port of the instrument as illustrated in Figure 2(b)

If a metal bar is inserted along the centre-line of a waveguide, a uniform single-ridged waveguide will be formed. If such a bar is placed along half the length of a standing wave detector slotted line and then

extended into a reflection-free terminating section, then, with the movable probe, standing wave patterns can be measured in the rectangular waveguide part and the ridged waveguide part, the latter being close to unity if the reflection-free termination is well made. In addition, it will be possible to measure the effect of the end of the ridge as a distortion of the electric field distribution in the vicinity of the interface between the rectangular and ridged waveguides. The two-dimensional standing wave detector would give additional detail on the way in which the ridge distorts the electric field distribution in cross-sectional planes in the vicinity of the interface.

If the input and output ports of the waveguide are terminated with high reflection coefficient components, such as short circuiting walls, then an electromagnetic resonant cavity will be formed. The conventional one-dimensional and the proposed two-dimensional standing wave detectors could be used to measure the electric field distribution near the top wall of the cavity and if the excitation frequency is set equal to a resonance then details of the resonant distribution will be obtained. If the resonator is a rectangular parallelopiped then details of each resonance can be predicted theoretically. These results may be used to evaluate the effect of various practical aspects of the microwave equipment being used for measuring the resonance characteristics. Thus it is possible to evaluate the effects of detector probe loading, excitation source coupling and variations due to probe movement due to non-uniformity of the slot in the one-dimensional case or the sliding surfaces in the two-dimensional standing wave detector assembly.

One more guiding principle must be understood. In using the one-dimensional or the two-dimensional standing wave detector to measure field distributions in cavities at resonance, it may not be possible to introduce the excitation signal through either of the terminating walls of the fixed waveguide part of the assembly. The simplest solution, if such a constraint is imposed, is for the excitation function, as well as the detection function, to be performed by the movable electric field probe. A simple way of doing this is to remove the simple diode detector and tuning stub from the probe shown in Figure 2(a) and connect a microwave reflectometer in its place to measure incident and reflected quantities at

that coaxial port as shown in Figure 3(c).

4.2 Demonstration of the new method with a commercially available standing wave detector.

A commercially available standing wave detector can be used to demonstrate the new method of measuring microwave cavity resonances and their associated electric field distributions by assembling it with additional microwave components in the following array. Connecting a short circuiting plate or plunger to each end of the slotted waveguide section creates a rectangular cross-section parallelpiped cavity of known physical dimensions. The resonant frequencies of such a cavity can be accurately calculated from the dimensions. Also the relative distribution of electric field along the path of the longitudinal slot for each of the resonances can be set down as an integral number of half sine wave loops as shown in Figure 3. Part (b) of that figure illustrates the relative electric field distributions for the six resonances designated TE_{106} through to $TE_{10(11)}$.

Part (a) of that figure shows the electric field probe schematically at the position mid-way between the short-circuits at the ends of the cavity. Referring to part (b) it is clear that half-way along the cavity the probe will be at a position where the electric field associated with resonances is either zero or a maxmimum. Resonances that make the cavity an even number of half wavelengths long (identified by the third mode subscript being even, ie. 6, 8 and 10) have zeroes half-way along the cavity while resonances with odd numbers 7, 9 and 11, in the third subscript position have maxima at the mid-point.

The measuring equipment assembly shown in Figure 3(c) can be used to identify the frequency at which each one of the resonances set out in Figure 3(b) occurs in an actual rectangular cavity. A housing for test purposes is assembled from a Hewlett Packard Model X810B slotted waveguide section illustrated in Ginzton on page 258 [2], probe carriage Model HP809C and coaxial probe Model HP442B, together with two microwave short circuiting plungers, one for each end of the slotted waveguide section. The coaxial probe does not have a detector or a tuning stub, but its penetration into the cross-section of the waveguide can be

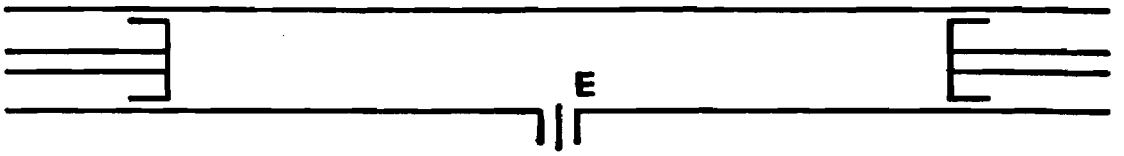

(a) Rectangular cross-section cavity with E-field probe that can be moved along a slot on the center-line of the broad wall to any longitudinal position

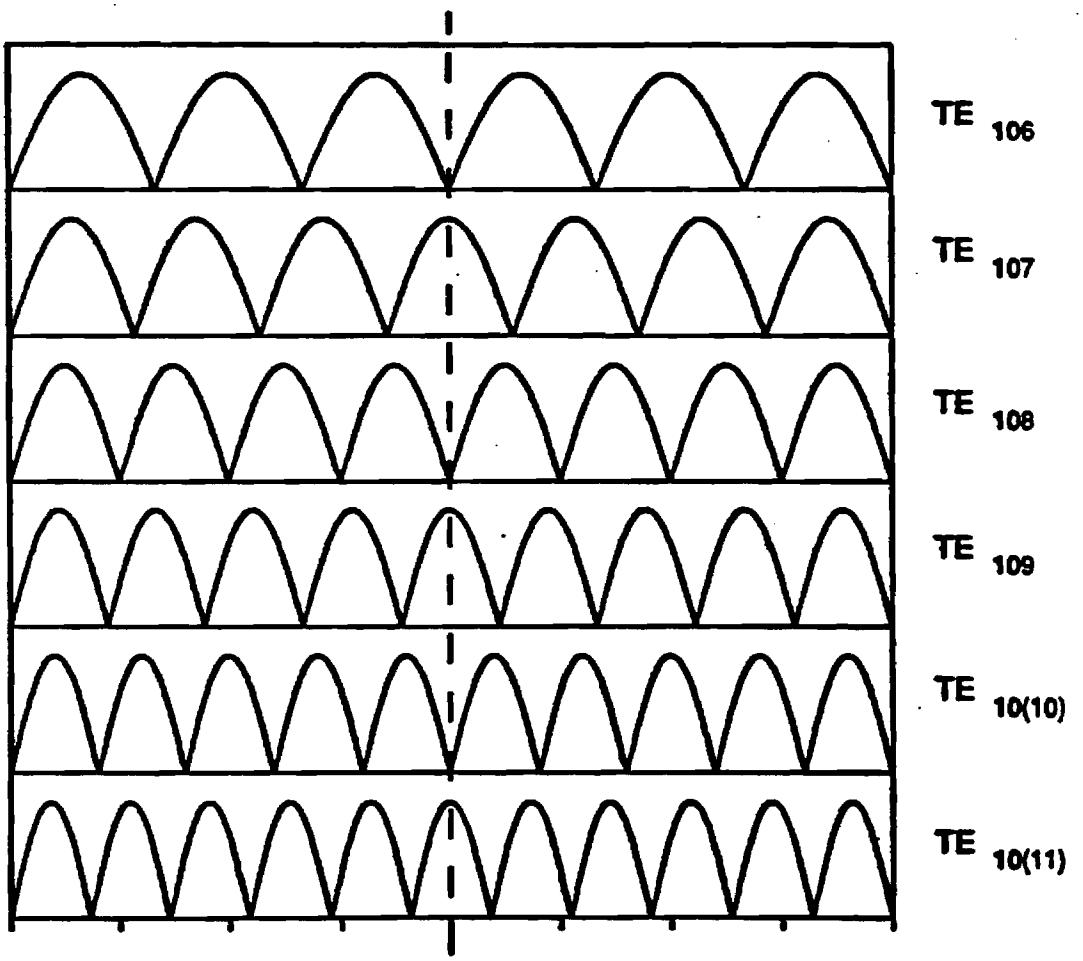

(b) Electric field standing wave patterns corresponding to TE_{106} through to $TE_{10(11)}$ resonant modes within the cavity

Figure 3 (a) and (b) A resonant cavity made with a slotted waveguide and short circuit plungers that demonstrates resonant field distribution measurement.

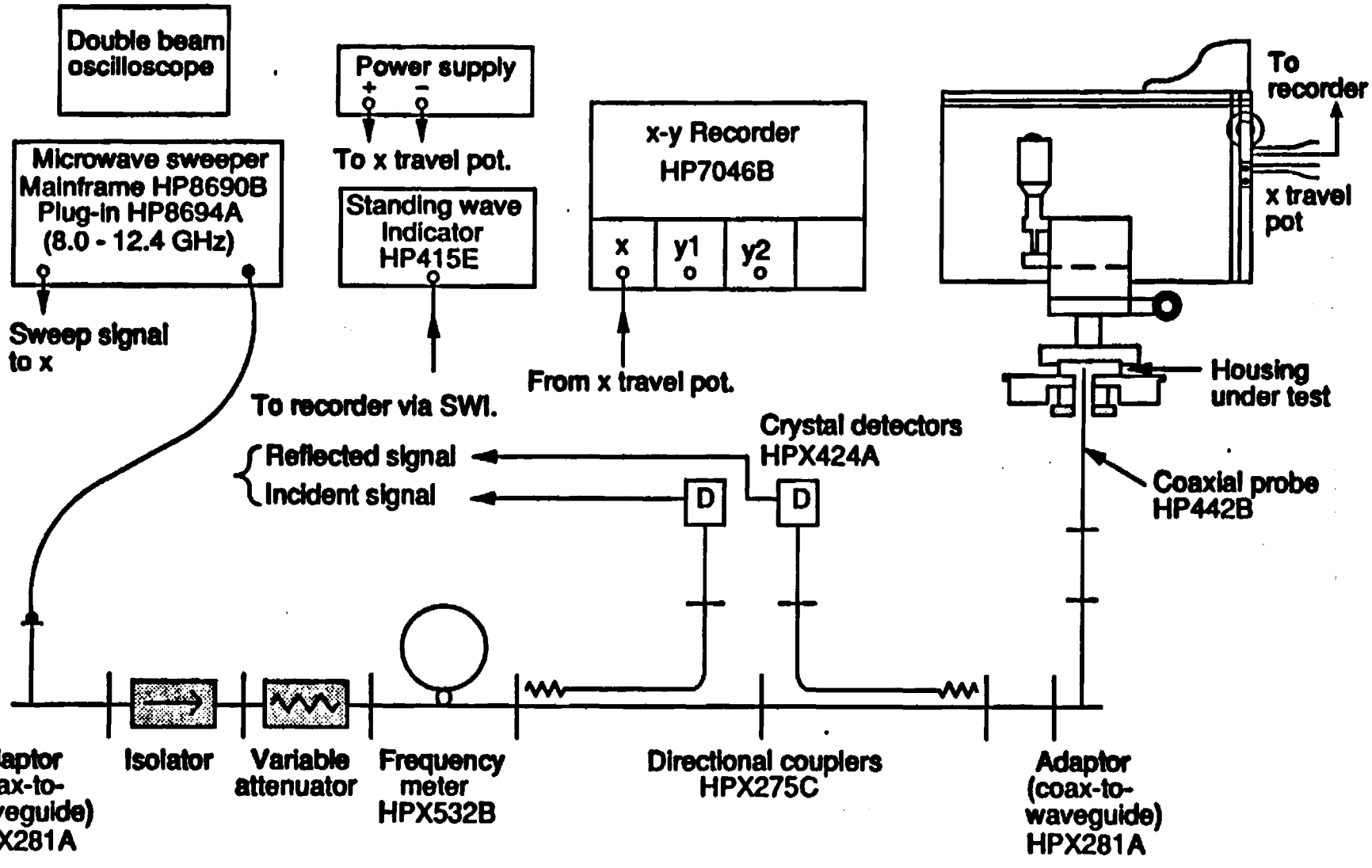

Figure 3(c) Schematic of the assembly used for measuring electric field distributions associated with resonances inside microwave module housings and packages.

adjusted to maximise the power absorbed by the cavity at resonance. This means that the reflected power will have a small value compared with the incident power at resonance, provided the position of the probe as well as the penetration are adjusted properly.

If the probe is positioned half-way along the cavity and the microwave signal source is swept over the frequency range 8.0 to 12.4 GHz then recordings of incident and reflected power like those shown in Figure 4(a) can be obtained. Markers on these recordings at 9.0 and 11.0 GHz can be set within the microwave source and appear as sharp reductions in both incident and reflected power at those frequencies. On the recording of reflected power three additional absorption lines appear and as explained above they correspond to cavity resonances in modes TE_{107}, TE_{109} and $TE_{10(11)}$. Probe penetration has been adjusted to give almost complete absorption of incident power. In fact it has been reduced slightly so that 10 percent or more of the incident power is reflected. The cavity resonances are then said to be undercoupled compared with conditions for total absorption which are referred to as critical coupling (reference [2], page 396).

The probe carriage Model HP809C, like most commercially available probe carriages, is not equipped to provide an output voltage proportional to probe displacement along the slotted waveguide section. Swept frequency recordings of incident and reflected power at 2 millimetre intervals as the probe is moved from the half-way position by a total of 30 millimetres are presented in Figures 4(a) through to 4(p). Only the position of the probe is altered and as a result the incident power recording obtained from the incident power directional coupler and detector of Figure 3(c) is the same in all of the Figures 4(a) through to 4(p). Figure 3(b) clearly illustrates that movement of the probe away from the half-way position leads to a slight decrease in the field at the probe for the odd numbered resonances and therefore a decrease in the coupling to the source. This in turn leads to less power absorption and more reflection. The effect is barely perceptible with 2 millimetres displacement but is quite evident after 4 millimetres. At the same time the electric field at the probe for the even numbered resonances becomes finite and increases as displacement increases. The recording of the reflected power

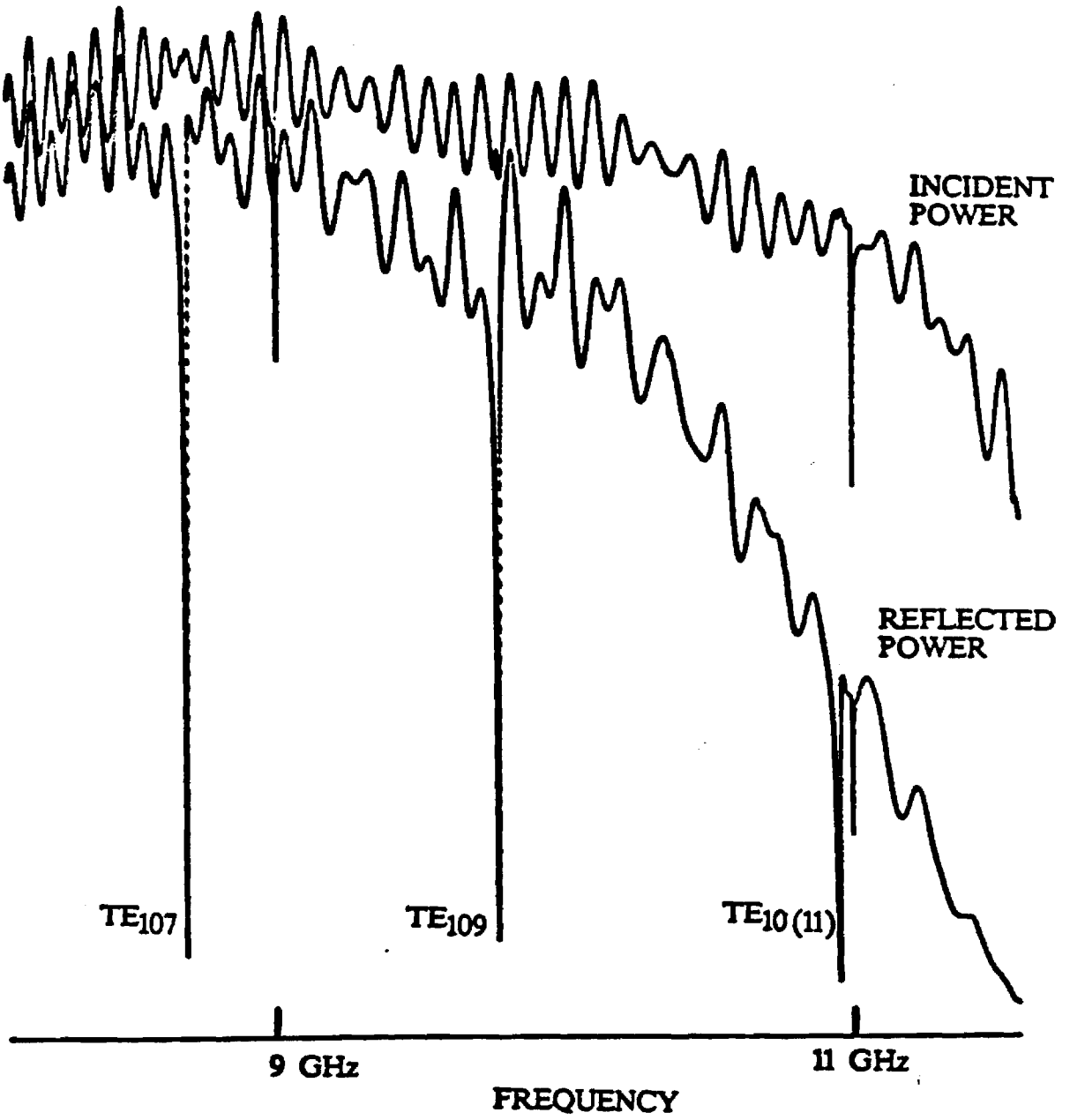

Figure 4(a). Coupling probe position 0.00 cms (mid-way along cavity). The effect of the probe position on incident and reflected power as a function of frequency for a long rectangular cavity resonator 0.900 x 0.400 x 7.297 inches (18.53cms). Frequency markers at 9.000 and 11.000 GHz.

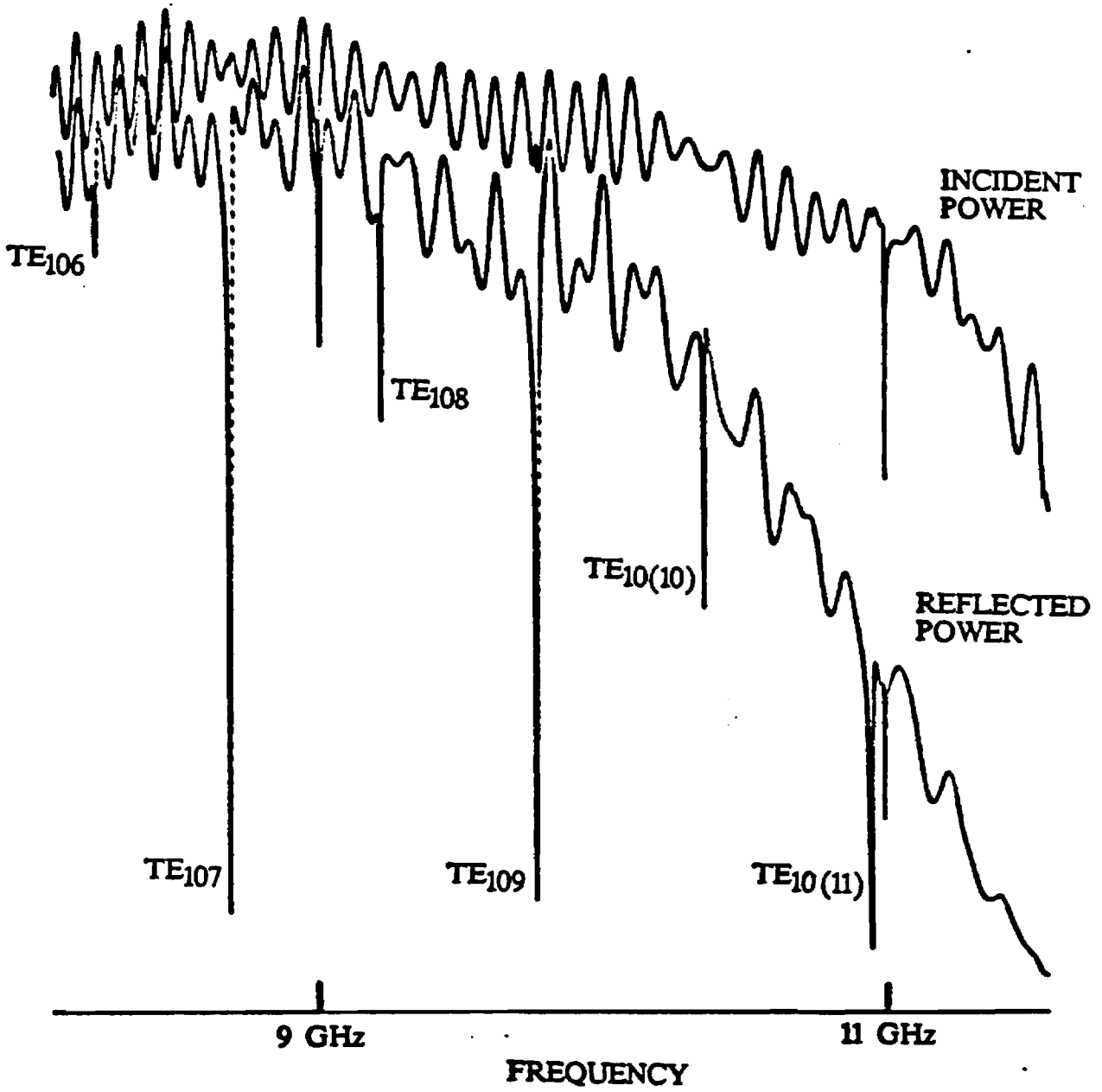

Figure 4(b). Coupling probe position 0.20 cms.

The effect of the probe position on incident and reflected power as a function of frequency for a long rectangular cavity resonator 0.900 x 0.400 x 7.297 inches (18.53cms).
Frequency markers at 9.000 and 11.000 GHz.

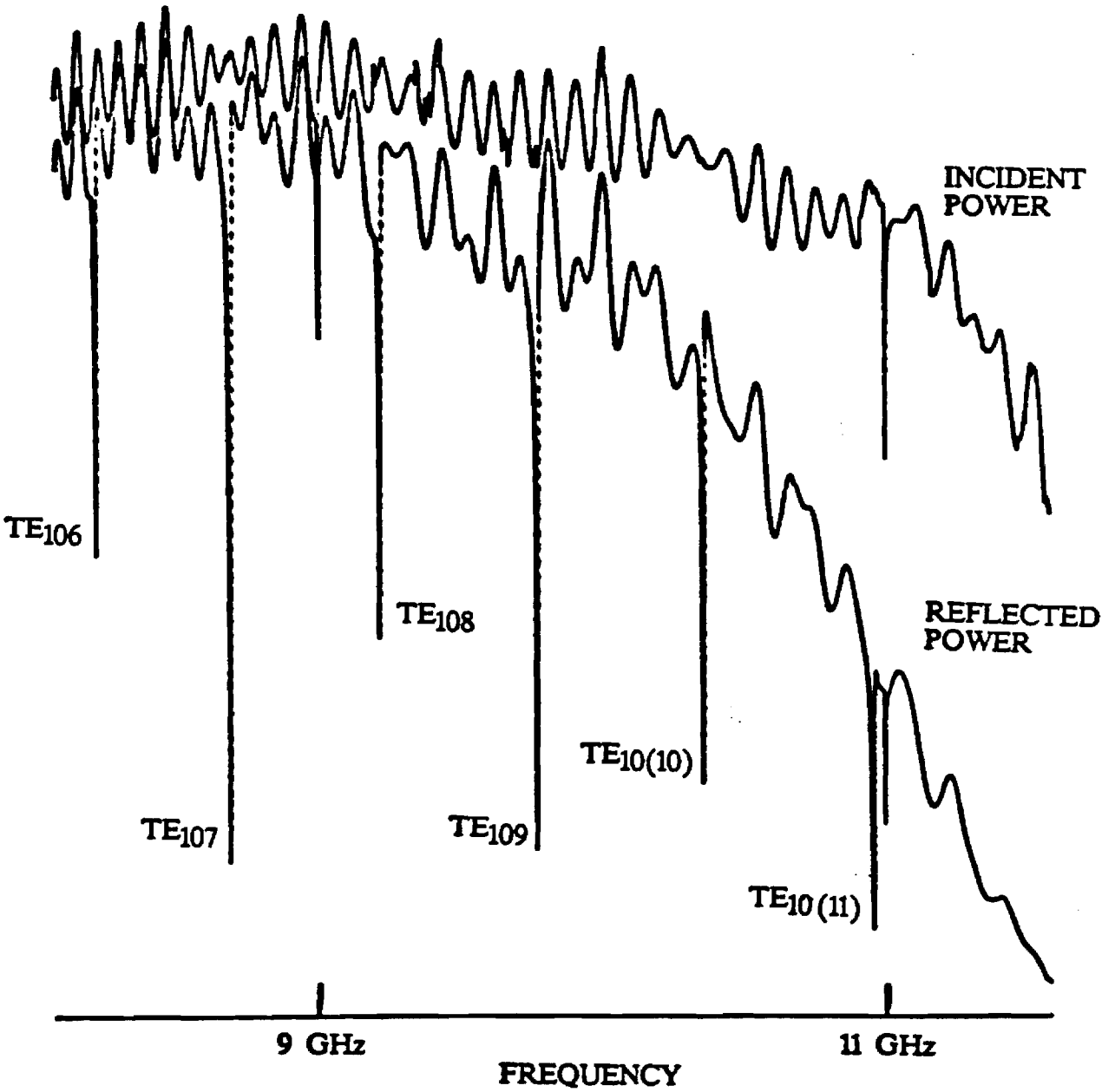

Figure 4(c). Coupling probe position 0.40 cms.

The effect of the probe position on incident and reflected power as a function of frequency for a long rectangular cavity resonator 0.900 x 0.400 x 7.297 inches (18.53cms).
Frequency markers at 9.000 and 11.000 GHz.

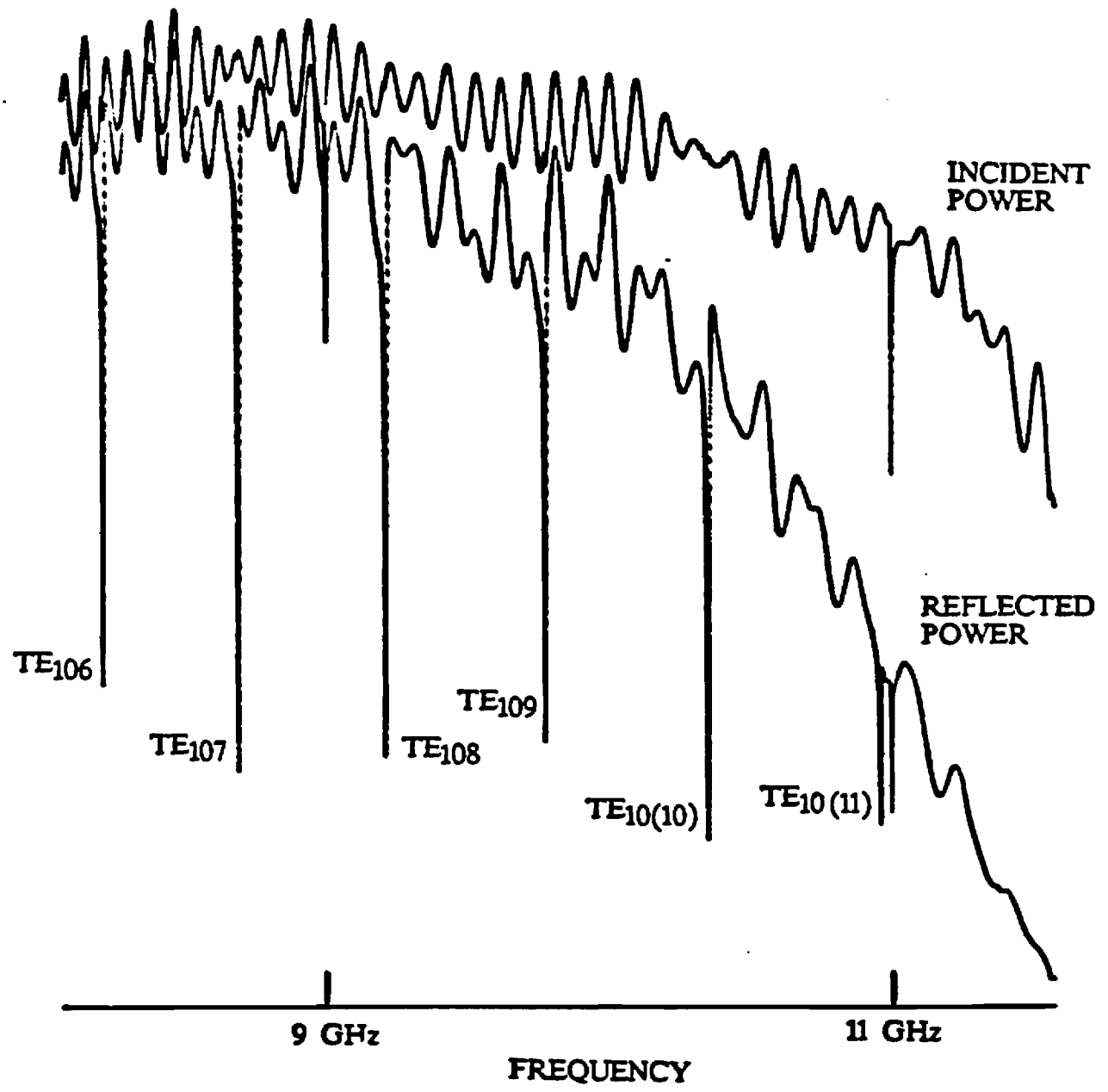

Figure 4(d). Coupling probe position 0.60 cms.
The effect of the probe position on incident and reflected power as a function of frequency for a long rectangular cavity resonator 0.900 x 0.400 x 7.297 inches (18.53cms).
Frequency markers at 9.000 and 11.000 GHz.

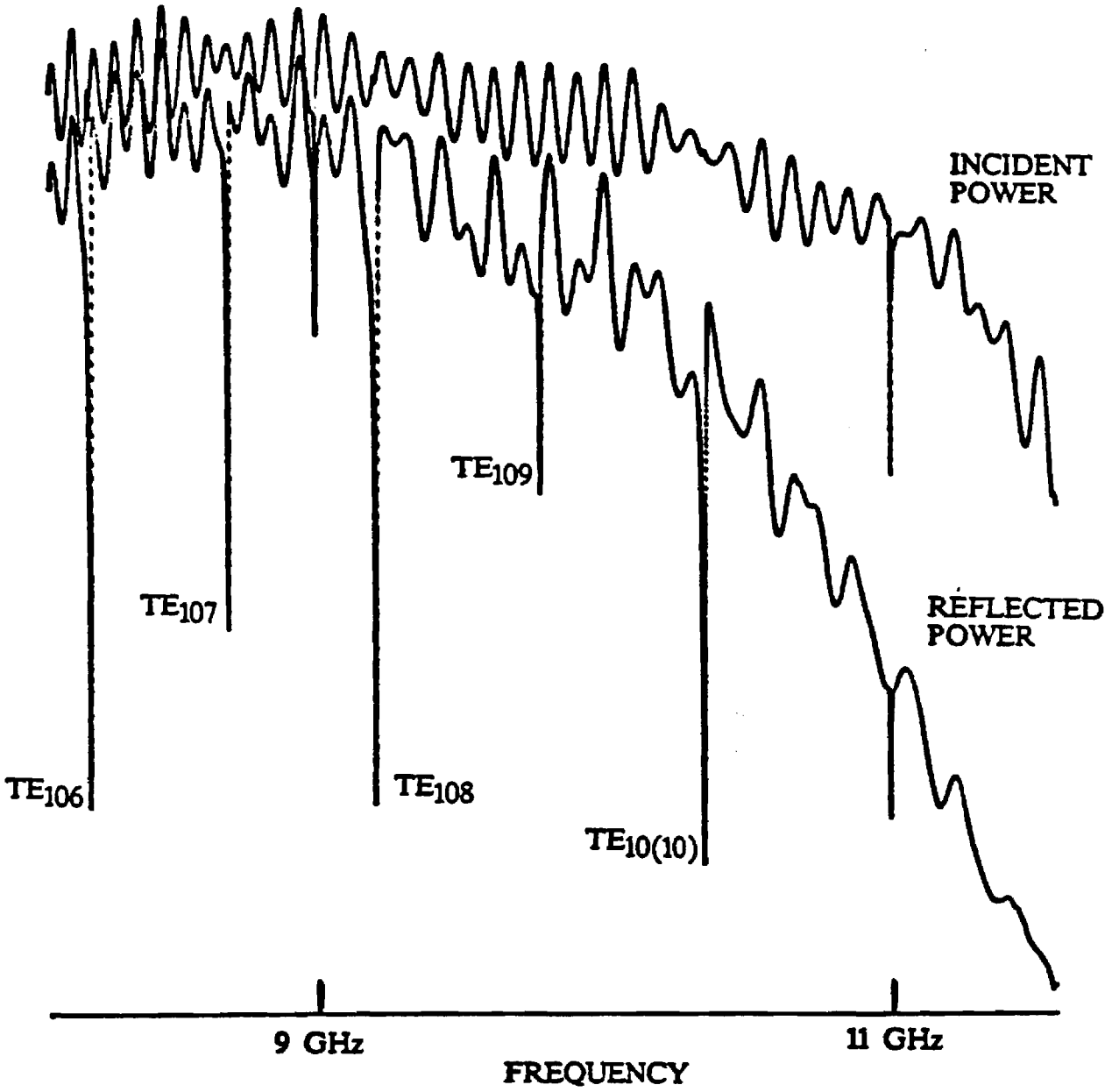

Figure 4(e). Coupling probe position 0.80 cms.
The effect of the probe position on incident and reflected power as a function of frequency for a long rectangular cavity resonator 0.900 x 0.400 x 7.297 inches (18.53cms).
Frequency markers at 9.000 and 11.000 GHz.

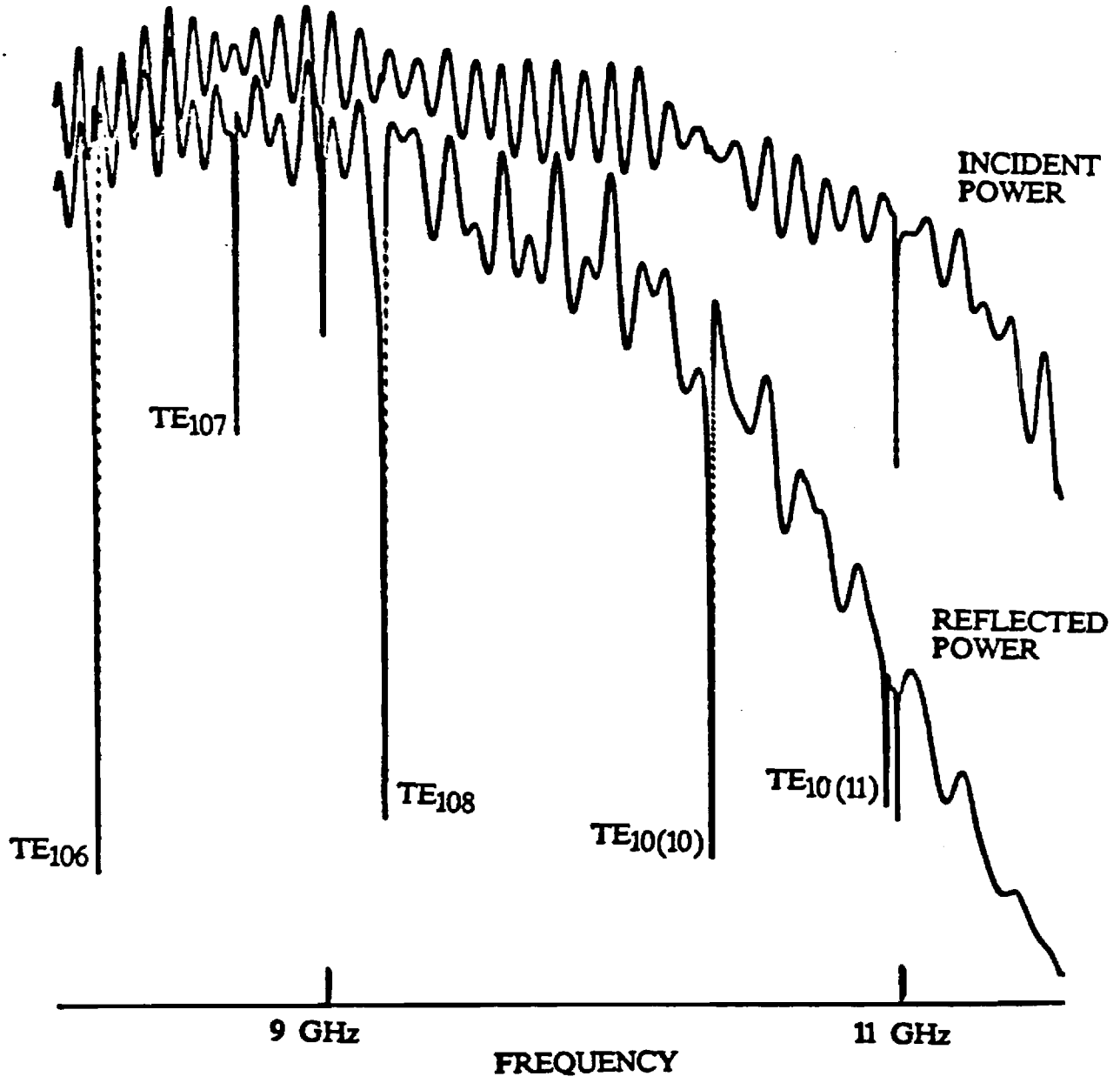

Figure 4(f). Coupling probe position 1.00 cms.
The effect of the probe position on incident and reflected power as a function of frequency for a long rectangular cavity resonator 0.900 x 0.400 x 7.297 inches (18.53cms).
Frequency markers at 9.000 and 11.000 GHz.

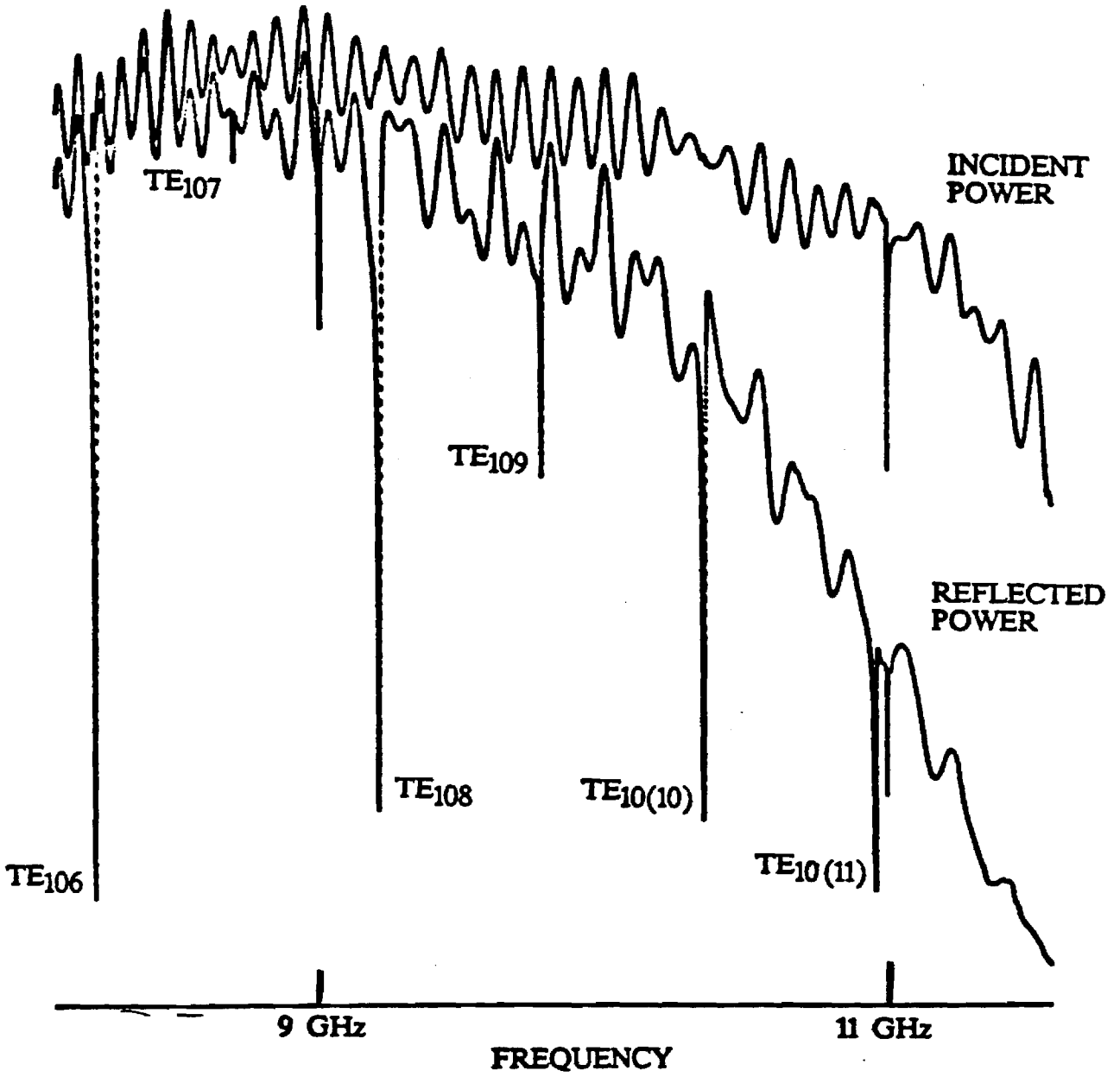

Figure 4(g). Coupling probe position 1.20 cms.
The effect of the probe position on incident and reflected power as a function of frequency for a long rectangular cavity resonator 0.900 x 0.400 x 7.297 inches (18.53cms).
Frequency markers at 9.000 and 11.000 GHz.

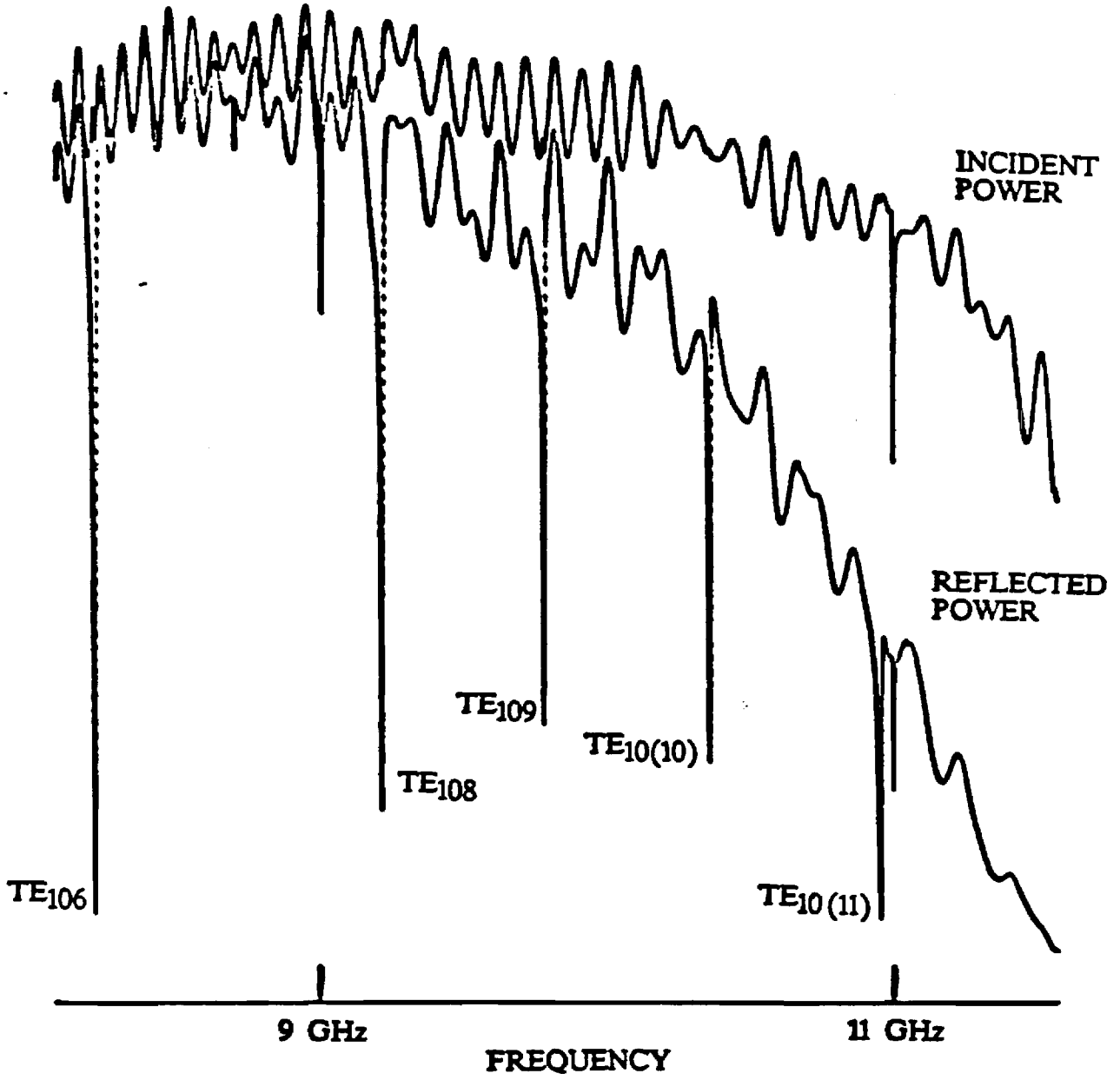

Figure 4(h). Coupling probe position 1.40 cms.
The effect of the probe position on incident and reflected power as a function of frequency for a long rectangular cavity resonator 0.900 x 0.400 x 7.297 inches (18.53cms).
Frequency markers at 9.000 and 11.000 GHz.

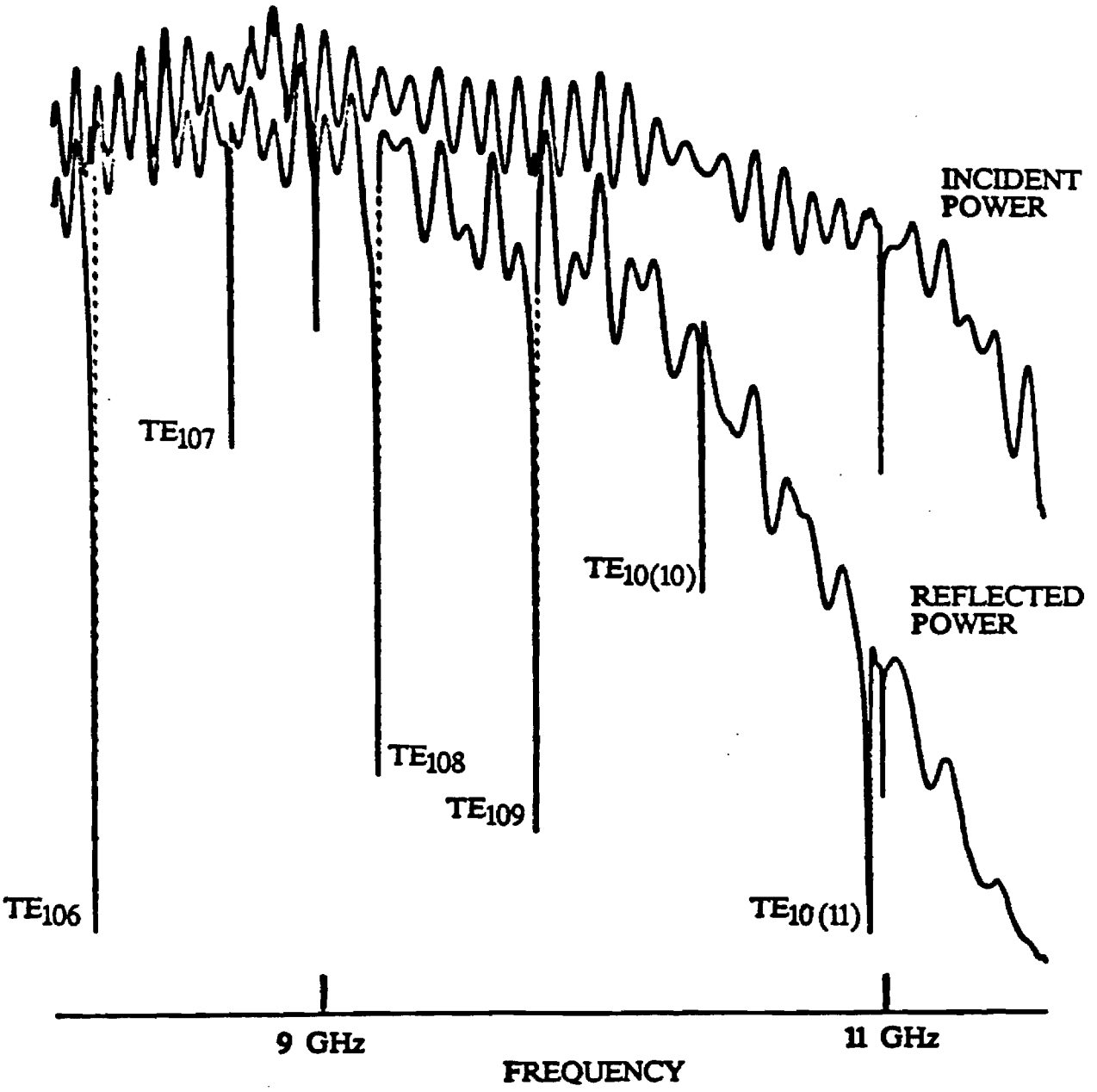

Figure 4(i). Coupling probe position 1.60 cms.
The effect of the probe position on incident and reflected power as a function of frequency for a long rectangular cavity resonator 0.900 x 0.400 x 7.297 inches (18.53cms).
Frequency markers at 9.000 and 11.000 GHz.

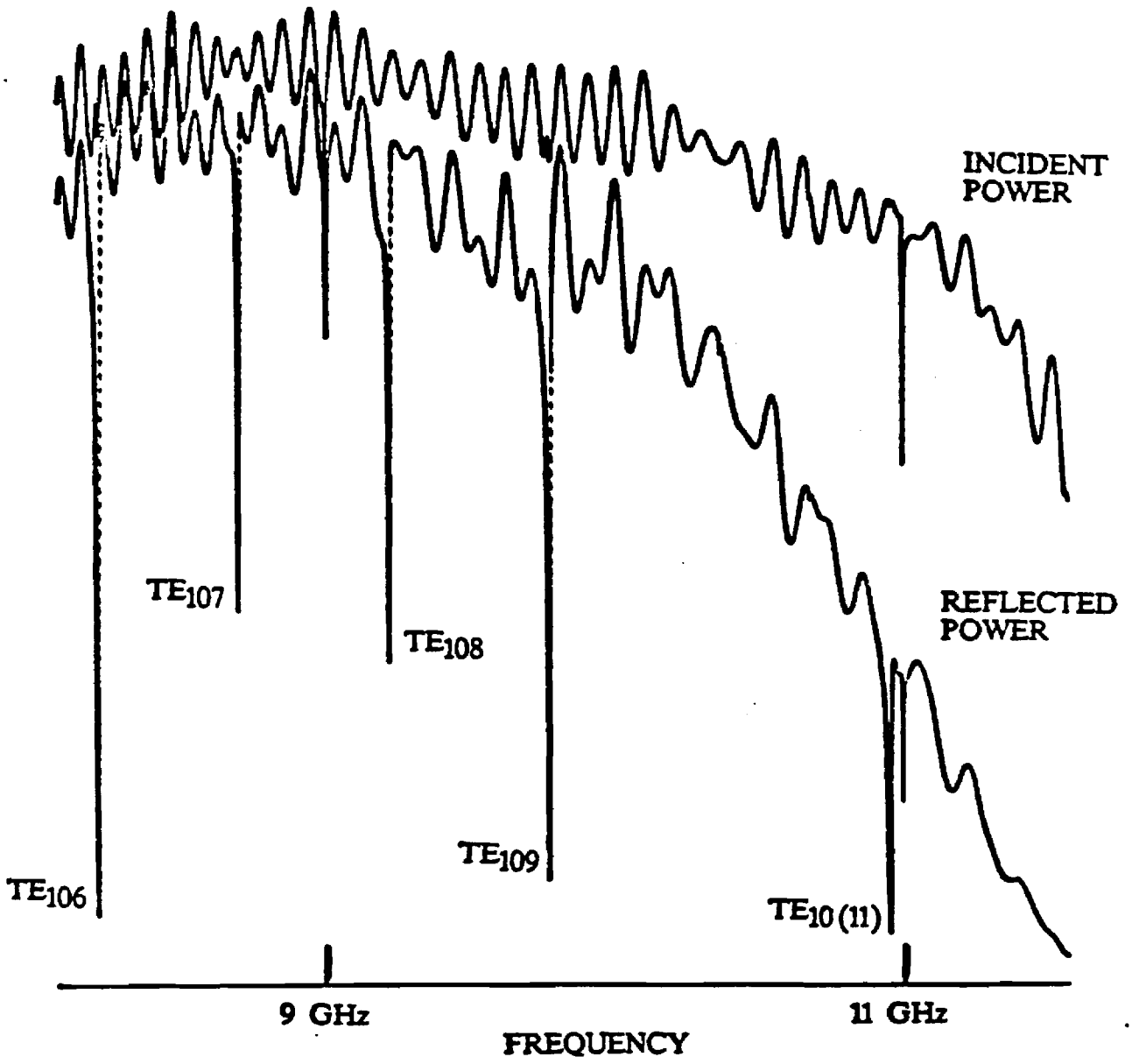

Figure 4(j). Coupling probe position 1.80 cms.
The effect of the probe position on incident and reflected power as a function of frequency for a long rectangular cavity resonator 0.900 x 0.400 x 7.297 inches (18.53cms).
Frequency markers at 9.000 and 11.000 GHz.

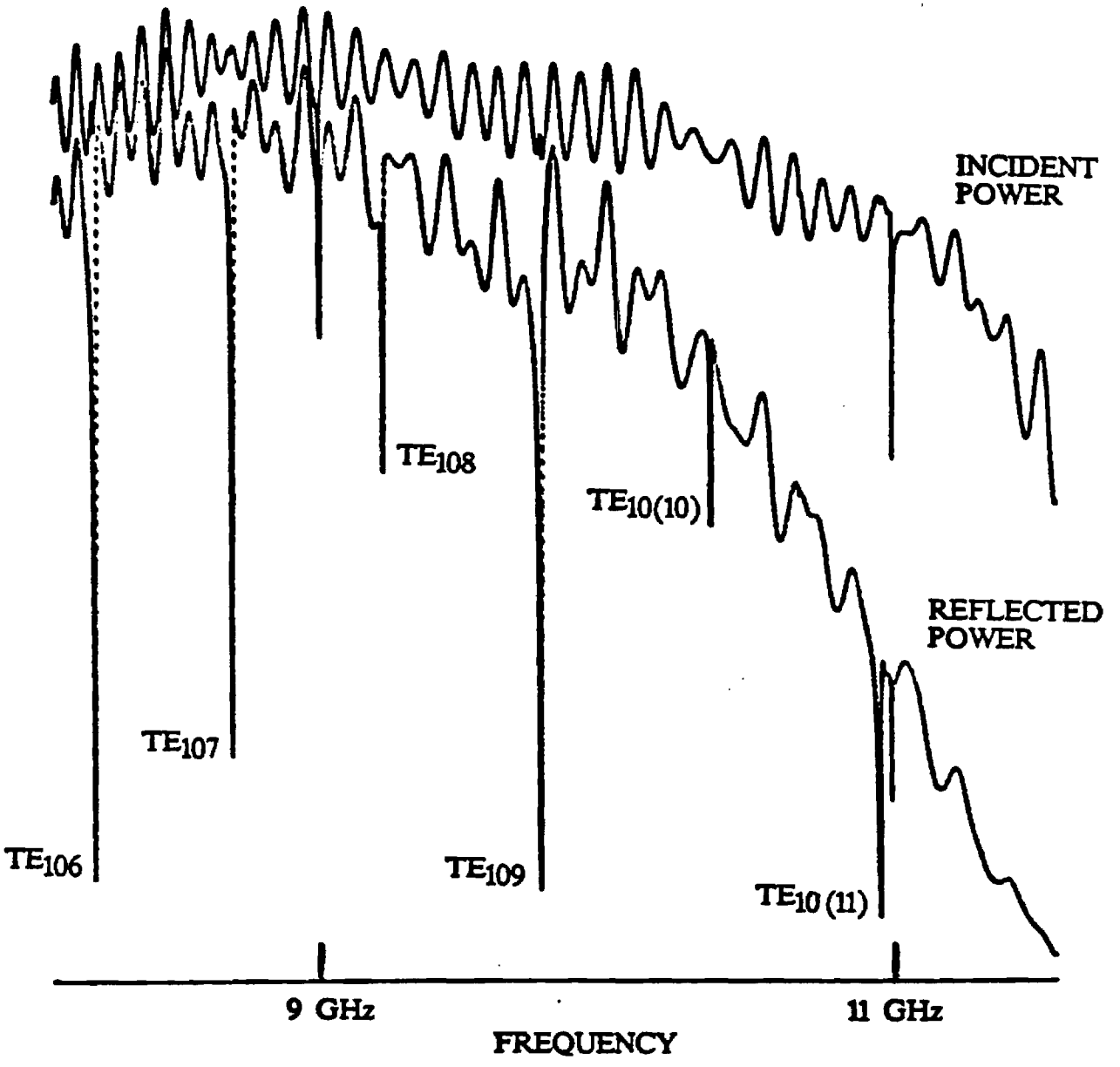

Figure 4(k). Coupling probe position 2.00 cms.
The effect of the probe position on incident and reflected power as a function of frequency for a long rectangular cavity resonator 0.900 x 0.400 x 7.297 inches (18.53cms).
Frequency markers at 9.000 and 11.000 GHz.

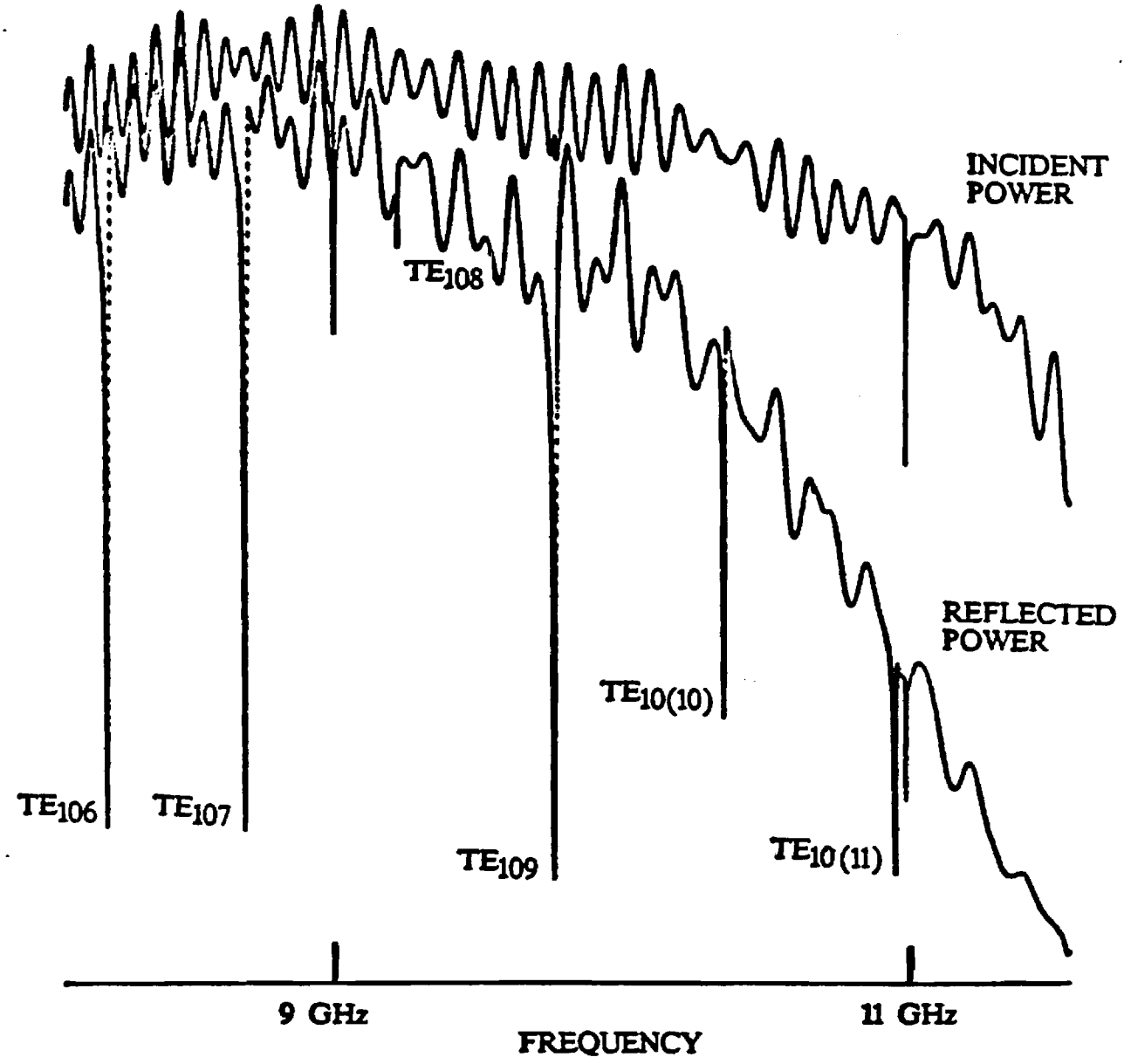

Figure 4(1). Coupling probe position 2.20 cms.
The effect of the probe position on incident and reflected power as a function of frequency for a long rectangular cavity resonator 0.900 x 0.400 x 7.297 inches (18.53cms).
Frequency markers at 9.000 and 11.000 GHz.

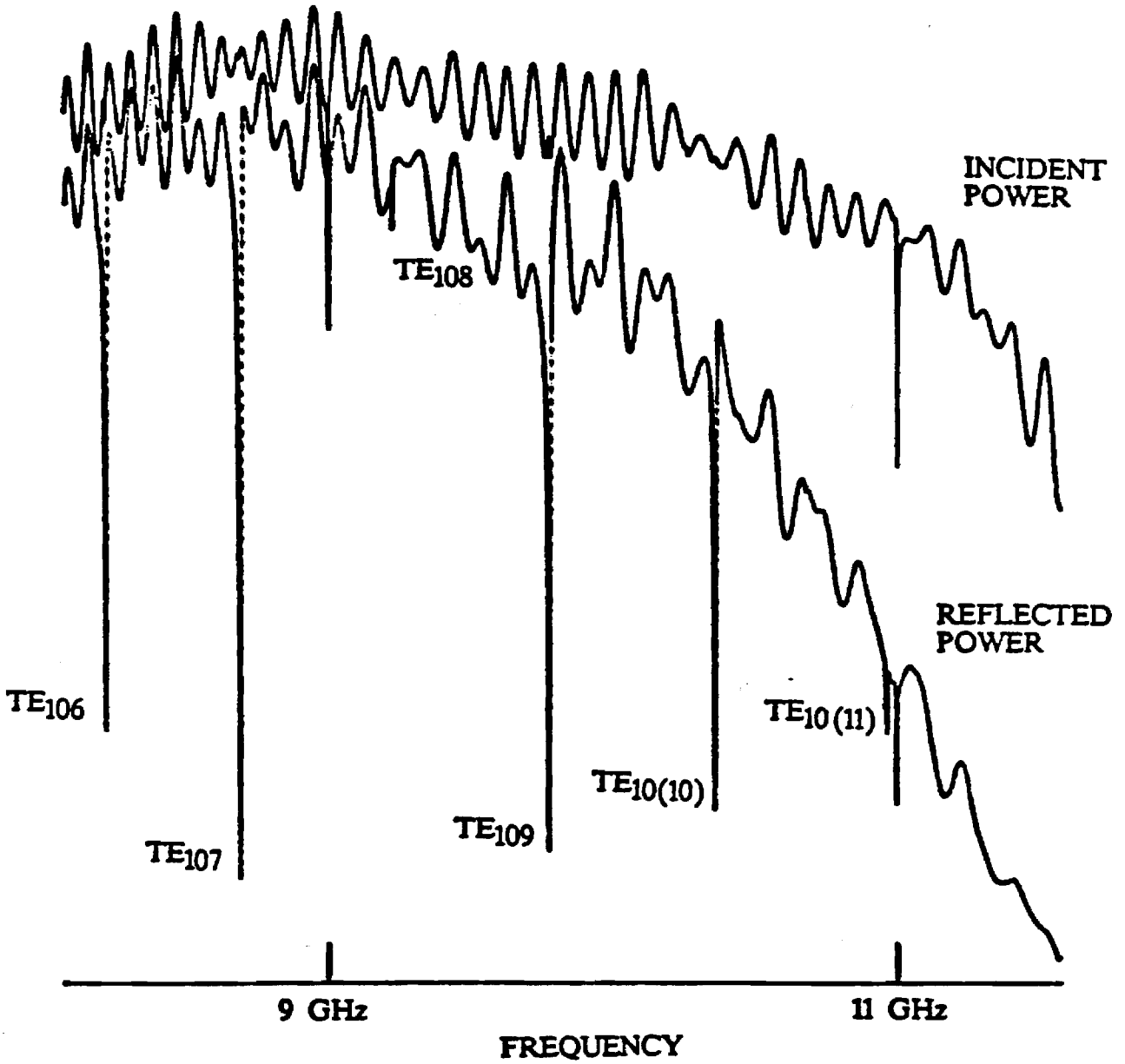

Figure 4(m). Coupling probe position 2.40 cms.
The effect of the probe position on incident and reflected power as a function of frequency for a long rectangular cavity resonator 0.900 x 0.400 x 7.297 inches (18.53cms).
Frequency markers at 9.000 and 11.000 GHz.

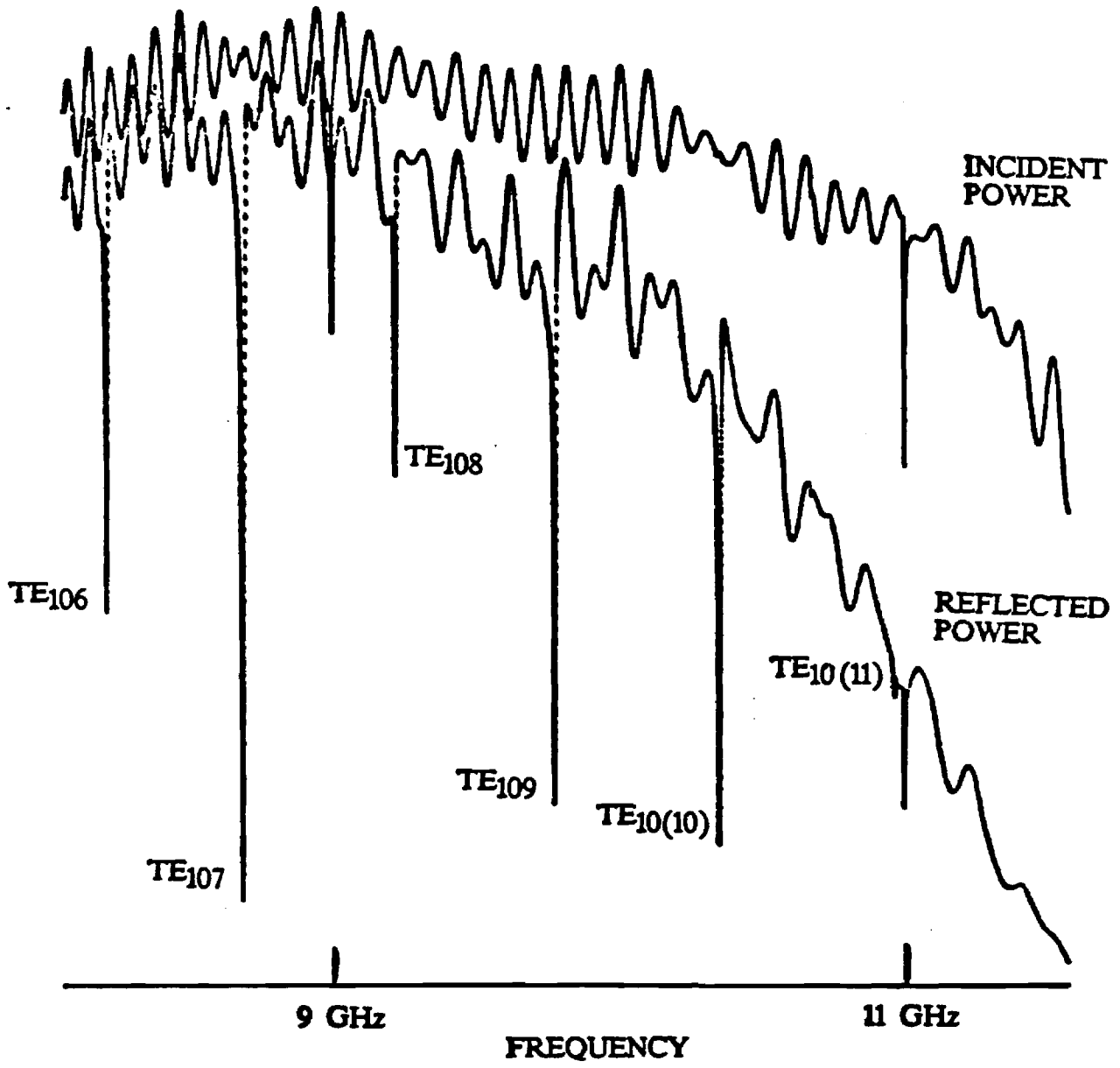

Figure 4(n). Coupling probe position 2.60 cms.
The effect of the probe position on incident and reflected power as a function of frequency for a long rectangular cavity resonator 0.900 x 0.400 x 7.297 inches (18.53cms).
Frequency markers at 9.000 and 11.000 GHz.

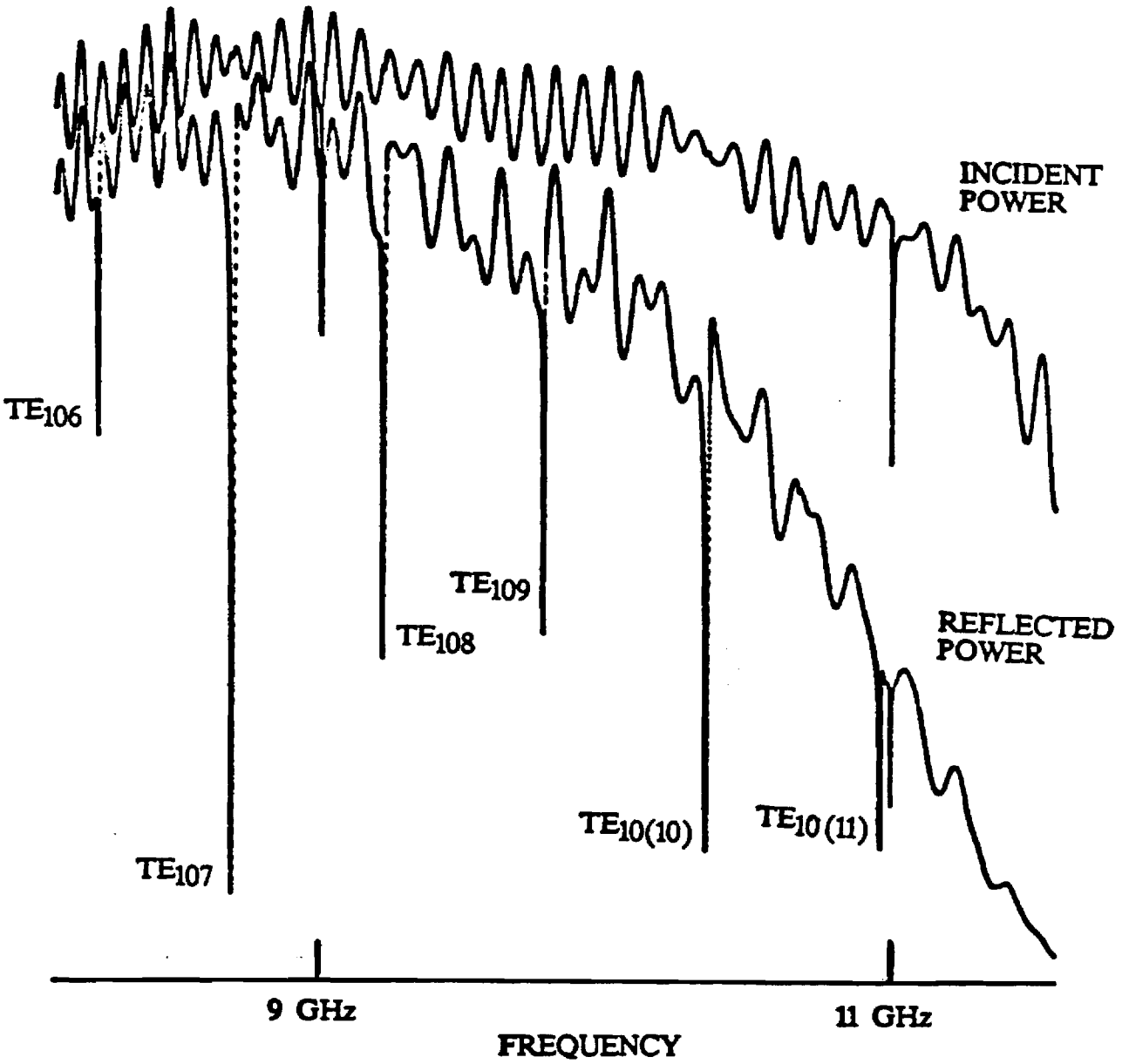

Figure 4(o). Coupling probe position 2.80 cms.
The effect of the probe position on incident and reflected power as a function of frequency for a long rectangular cavity resonator 0.900 x 0.400 x 7.297 inches (18.53cms).
Frequency markers at 9.000 and 11.000 GHz.

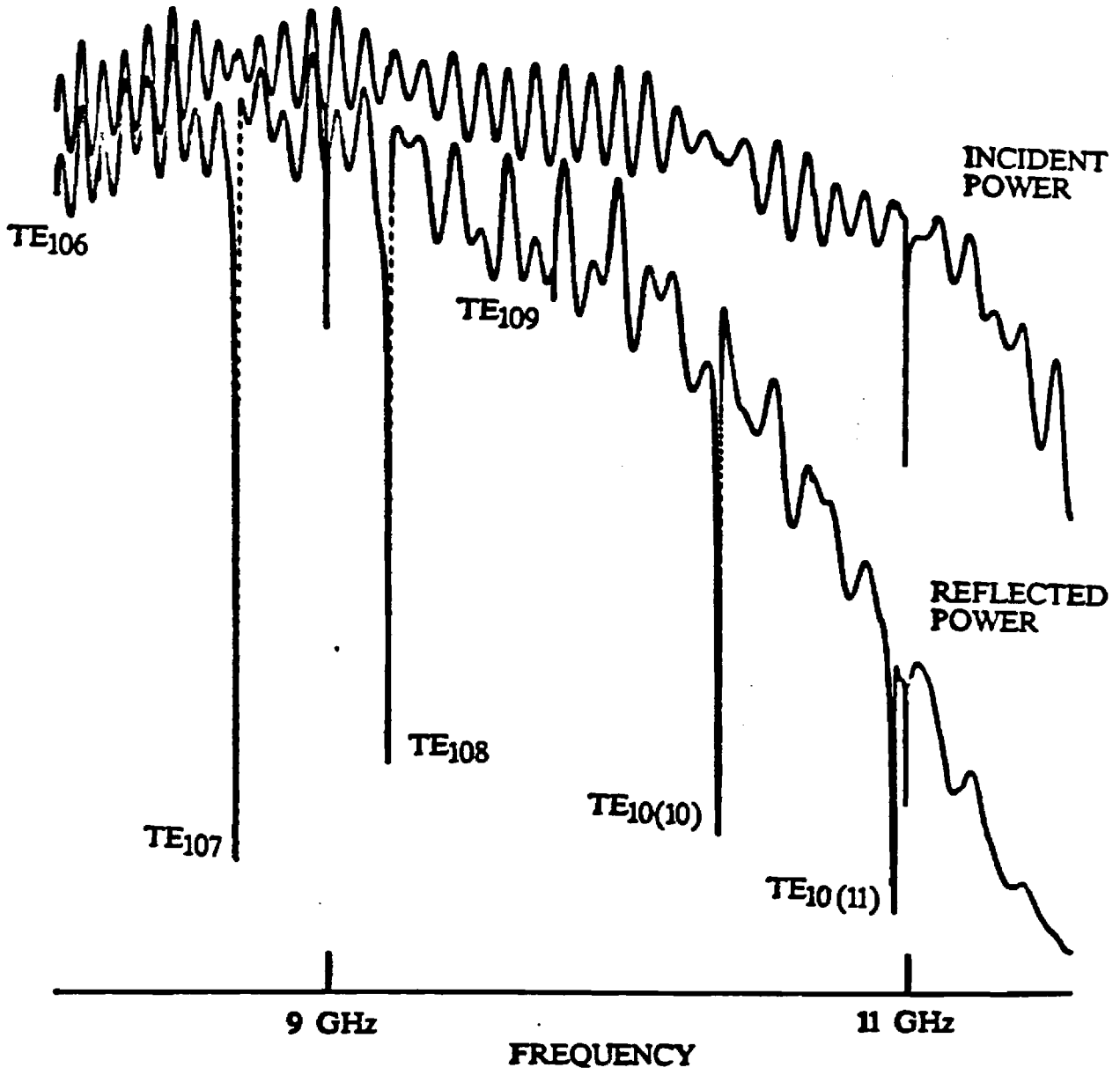

Figure 4(p). Coupling probe position 3.00 cms.
The effect of the probe position on incident and reflected power as a function of frequency for a long rectangular cavity resonator 0.900 x 0.400 x 7.297 inches (18.53cms).
Frequency markers at 9.000 and 11.000 GHz.

in Figure 4(b) exhibits three additional absorption dips corresponding to cavity resonances in modes TE_{106}, TE_{108} and $TE_{10(10)}$.

As displacement is increased it is clear from Figure 3(c) that the absorption due to the $TE_{10(11)}$ resonance will be the first of the odd numbered modes to disappear and this occurs at a displacement of about 8 millimetres. The same effect occurs for the TE_{109} resonance at a displacement of about 10 millimetres and in between these two positions the coupling to the $TE_{10(10)}$ resonance passes through a maximum indicated by a minimum in the reflection.

By concentrating on any resonance and flipping through the sequence of recordings of reflected power, the maxima and minima of the electric field standing wave patterns of Figure 3(b) can be followed as minima and maxima of the reflected power. All of the features of all of the resonances are revealed in an orderly fashion and it is clear that an empirical law might be derived from such measurements that relates the field distribution to the measurable reflected power. (The top right-hand corners of pages 24 to 39 have been removed to identify the "flip section".)

The maxima and minima of the electric field distribution for each of the cavity resonances are revealed by reverse features, namely minima and maxima in the reflected power where the maxima are in fact the level of reflection without any incident power being absorbed by the resonance. By simply turning the recording upside down attention is focussed on the absorption associated with resonance as the height of the plotted response above, what is admittedly, a far from smooth curve that defines zero resonance absorption. As the probe is moved the maxima and zeroes of resonance absorption occur at the locations where the maxima and zeroes of the electric field sketched in Figure 3(b) occur. If an empirical law is to be derived then it would appear to be simpler and more direct to do so by relating measured resonance absorption to known relative electric field distributions. Rather than using recordings like those of Figures 4(a) to (p) with frequency as the x-axis variable, recordings at a fixed frequency with probe position along the slot in the top wall of the cavity as the independent variable are needed for deriving an empirical law or testing an

analytically derived relationship.

4.3 An equivalent circuit explanation of the new method of measuring the electric field distribution in a resonating cavity.

The measurement method, that can be demonstrated in the way described in section 4.2, can be explained in terms of the properties exhibited by equivalent circuits at all of the positions of the electric field probe in the resonating cavity. The importance of such an explanation at this stage of this report is that it reveals problems pertaining to the method of measurement, and the measuring apparatus, that must be solved if the method is to be successfully developed as a means of measuring electric field distributions over an area with a special purpose two-dimensional standing wave detector. The reality of the problems identified by studying equivalent circuit representations can be confirmed by re-examination of the measurements presented in Figures 4(a) to (p) together with additional results obtained with the same apparatus.

A schematic of the resonating cavity is shown in Figure 5(a). It is assumed to be a waveguide of uniform cross-section terminated with short circuits at S_L to the left and S_R to the right which are an integral number of half-wavelengths apart along the axis of the waveguide. A single half-wavelength long part of the cavity is shown in detail extending just beyond cross-sectional planes at AA' and EE'. Figure 5(b) shows schematically the amplitude distribution of transverse components of electric (E) and magnetic (H) field intensity which are assumed to be parts of the sinusoidal standing wave patterns that extend throughout the cavity from S_L to S_R. Transverse reference plane AA' is to the right of a null in the E-field pattern, CC' is to the right of the maximum in that field and EE' is to the left of the next null. Reference planes BB' and DD' are chosen between nulls and the maximum.

If the electric field probe is successively positioned along a line parallel to the axis of the cavity at A, B, C, D and E then the effect in equivalent circuit terms is to connect an excitation source and an impedance across the line at each position in turn. The shunt impedance can be represented by a parallel combination of capacitance, C_p, and resistance,

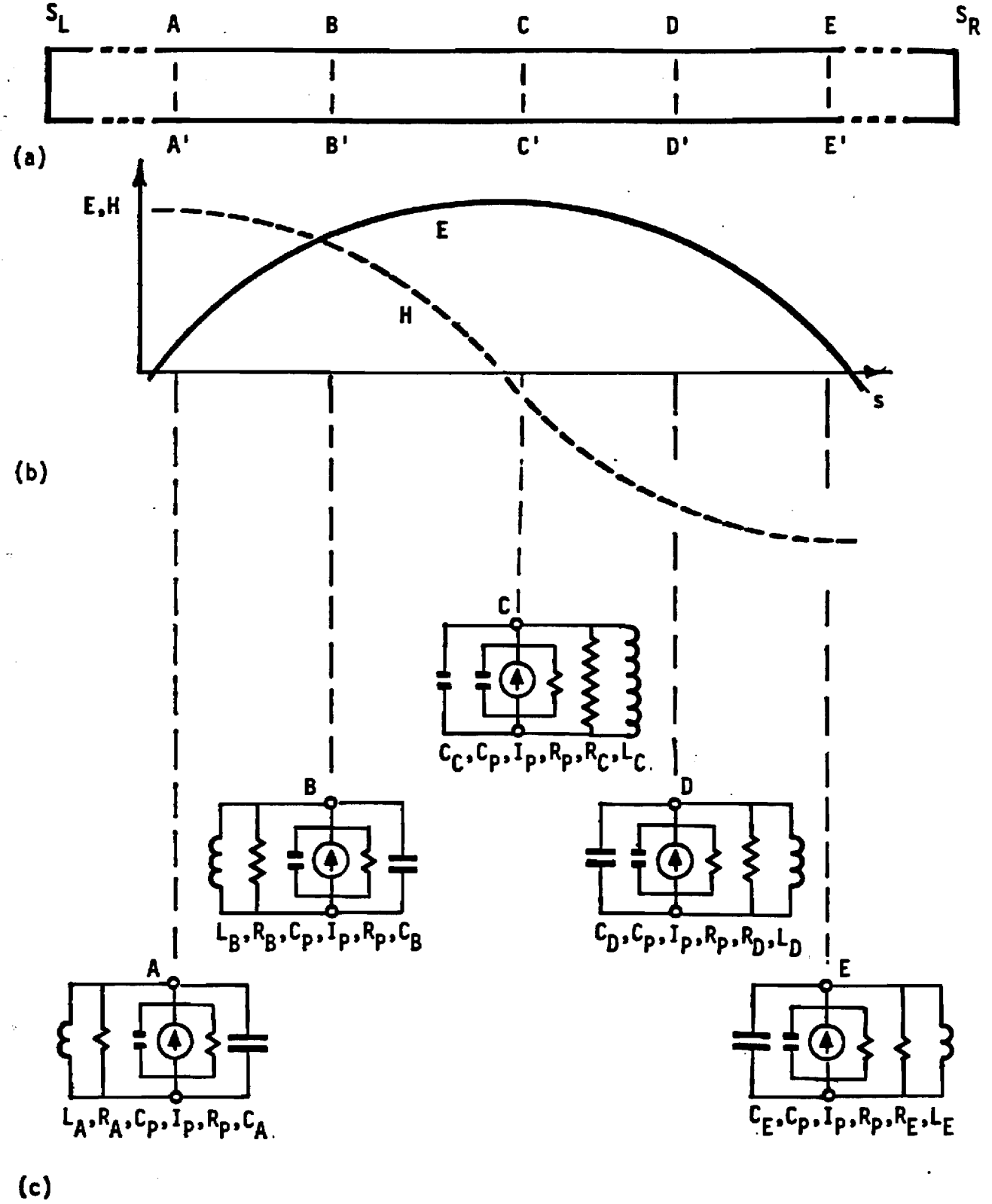

Figure 5 Equivalent circuits at various probe positions in the E-field standing wave pattern of a rectangular cavity resonator.

R_p, (reference [1] page 484 and reference [2] page 243) where C_p is related to the capacitance between the probe tip and the far wall of the waveguide and R_p is related to the extent to which the resistive load connected to the coaxial line that leads signals to and from the probe is coupled across the cavity and therefore contributes to the total power loss in the cavity. The components C_p and R_p depend upon the geometry of the probe that extends into the cavity and the coaxial connection to it and they are independent of the position along the axis. It is clear that the probe does have an effect on the electric field intensity to be measured. Thus the true field distribution will not be obtained directly from readings made via the probe. The direct recordings of reflected power in Figures 4(a) to (p) can be regarded as distorted versions of the true relative electric field at the various resonant frequencies and probe positions. It is an analytical task to determine the true relative electric field distribution from the measurements by using correct equivalent circuits for the conditions of measurement. The excitation source introduced by the probe is shown as an equivalent current generator I_p in the cavity in parallel with C_p and R_p. An excitation voltage will develop across the cavity at the position of the probe according to what total impedance is presented to this current generator by the probe and cavity. The components C_p and R_p and the current generator I_p are independent of the probe position in the cavity and therefore form part of each equivalent circuit drawn at positions A, B, C, D and E.

The resonating cavity can be represented at each of these positions by a parallel combination of resistance R_x, inductance L_x and capacitance C_x where x refer to the position along the cavity such as A, B, C, D or E. At the position A the length of guide from the short circuit at S_L to A is slightly more than an integral number of half-wavelengths and therefore presents a normalised impedance,

$$z_L = j\tan\beta\Delta s = jw_oL_A \qquad (1)$$

where β is the phase constant for propagation in the waveguide

Δs is the distance from A to the nearest null in electric field to the left of A, and,

w_o is the resonant frequency in radians per second.

The length of waveguide to the right of A is slightly shorter than an integral number of half-wavelengths and presents a normalised impedance given by,

$$z_R = -j\tan\beta\Delta s = 1/jw_oC_A \qquad (2)$$

Expressions (1) and (2) are obtained simply from the expression for the normalised input impedance of a length, l, of lossless equivalent transmission line terminated in a load impedance Z_R, namely,

$$Z_{IN}/Z_0 = \frac{Z_R/Z_0 + j\tan\beta l}{1 + j(Z_R\tan\beta l)/Z_0} \qquad (3)$$

by substituting $Z_R = 0$ and $l = n\lambda_g/2 \pm \Delta s$. Losses in the cavity arise from the finite resistance of the walls and are therefore distributed over all internal wall surfaces. This can be taken into account by replacing (3) by a more general formula but the result is that at a position such as A along the cavity the equivalent circuit must include the resistance R_A to account for the losses inside the resonator. These losses can be regarded as giving rise to an unloaded quality factor Q_U for the resonance under consideration such that,

$$Q_U = R_A/w_oL_A \quad \text{at position A} \qquad (4)$$

For any particular resonance in the cavity the unloaded quality factor is a constant and therefore it must be the same for all equivalent circuits irrespective of reference plane position along the cavity. In the case of positions B, C, D and E the distances to the short circuits at S_L and S_R are different and when equation (3) is used to yield equations equivalent to (1) and (2), the inductance and capacitance values will be different. In fact L_B will be greater than L_A, C_B and will be smaller than C_A and R_B will be greater than R_A in keeping with,

$$Q_U = R_A/w_oL_A = R_B/w_oL_B \qquad (5)$$

Further to the right, if C is chosen just past the position of maximum resonant electric field, the guide to the left terminated in short circuit S_L will present a capacitive impedance shown as C_C whereas the guide to the

right terminated in S_R will present an inductive impedance denoted by L_C. The factor $\tan\beta l$ in each case will have a large value and from equation (1) the value of L_C will be relatively large and from (2) the value of C_C will be relatively small. As well as the unloaded quality factor being invariant with position, the resonant frequency with no probe present is also invariant and therefore for all positions A, B, C, D and E,

$$Q_U = R_A/w_oL_A = R_B/w_oL_B = R_C/w_oL_C = R_D/w_oL_D = R_E/w_oL_E \text{ , and} \quad (6)$$

$$1/w_o^2 = L_AC_A = L_BC_B = L_CC_C = L_DC_D = L_EC_E \quad (7)$$

In Figure 5(c) the relative magnitudes of the equivalent inductances, capacitances and resistances representing internal losses are indicated by the size of the symbol used. Near the electric field maximum the inductance L_C is large and its reactance approaches an open circuit. Also the capacitance C_C is small and its reactance approaches an open circuit. At the other extreme near electric field nulls the inductances L_A and L_E are small, capacitances C_A and C_E are large and all of these shunt reactances approach a short circuit condition.

Several effects that are important from the point of view of exploiting the assembly to measure electric field distributions are evident from the complete equivalent circuits of Figure 5(c).

(a) The loaded quality factor, Q_L, of the cavity at resonance depends upon the position of the probe. When the probe is near a minimum in the electric field distribution the value of Q_L approaches that of Q_U because R_p is large compared with R_A or R_E. Thus,

$$Q_{L(A)} = \frac{R_A R_p}{(R_A + R_p)wL_A} = Q_U \left[\frac{1}{1 + R_A/R_p} \right] \rightarrow Q_U \text{ as } R_A/R_p \rightarrow 0. \quad (8)$$

(b) The loaded quality factor can be set to a value of $Q_U/2$ if the probe penetration is adjusted until $R_p = R_{max}$ where R_{max} is the shunt resistance that represents internal cavity losses at the maximum electric field position near reference position C. If the probe is adjusted for this condition then the loaded quality factor will vary between the

limits $Q_U/2$ and Q_U as the probe is moved from a maximum near C to a zero electric field position, near A or E.

(c) If the probe is attached to a flat plate that forms the top wall of the cavity as explained in section 4.1, then as the plate is moved to reposition the probe the internal losses in the cavity must not change. If they do then instead of values R_A, R_B, R_C, R_D and R_E corresponding to constant internal losses, variations in those losses will give rise to different, unpredictable values of internal loss resistances in the equivalent circuit. These in turn will lead to measurable quantities from which correct relative field distributions are not obtainable.

(d) The fixed capacitance C_p associated with the probe detunes the cavity from the frequency ω_o at which resonance occurs with the probe absent. At positions A and E close to electric field zeroes, detuning is negligible because C_p is small compared with C_A or C_E. At position C, near a maximum in the electric field, C_C is small and so the detuning effect of C_p will be near its maximum.

The first two effects, (a) and (b), are relevant to the development of a procedure to be followed in making measurements and interpreting them. The third effect, (c), is a problem that must be solved in the design of the apparatus. The fourth effect, (d), must either be taken into account in developing an analytical procedure for interpreting measurements or eliminated by electronically adjusting the test frquency to the resonant frequency of the cavity as the probe is moved through the range of positions from A through to E in this example.

4.4 Demonstration of the relevance of probe coupling to the measurement method.

The effect of probe coupling on the resonant frequency and the loaded quality factor of any resonant mode that is energised by slowly sweeping over a frequency range that includes it, is shown in the results of Figures 6(a) to (f). The probe is positioned half-way along the cavity and will be coupled to modes with 7, 9 and 11 half-wavelengths as explained in

section 4.2 and illustrated in Figure 3(b). The results shown in Figure 6(a) are for a small probe penetration which gives such an undercoupled condition that absorption at each resonance is barely perceptible. Figure 6(b) shows results for larger probe penetration that is still less than critical coupling while Figure 6(c) clearly shows almost complete absorption at each resonance corresponding to critical coupling. Close inspection reveals that the frequency range over which absorption occurs has tended to increase corresponding to a loaded quality factor that has ranged from a value close to the unloaded quality factor in Figure 6(a) to half that value in 6(c).

Increasing the probe coupling still further has the effects shown in Figures 6(d) and (e) where it is evident that the loaded quality factor has been reduced well below $Q_U/2$ by over-coupling. In Figure 6(e) the even numbered resonances are being excited which is probably caused by the probe not being positioned precisely half-way along the cavity where these modes have zero electric field in their distribution patterns.

The shift in resonant frequency caused by increasing the probe coupling is evident by examining the position of the mode near the 11GHz marker. Increasing the probe penetration increases the capacitance C_p which tunes the resonance to a lower frequency which is clearly seen by comparing Figures 6(a) and (e).

This mode of resonance has been recorded in greater detail by sweeping the frequency over a smaller range. The results for very small coupling, undercoupling and near critical coupling are shown in Figure 6(f).

It is clear that if power absorption is to be used as a means of measuring the relative distribution of the electric field then there is nothing to be gained and indeed a lot of unnecessary complication to be created if overcoupling exists between the cavity and the measurement assembly via the probe. This is because as the probe is moved to lower field regions the absorption will not fall until coupling has decreased below the critical level. Thus excessive probe penetration into the cavity is to be avoided.

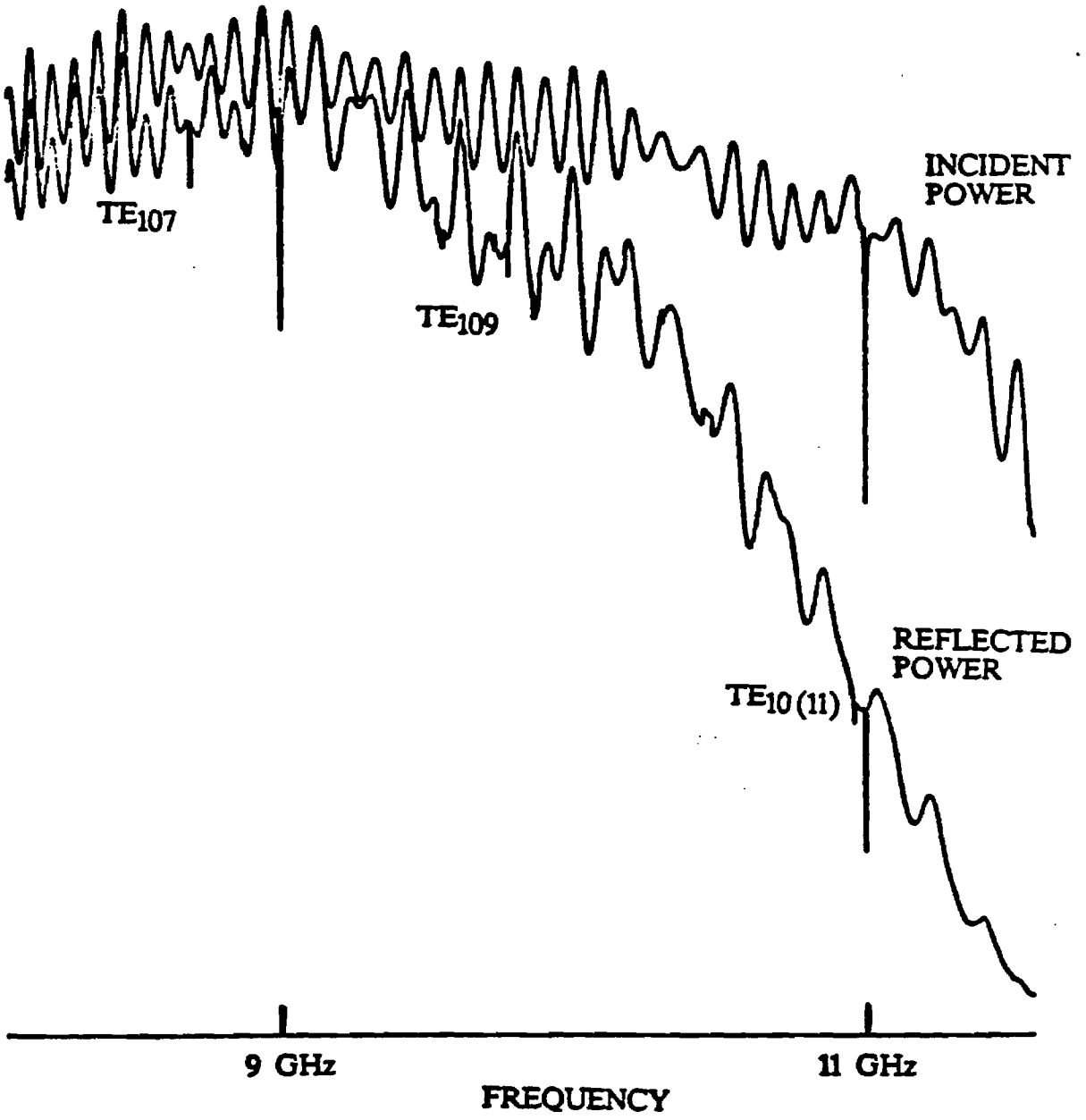

Figure 6(a) Very small coupling – negligible probe penetration at midpoint along the cavity.
The effect of probe coupling on the shape of resonant absorption lines and the frequencies at which maximum absorption occurs.

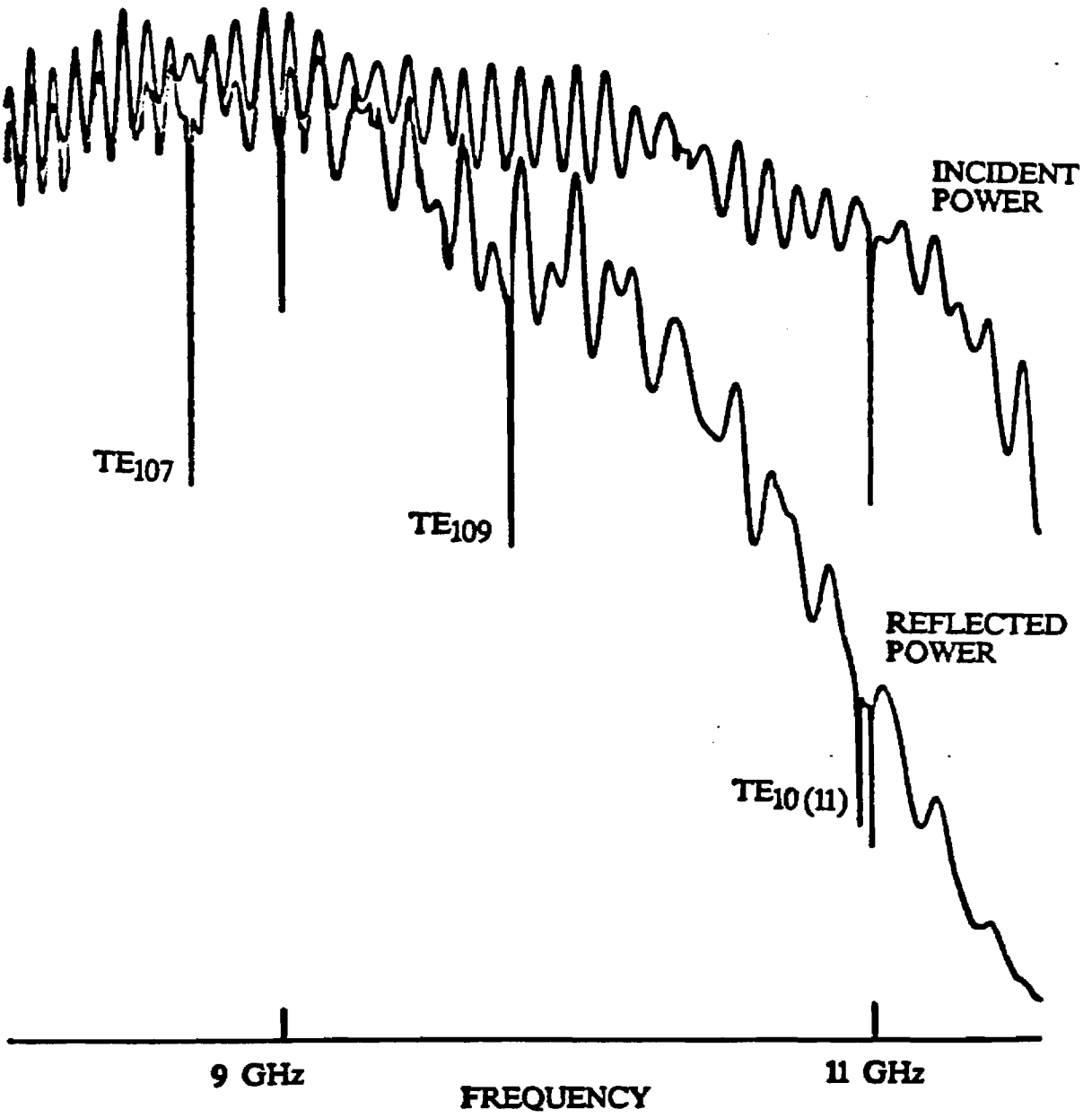

Figure 6(b) Undercoupled operating conditions – probe at midpoint. The effect of probe coupling on the shape of resonant absorption lines and the frequencies at which maximum absorption occurs.

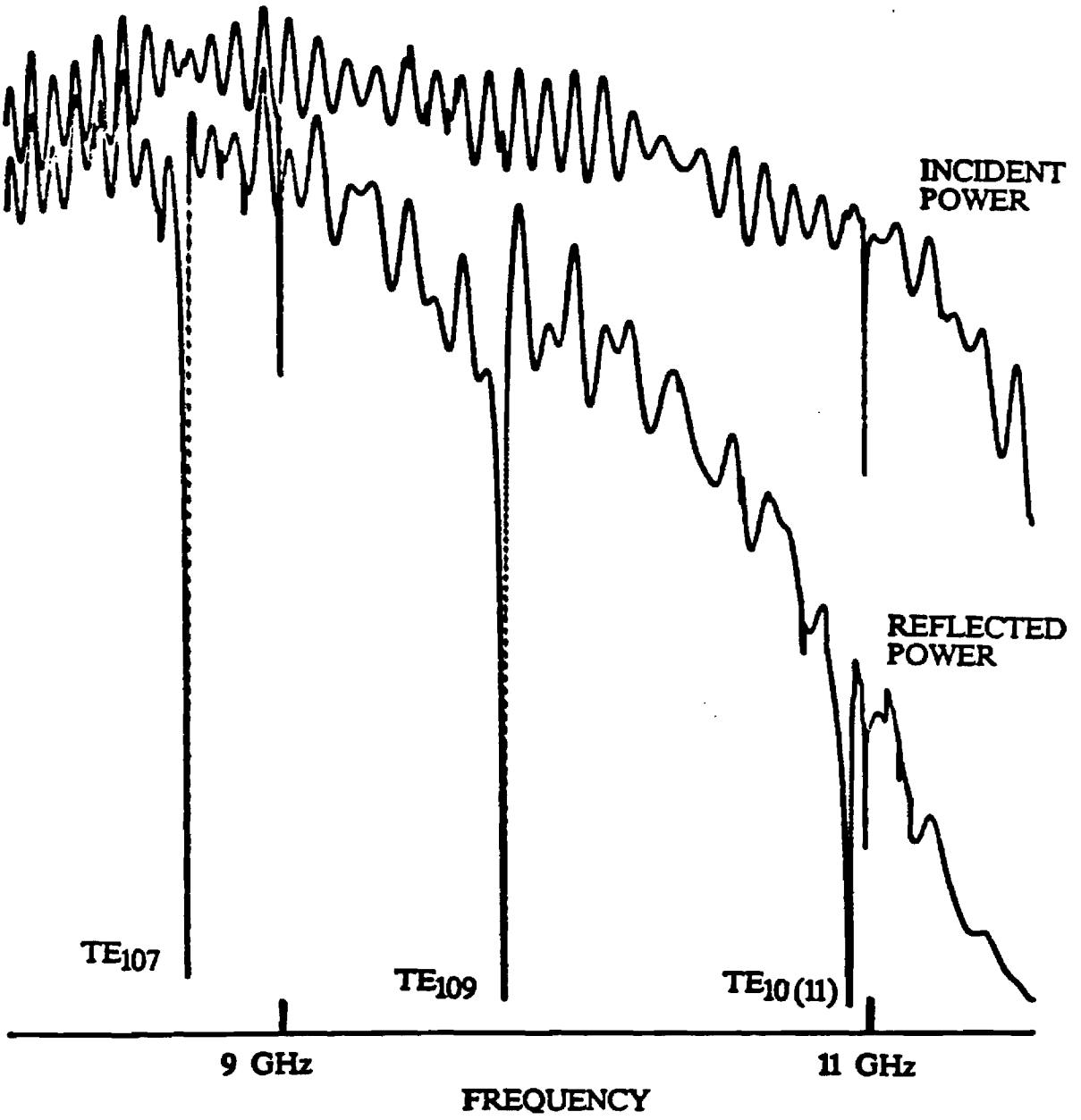

Figure 6(c) Close to critical coupled operation – probe at midpoint. The effect of probe coupling on the shape of resonant absorption lines and the frequencies at which maximum absorption occurs.

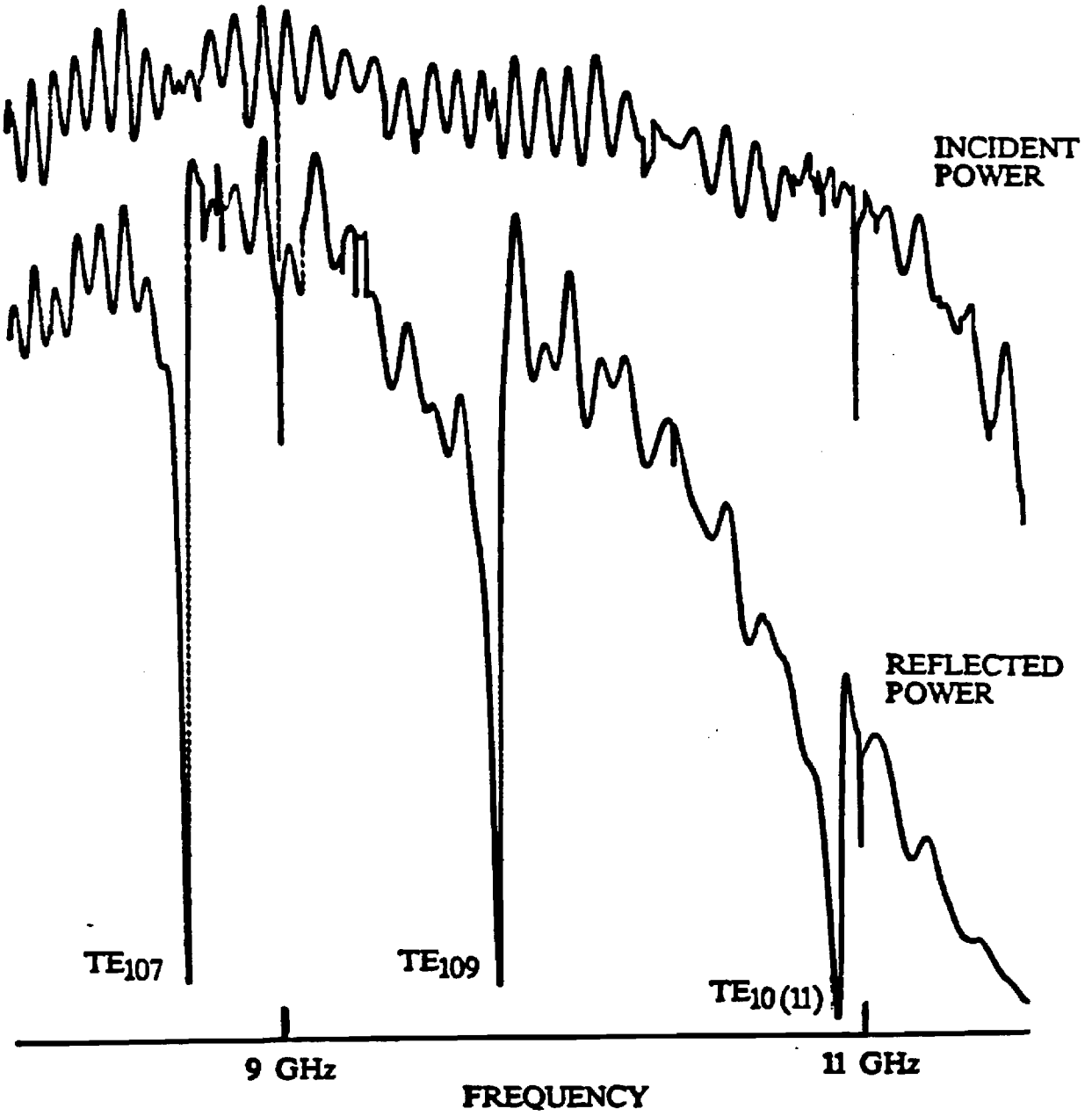

Figure 6(d) Overcoupled operation – probe at midpoint.
The effect of probe coupling on the shape of resonant absorption lines and the frequencies at which maximum absorption occurs.

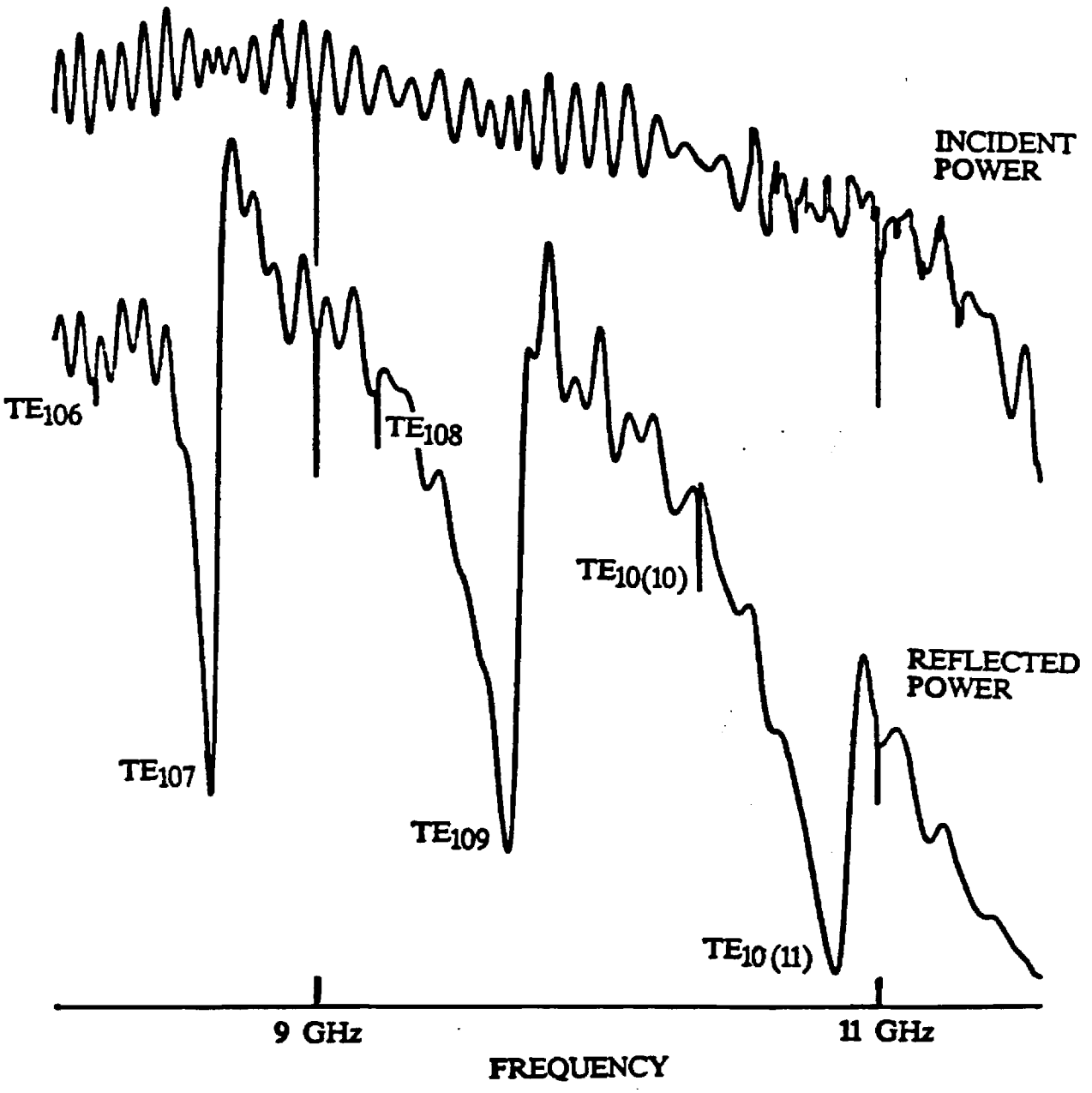

Figure 6(e) Heavily overcoupled operation – probe at midpoint. The effect of probe coupling on the shape of resonant absorption lines and the frequencies at which maximum absorption occurs.

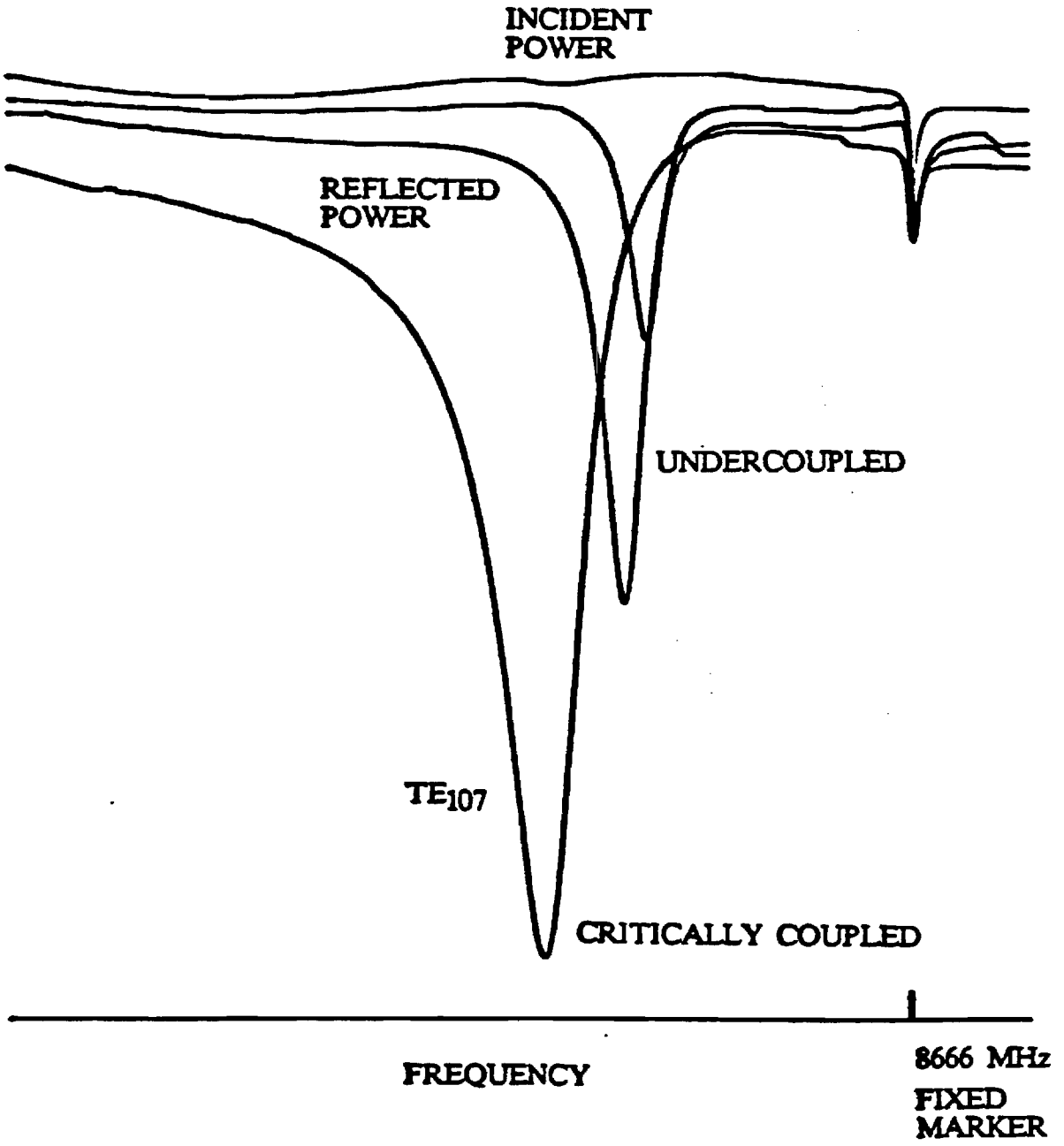

Figure 6(f) The effect of probe coupling on the shape and position of the TE_{10} resonant absorption line recorded against an expanded frequency scale.

At the other extreme of probe penetration if the cavity and the measurement assembly are lightly coupled at the position of maximum field intensity then the range of power absorption variation between maximum and minimum field positions will be a limiting factor on the accuracy of measurement if simple measuring apparatus like that shown in Figure 3(c) is used. This disadvantage is reduced to some extent by the reduction in detuning variation as the probe is moved to different positions.

For qualitative indication of relative field distributions using simple measuring apparatus a procedure that involves setting the probe so that close to critical coupling at the maximum field position occurs as the probe is moved about appears most desirable. Swept frequency recordings of the reflected power like those of Figures 4(a) to (p) and 6(a) to (e) can be used to set this condition with adequate accuracy for the purpose of investigating the method experimentally and analytically.

4.5 An equivalent circuit explanation of the quantities that are measured and their relationship to the resonator electric field distribution.

The equivalent circuits derived in section 4.3 represent the behaviour of the cavity, with the probe coupling structure at various chosen reference planes within the cavity. In order to relate the quantities that can be measured with the waveguide instruments between the excitation source and the probe coupling unit it is necessary to derive an equivalent circuit for the resonant cavity and probe coupling at a reference plane in the guide between the measuring assembly and the probe unit. Such an equivalent circuit is shown in Figure 7.

For an arbitrarily chosen position of the probe it has been shown that the cavity can be represented by a parallel combination of inductance L_x, capacitance C_x and resistance R_x and that resonance in the absence of any external connection will occur at a frequency given by,

$$\omega_o^2 = 1/L_x C_x \qquad (1)$$

If this circuit is to be transformed through the probe structure to a

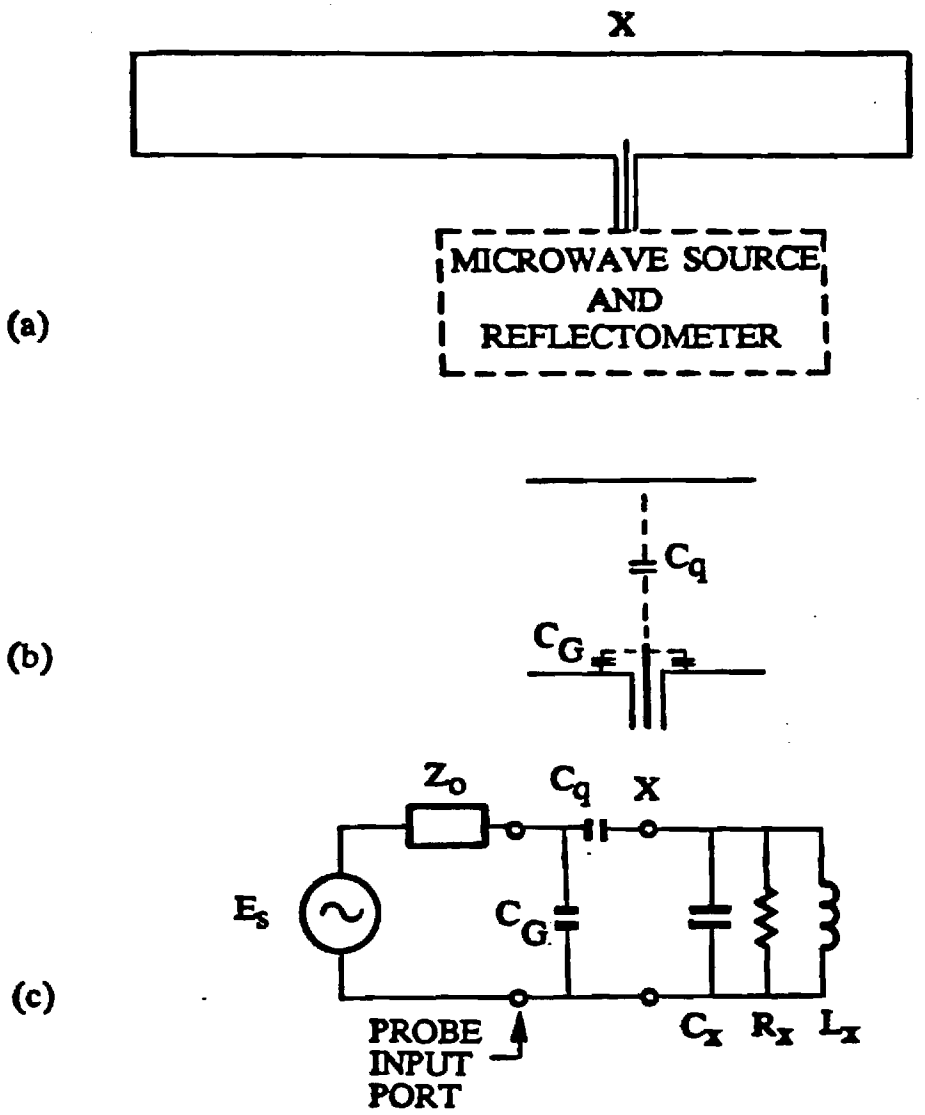

Figure 7 Equivalent circuit of probe coupled cavity referred to the input port to the probe.

reference plane identified by the terminals HH in Figure 7 then a circuit representation of the probe unit by itself is needed. This is not the parallel combination of R_p, C_p and I_p shown in Figure 5(c) because that circuit was the representation of the source as well as the probe unit at the reference plane within the cavity. The probe can be represented by two lumped capacitors, C_G between the probe and the cavity wall through which the probe extends and C_q between the probe and the opposite wall of the cavity. The values of these capacitors depend primarily on the physical dimensions of the probe and the cavity walls in the vicinity of the probe and also the dielectric properties of the materials that fill the space between the probe and the cavity walls.

The impedance Z_L presented to the source and the reflectometer assembly is the combination of C_G, C_q, L_x, C_x and R_x. The exact expression is,

$$Z_L = \frac{A + B - j\,(C + D)}{E + F} \tag{2}$$

where

$$A = R_x\left[1 - w^2 L_x \left[C_x + C_q\right]\right]\left[- w^2 L_x\left[C_G + C_q\right]\right] \tag{3}$$

$$B = w^2 L_x R_x\left[C_G\left[1 - w^2 L_x\left[C_x + C_q\right]\right] + C_q\left[1 - w^2 L_x C_x\right]\right] \tag{4}$$

$$C = w^3 L_x^2 \left[C_G + C_q\right] \tag{5}$$

$$D = w R_x^2\left[1-w^2 L_x\left[C_x+C_q\right]\right]\left[C_G\left[1-w^2 L_x\left[C_x+C_q\right]\right]+ C_q\left[1-w^2 L_x C_x\right]\right] \tag{6}$$

$$E = \left[w^2 L_x\left[C_G+C_q\right]\right]^2 \tag{7}$$

$$F = w^2 R_x^2\left[C_G\left[1-w^2 L_x\left[C_x+ C_q\right]\right] + C_q\left[1-w^2 L_x C_x\right]\right]^2 \tag{8}$$

Measurements are made at the resonant frequency of the cavity which is determined by setting the probe at a position of maximum electric field intensity, adjusting it for critical coupling and selecting the frequency that gives near zero reflection. Let us assume that this corresponds in mathematical terms to the condition,

$$w^2 L_x\left[C_x+C_q\right] = w^2 L_{max}\left[C_{min}+C_q\right] = 1 \tag{9}$$

and consequently,

$$F = w^2R_x^2\left[\,0 + C_q\,\left[1-w^2L_xC_x\right]\right]^2$$

$$= w^2R_x^2C_q^2\left[w^2L_xC_q\right]^2 \text{ which is small because } C_q \text{ is small,}$$

$$E+F = \left[w^2L_x\left[C_G+C_q\right]\right]^2$$

$$A = 0$$

$$B = w^2L_xR_x\left[0 + C_q\left[w^2L_xC_q\right]\right]$$

$$\frac{A+B}{E+F} = \frac{\left[w^2L_xC_q\right]^2R_x}{\left[w^2L_x\left[C_G+C_q\right]\right]^2} = \left[\frac{C_q}{C_G+C_q}\right]^2 R_x$$

$$D = 0$$

$$C+D = w^3L_x^2\left[C_G+C_q\right]$$

$$\frac{C+D}{E+F} = \frac{w^3L_x^2\left[C_G+C_q\right]}{\left[w^2L_x\left[C_G+C_q\right]\right]^2} = \frac{1}{w\left[C_G+C_q\right]}$$

The final result is that

$$Z_L = R_x\left[C_q/\left[C_G+C_q\right]\right]^2 - j\left[1/w\left[C_G+C_q\right]\right] \qquad (10)$$

at an arbitrarily chosen position in the cavity standing wave pattern with w, the resonant frequency according to the condition of equation (9).

The presence of a reactance requires reconciliation with the initial settings of resonance and critical coupling. Changing the probe penetration to achieve critical coupling changes C_q in expression (10). This causes relatively large changes in the resistive component compared with the reactive part of Z_L and on a Smith chart will tend to follow a constant capacitive reactance contour from values of normalised resistance that are less than unity to values greater than unity or vice versa. That locus will pass close to the centre of the Smith chart if the capacitive reactance is small. However, if it is not small, then the test frequency can be altered

so that instead of the condition (9) being resonance, a net reactance from the cavity is created that cancels the reactance part of expression (10). Of course as the probe is moved away from the maximum electric field position the actual resonance will shift slightly away from the test frequency as has been noted already in the equivalent circuit study of behaviour in section 4.3.

If detuning effects due to probe movement could be made small enough to have negligible effect on the measurement of electric field distributions then the relation connecting the measurable quantity and the electric field would simply be,

$$Z_L = R_x \left[C_q/[C_G+C_q]\right]^2 = \text{constant} \times R_x \qquad (11)$$

This equivalent circuit model gives excellent qualitative understanding of the measurement method but it requires revision in more rigorous terms before a judgement can be passed on whether or not measurable quantities can be accurately related to the electric field through an analytical expression. As well as the problem of detuning occurring as the probe is moved the losses in the cavity need to be modelled as distributed losses to avoid singularities that arise if the expressions (1) and (2) of section 4.3 are used.

5. CONSTRUCTION AND OPERATION OF A SPECIAL PURPOSE TWO-DIMENSIONAL STANDING WAVE DETECTOR.

5.1 The special purpose application - resonant field distributions in MMIC module housings with flat lids impose stringent requirements.

The new method that has been demonstrated in chapter 4 of this report, has been developed and operated successfully as a means of measuring the electric field distribution at the inside surface of flat lids on MMIC module housings at frequencies that cause electromagnetic cavity resonances. This special purpose application imposes particularly stringent requirements on the design of the test platform that carries the measurement probe and takes the place of the flat lid on the module housing. Those requirements have been explained in detail in chapter 3 and in sections 4.1 and 4.3(c) of chapter 4. In particular, movement of the housing relative to the test platform and therefore the probe should not affect the microwave impedance between the top edges of the housing side walls and the substitute for the flat lid, namely the test platform. That impedance should be as small as practical and should remain constant with regard to both its resistive and reactive parts despite movement between the two surfaces. The resultant impedance should be small compared with the surface impedance of the inside of the housing so that the unloaded quality factor and the resonant frequencies are not affected to any significant extent by replacement of the lid.

5.2 The engineering solution for these stringent requirements.

It is known that the performance of various microwave and millimetre wave components can exhibit a degree of non-repeatable or random variation whenever metal-to-metal contact is involved. It occurs in coaxial connectors, waveguide flanges, calibration components for use with automatic test equipment, contacting type short circuit plungers for various guiding structures, point contact diodes, etc. It can usually be traced to variation in the contact resistance between the two metal surfaces and is affected by surface condition, pressure, types of metal, temperature, etc. The most sensitive way of measuring these effects is to arrange for the contact to be within a microwave resonator and carrying microwave current

at the test frequency of interest. Thus the stringent requirements explained in the previous section can be identified with a well known problem that happens to be associated in this special purpose application with the worst possible operating conditions, namely, cavity resonance conditions.

The solution is simple and elegant in concept but must be implemented with due care and attention to detail. The test platform must be made flat, optically flat, and therefore like a perfect metal mirror. It must then be coated with a low-loss dielectric layer that is uniform and as thin as practical and is also wear resistant. In addition it should be non-abrasive and preferably have a low coefficient of friction. The edges of the side walls of the module housing to be tested should be polished so that they lie in a plane and have minimum surface roughness although this treatment is not essential. The pressure between the housing and the test platform should be constant as the two are moved relative to each other. It is preferable that it be small and may be due to little more than the weight of the housing. As a consequence of this and because it is convenient to be able to keep the measurement assembly, including the test platform, stationary, the housing may be inverted and put on top of the test platform and moved by means of micropositioners laterally and longitudinally relative to the probe, that protrudes from the centre of the plate. If the housing to be tested contains a complete, serviceable microwave system and it is desirable to measure resonant field distributions with the system operating, then flexible signal, control and bias lead connections must be made in such a way that they do not unduly affect the movement or the contact pressure of the housing on the test platform. To set the microwave coupling factor, the extent to which the probe protrudes into the cavity within the housing must be adjustable. This means that the test platform may be moved up or down relative to the measuring equipment assembly and the subassembly for positioning the housing must be designed to accommodate this movement, small as it may be.

An experimental assembly that incorporates all of features described in the previous paragraph is shown in the photographs of Figures 8(a) to (c).

5.3 Features of the experimental assembly and the operating procedure

The experimental assembly shown in Figure 8(a) is designed to be connected to a simple microwave reflectometer as shown in the schematic drawing of Figure 3(c) and the photograph of Figure 9. Microwave power is fed to the housing under test via rectangular cross-section waveguide and coaxial line components connected to the HP442B probe unit. The amount by which the probe extends into the housing cavity is measured with the micrometer clearly seen underneath the test platform in Figure 8(c). The test platform has a 6 inch diameter optically flat top face clearly seen in Figure 8(b). This is the largest plate that could be conveniently polished to the required tolerance on flatness and is adequate for testing the housing shown in detail in Figures 1(a) to (d) and clearly seen inside a plexiglas frame in Figure 8(b). The probe is just perceptible at the centre of the circular plate and it follows that the radius of the plate must be greater than the largest plan view dimension of the housing if the probe is to be scanned through all positions within the lid aperture shown in Figure 8(b). The test platform is made thick enough to provide a rigid seat for the coaxial probe unit as well as easy engagement with the guide fork on the polishing machine.

The optically flat surface of the test platform presents a different appearance in Figure 8(b) compared with other parts of that aluminium item, because of the thin layer of dielectric that has been deposited on it. Vacuum deposition of silicon monoxide was attempted initially because of the promise of high quality sub-micron thick dielectric material that would give relatively large capacitance per unit area with the edges of the housing side walls and therefore negligible reactance in series with microwave currents between the walls and the substitute lid. The desired properties were not realised, and rather than spend development effort, a non-optimum alternative was used that proved to be adequate for demonstrating that this instrument would perform as predicted. A thin layer of photoresist was spun onto the plate and baked as specified. Results show that it is satisfactory with respect to dielectric properties, layer thickness and uniformity but is lacking with respect to wear resistance and coefficient of friction. A better type of layer is needed.

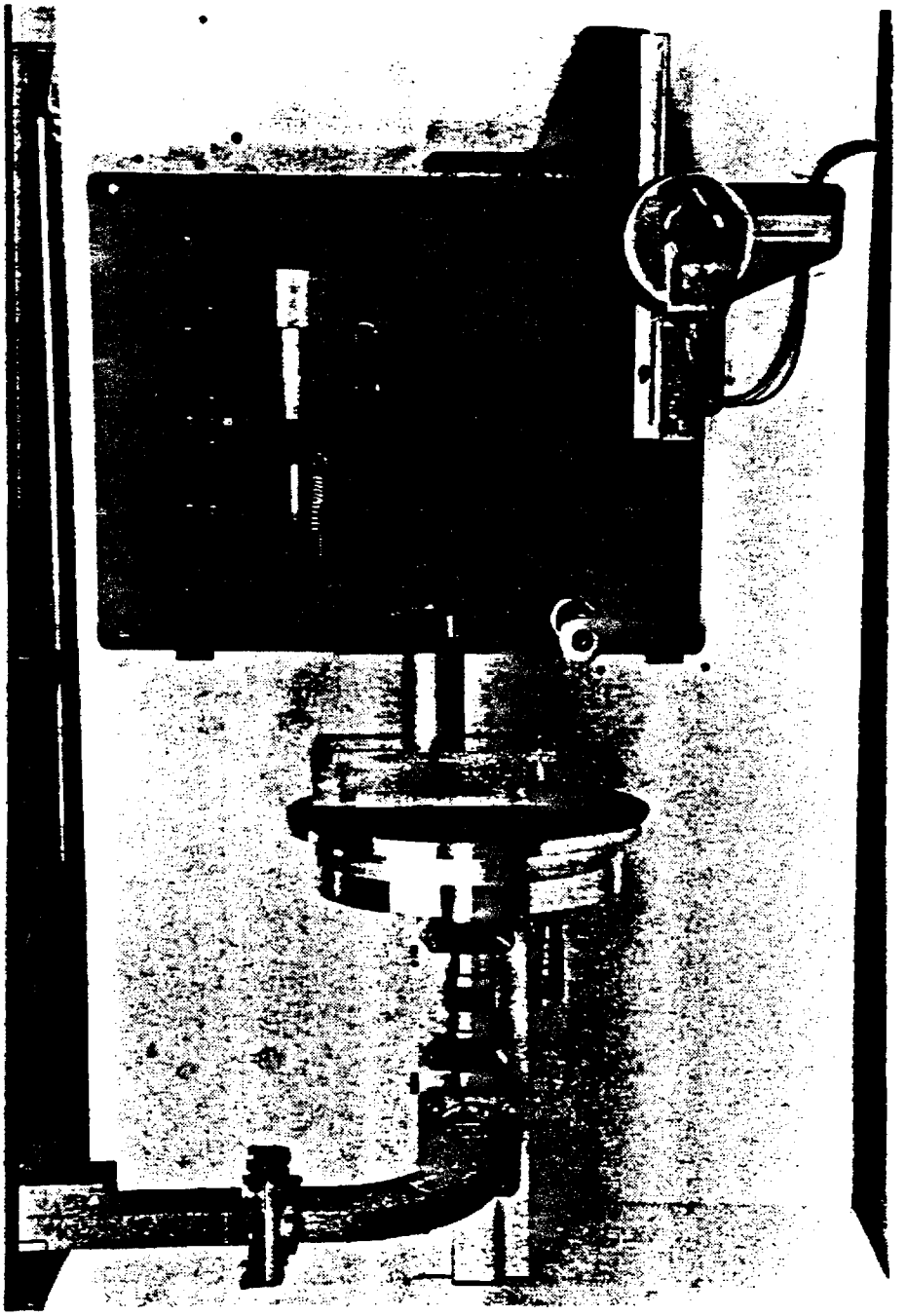

Figure 8(a) Photograph showing the micropositioner subassembly used to scan the coupling probe over the area of the module housing lid by moving the housing on a flat plate that carried the electric field coupling probe.

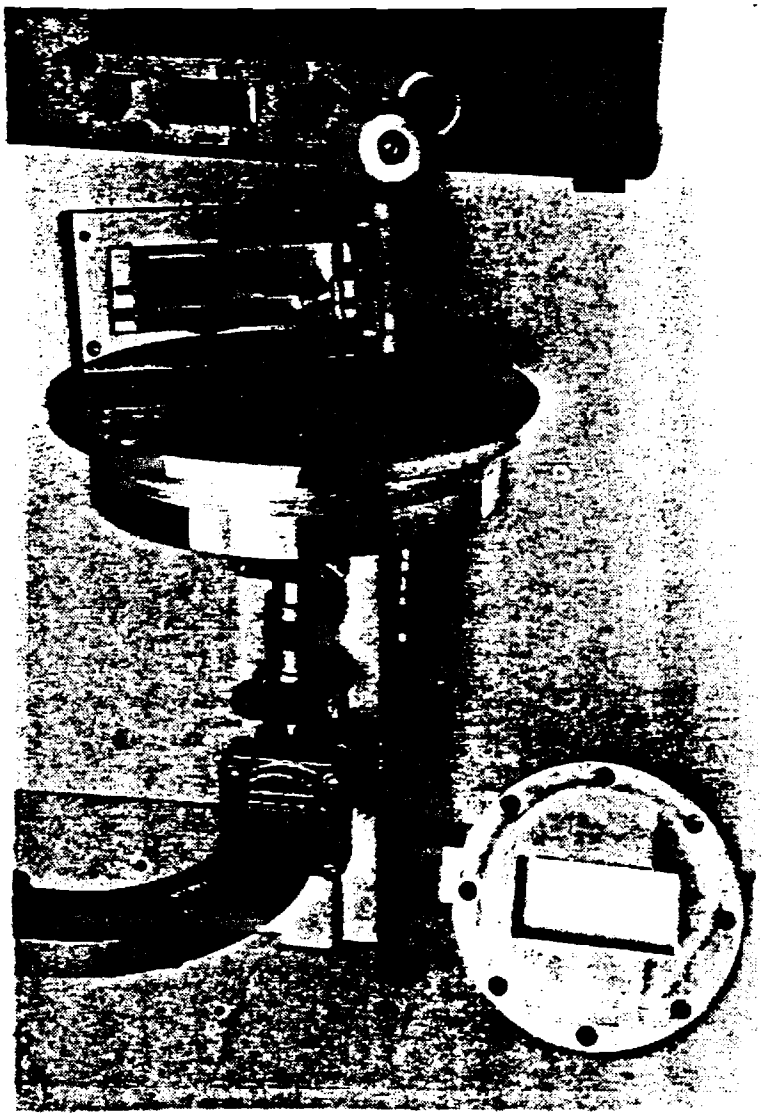

Figure 8(b) Photograph showing the electric field coupling probe at the center of the round flat base plate over which the module housing is moved so that the electric field distribution of the resonant mode might be measured.

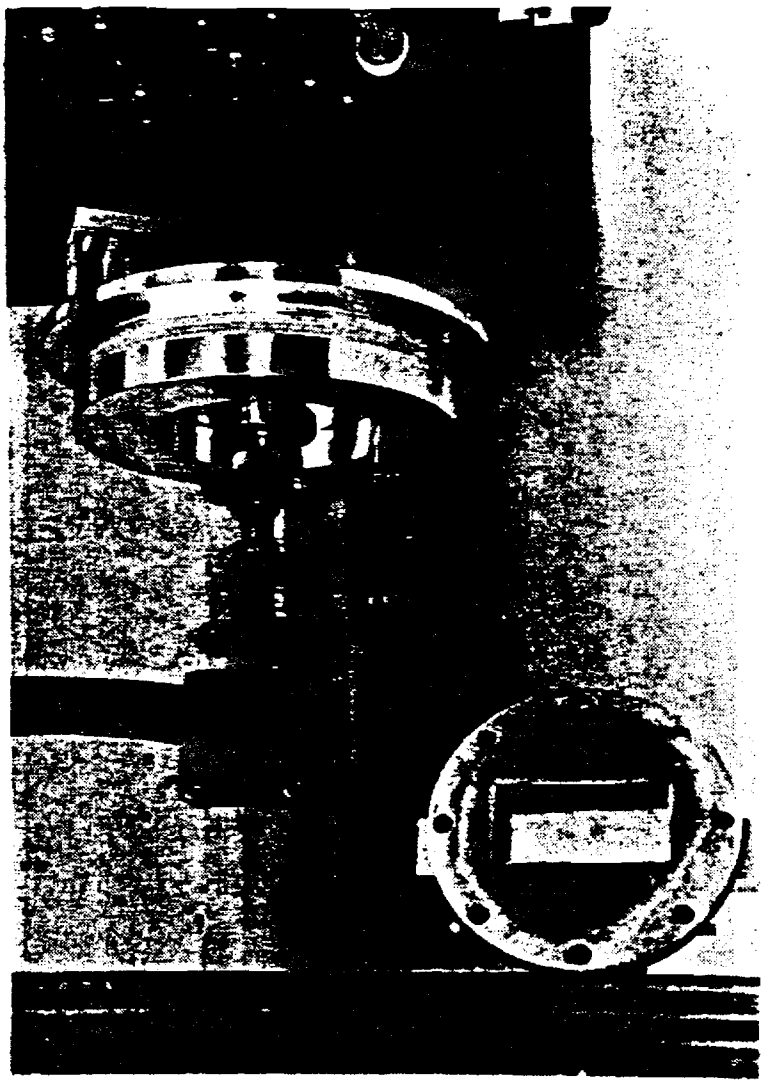

Figure 8(c) Photograph showing the probe clamping arrangement and the micrometer for measuring probe penetration.

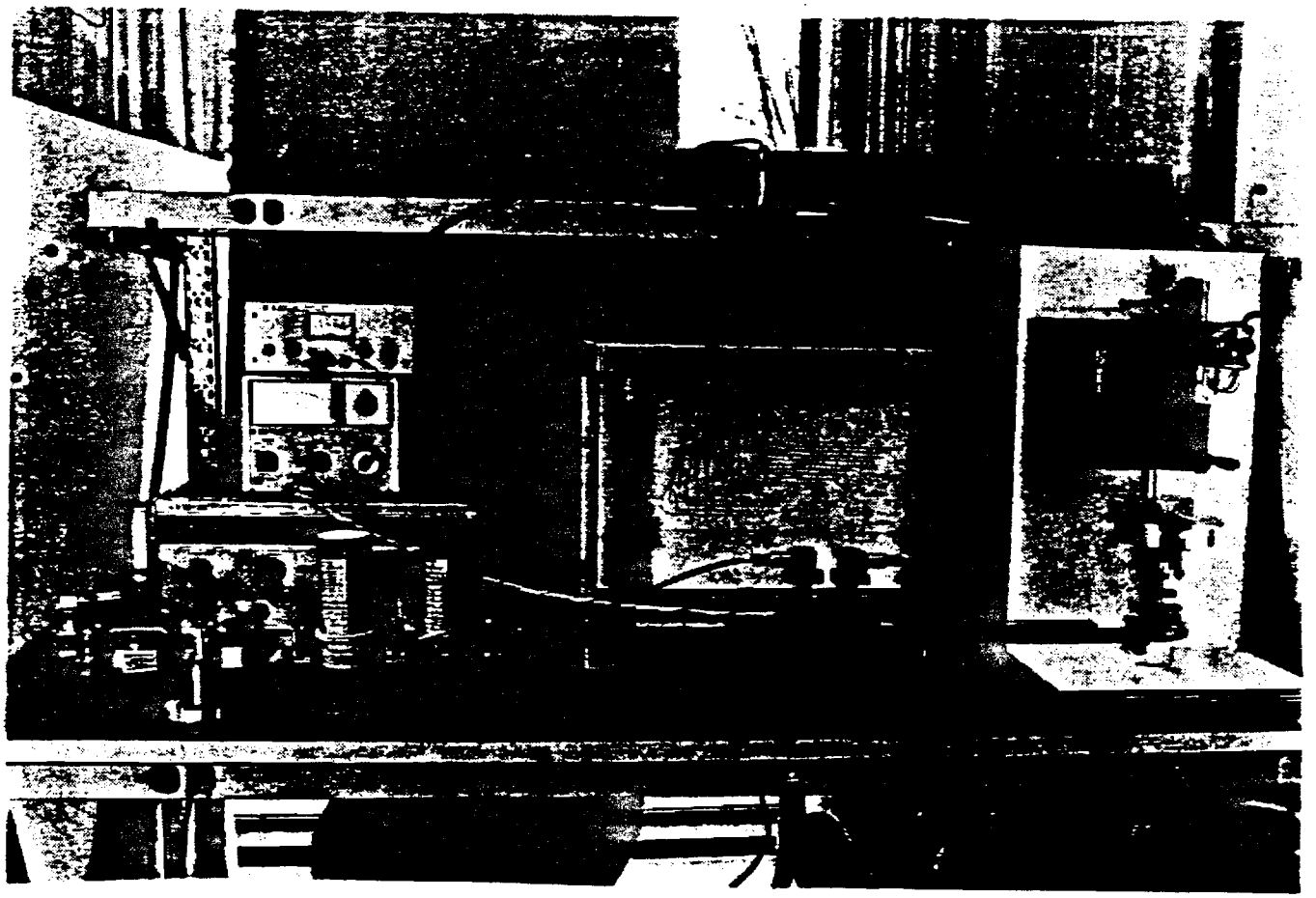

Figure 9 Photograph of the assembly used for measuring electric field distributions associated with resonances inside microwave module housings and packages.

The housing under test is an easy sliding fit in a rectangular aperture cut in the plexiglas frame shown in Figure 8(a) and (b). Thus the housing sits on the test platform under its own weight but can be moved laterally by the horizontal micropositioner immediately above it and longitudinally by means of the drive knob for a rack and pinion type translation mechanism in the upper right hand corner of Figure 8(a). A ten turn potentiometer is direct coupled to the drive knob so that with a simple direct current supply a voltage can be derived proportional to the longitudinal displacement of the housing and used to drive the x-axis movement of a recorder as shown in Figure 3(c). The vertical micropositioner that can be seen in Figure 8(a) is used to adjust the height of the plexiglas frame relative to the surface of the test platform each time a different probe penetration is set by moving the platform up or down relative to the microwave test equipment that is fixed to the laboratory bench as seen in Figure 9.

The plexiglas frame has been specially made for testing the housing of Figure 1 without any signal control or bias connections. A different frame would be needed if housing tests were to be conducted with the microwave module assembly energised. There is adequate clear space around the item under test in Figure 9 for the additional test equipment and connections to be made.

A second test item is shown on the bench in Figures 8(b) and (c). It is a simple rectangular box shape that becomes a closed resonator when it is placed face down on the test platform. Instead of a frame being used to connect it to the micropositioner assembly a spanner-like attachment is used. Two metal pins enter the holes in the body of this item adjacent to the short end walls of the cavity. The pins are an easy sliding fit and can be used to move the test item logitudinally and laterally while allowing it to sit on the test platform under its own weight. The resonant field distributions can be calculated accurately for this item and used to determine the relationship between measured quantities and the actual fields.

Careful inspection of the photograph of the housing in the plexiglas frame in Figure 8(b) and comparison with the details in Figures 1(a) to (d) reveal that the housing shown in the photograph is empty except for a

metal disc in the position where a microwave circulator is mounted in a complete T/R module assembly. In fact empty housings were supplied for initial investigations on resonances and because of the perceived importance of the circulator housing, as seen in the axial cross-section drawing of Figure 1(b), a metal disc of approximately the same outline was made to simulate the resonant currents that may flow on the circulator metal shell.

The procedure for recording the two-dimensional standing wave pattern of a cavity resonance with this manually operated assembly is simple. Firstly, resonances are detected by sweeping the test frequency over as wide a band as possible and recording both the incident and reflected power. The probe position is adjusted to ensure that all resonances are found. Secondly, each resonance is investigated in detail in the following way. The sweep range is reduced so that a particular resonant absorption curve is displayed on an oscilloscope. The probe position is altered until the position for maximum absorption is found. Next the probe penetration is adjusted until critical coupling is achieved at the resonant frequency which is used for the rest of the test. Micropositioner and control knob settings are calculated so that in plan form a series of parallel scan paths are devised that cover the area of the lid of the housing. In that plan care must be taken to avoid contact with the side walls of the housing and any interior walls otherwise the probe, which is a relatively fragile extension of the inner conductor of a coaxial line, may be bent. In addition, the equivalent circuit used to represent the probe, particularly C_p explained in section 4.3, will be altered if the probe comes too close to metal side walls. Having completed all these steps it is a simple but tedious matter to progressively record a family of curves depicting the relative field distribution at the resonant frequency chosen. An example can be seen in Figure 9.

6. TESTS ON THE TWO-DIMENSIONAL STANDING WAVE DETECTOR WITH A STANDARD RECTANGULAR RESONATOR.

6.1 Calculation of resonances in the standard rectangular resonator.

The standard rectangular resonator shown in the photographs of Figures 8(b) and (c) has the mechanical construction and dimensions shown in Figure 10. Selecting the largest dimension 2.005 inches as the length of the cavity, the resonator can be viewed as a waveguide of cross-sectional dimensions 1.005 by 0.387 inches. The dominant mode in such a waveguide is the TE_{10} mode with electric and magnetic field patterns as shown in Figure 11. If the waveguide is terminated in metal walls as in Figure 10 and an excitation frequency is selected that makes that length equal to two half waveguide wavelengths then the magnetic field distribution will be like that shown in the plan view designated 1 in Figure 10 when all of the energy in the resonator is stored in the magnetic. A quarter of a period later all of the energy will be stored in the electric field. Such a resonance would be designated as a TE_{102} mode of resonance.

The resonant frequency of the mode with subscripts (n, m, l) is given by the relationship,

$$\left[2\pi\, f_{nml}/c\right]^2 = \left[n\pi/A\right]^2 + \left[m\pi/B\right]^2 + \left[l\pi/L\right]^2 \qquad (1)$$

where A, B and L are the cross-sectional dimensions and length of the rectangular resonator,

c velocity of propagation of e.m. waves in the medium that fills the resonator.

Rearrangement of equation (1) yields an equation that can be used to construct a mode chart for a cavity with a specified cross-sectional aspect ratio A/B.

$$\left[f_{nml}A\right]^2 = \left[c/2\right]^2\left[(n)^2 + (m\,A/B)^2 + (l\,A/L)^2\right]$$

Plotting the left hand side as a function of $(A/L)^2$ yields a family of straight lines starting from points on the y-axis, detemined by choosing values of n and m in conjunction with the chosen A/B ratio.

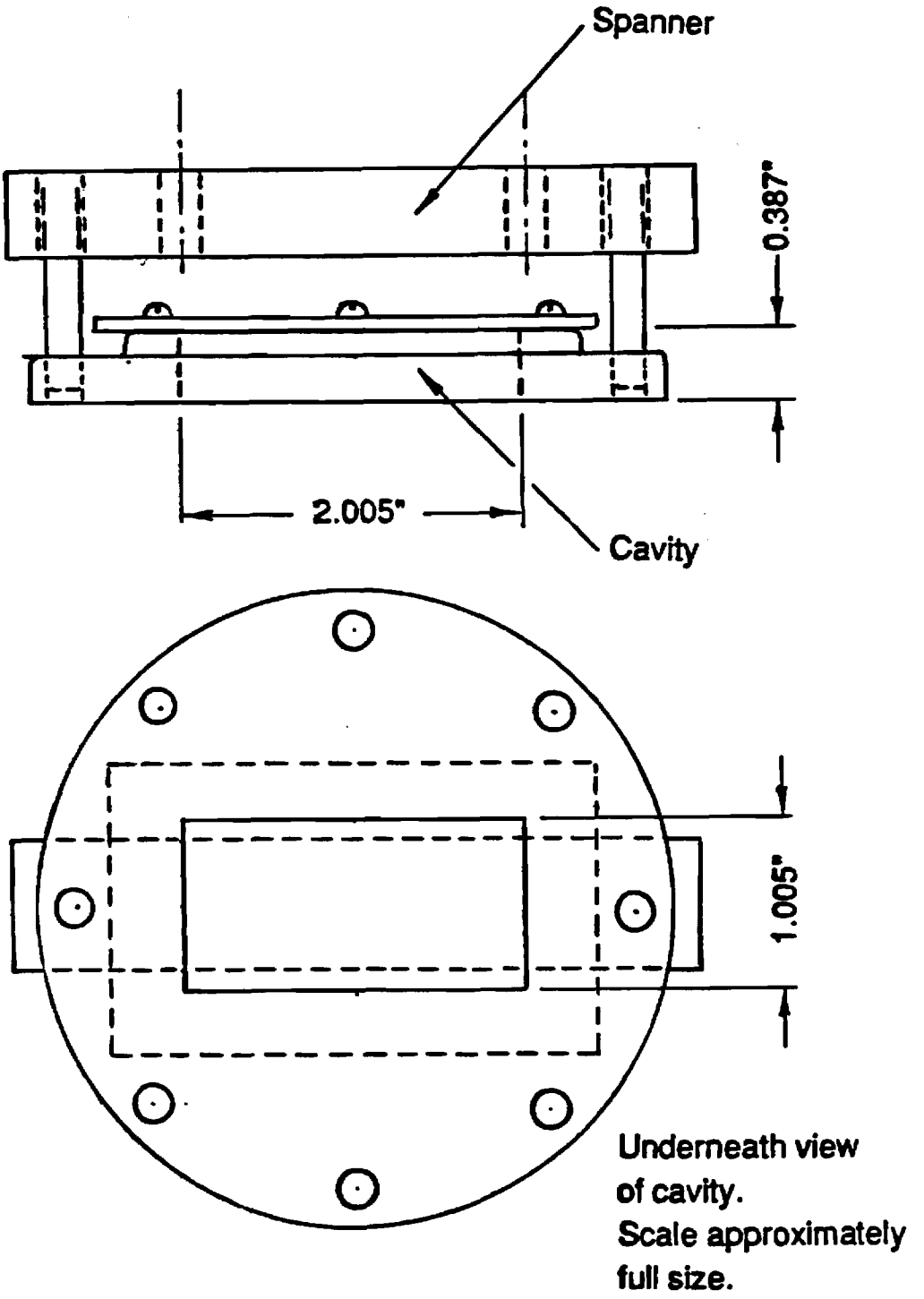

Figure 10 Sketch of standard rectangular test cavity with spanner-type mechanical coupling for attaching it to a x-y-z translation stage.

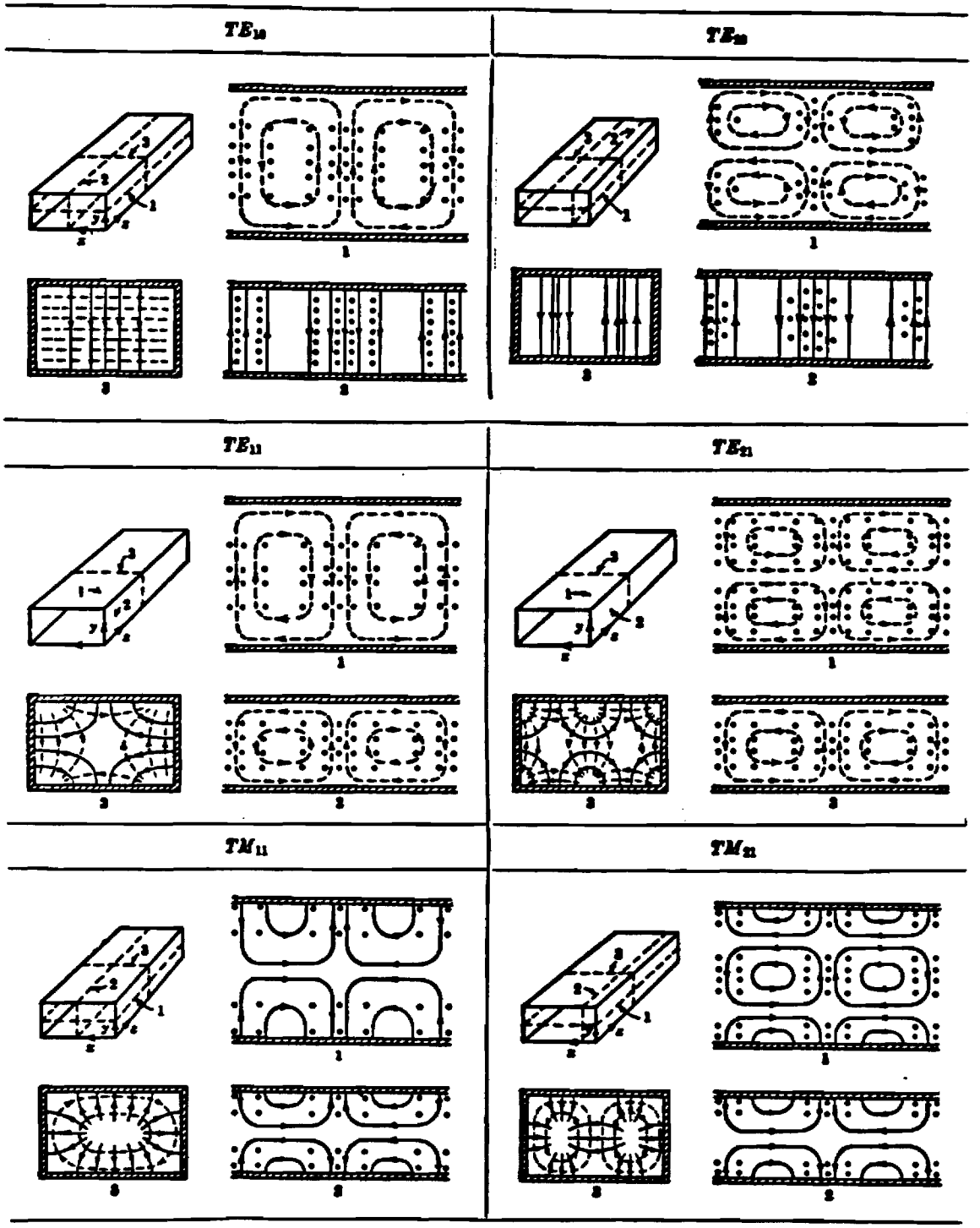

Figure 11 Sketches of electric and magnetic field distributions associated with travelling waves of various TE and TM modes in rectangular cross-section metal walled waveguides.

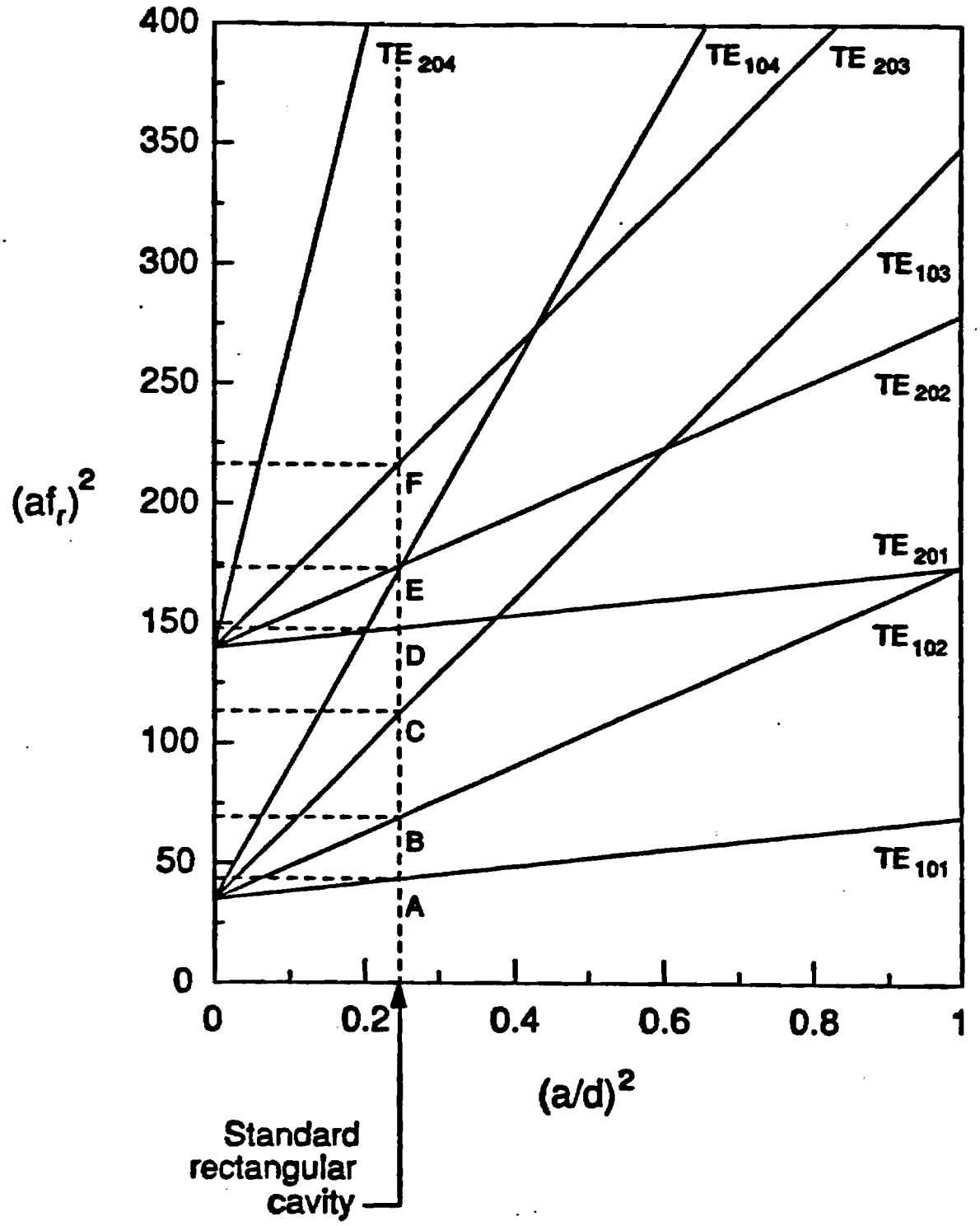

Figure 12 Mode chart for predicting resonances in metal walled rectangular box shaped resonators of cross-section 1.005 inches by 0.387 inches.

Such a mode chart for the resonator of Figure 10 is shown in Figure 12. It can be used to predict the resonant modes and the frequencies at which they will occur. In addition the field distributions can be predicted for each mode and are directly related to the propagating mode distributions depicted in Figure 11.

The resonances in increasing frequency can be read from Figure 12 at TE_{101}, TE_{102}, TE_{103}, TE_{104}, TE_{201}, TE_{202}, etc.

6.2 E-field probe measurements on the TE_{102} resonance.

The operating procedure explained in section 5.3 was followed in detail. From the theoretical electric field distribution for the TE_{102} resonance it was known that the maximum electric field occcurs on the centre-line of the lid and one quarter of the length of the cavity from each short-circuit. Probe penetration at the TE_{102} resonant frequency was adjusted at these points to give critical coupling and then recordings were made along the series of parallel scan paths shown in the upper part of Figure 13.

The recordings are reproduced in the lower part of Figure 13. The true electric field distribution along each of the paths in the absence of the probe is precisely two half sine wave loops with the maximum values on each scan path related through a sine law with its maximum on the centre-line and a zero at each side wall.

The recordings obviously differ in shape from the fields associated with a natural unloaded TE_{102} resonance and in the absence of an analytical method of relating the measurement to the ideal unloaded resonance an empirical relationship may be derived. The relationship obtained is close to a cube law, namely, $(E)^{2.9}$. Such a relationship has the effect of exaggerating the maxima and de-emphasising the minima in the overall distribution. It is clear from Figure 13 that there are two maxima in the locations expected from theory and that these maxima are surrounded by minima along all of the side walls and across the cavity half-way along its length. For many applications a clear pictorial view of the distribution is all that is needed. This may be adequate for example in

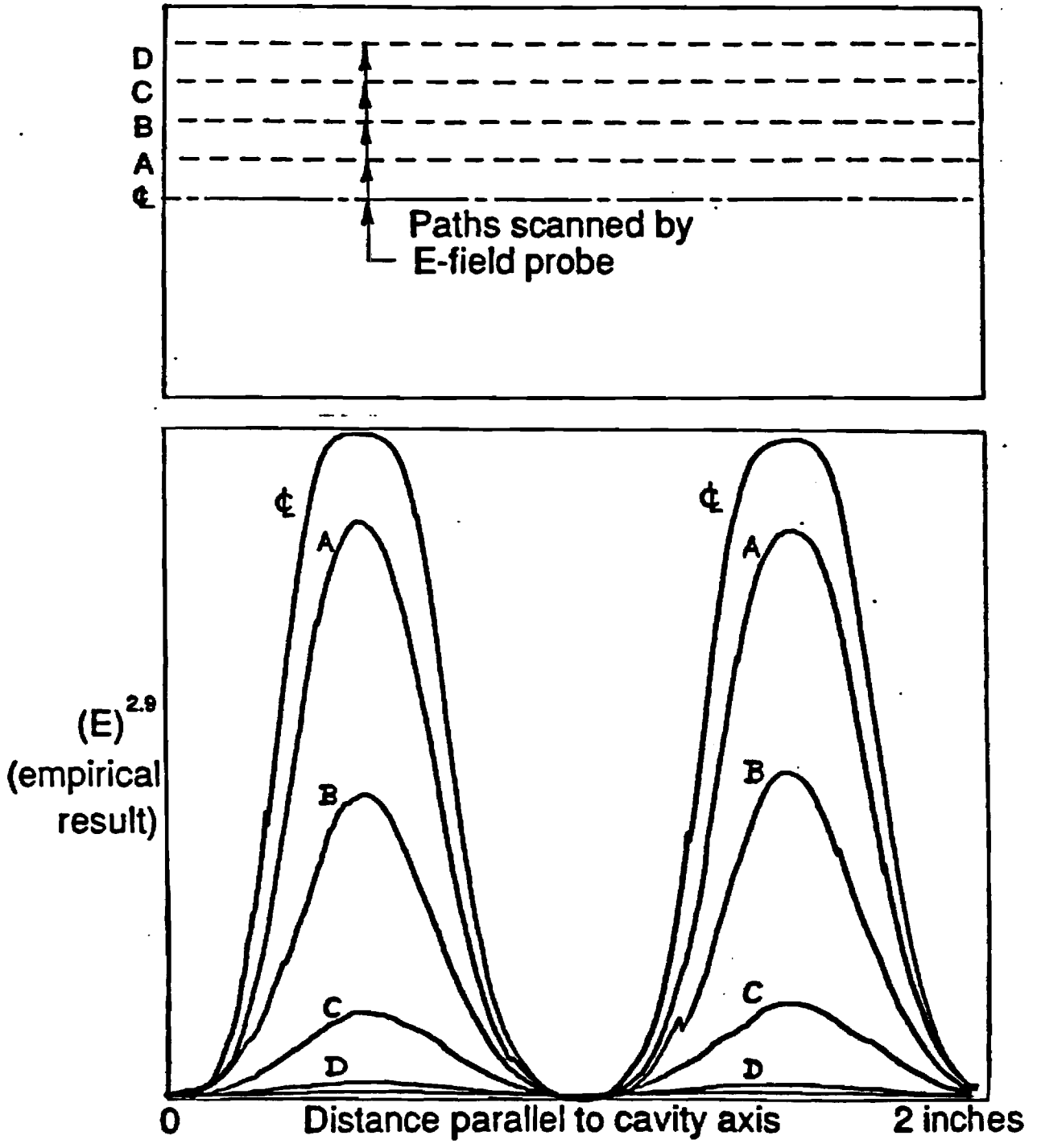

Figure 13 Experimentally measured plot of relative electric field distribution in a rectangular metal box resonator.

identifying unwanted resonances and testing the effectiveness of structures designed to prevent such resonances occurring.

7. TESTS ON A MMIC TRANSMIT-RECEIVE MODULE HOUSING KNOWN TO HAVE UNWANTED IN-BAND MALFUNCTION PROBLEMS

7.1 Preliminary tests and development of a measurement plan.

The module housing to be dealt with in this chapter provided the basic challenge for the development of the new measurement method described in earlier chapters. The detailed dimensions of the housing are set out in Figures 1(a) to (d) and have been referred to several times already. Preliminary tests were conducted to determine whether the housing exhibits any electromagnetic cavity resonances in the frequency band 8 to 12 GHz and if so where the E-field probe should be positioned for maximum coupling to each of the resonances.

In fact it was found that there were three resonances within the frequency range of interest and that each one could be excited with the probe positioned in the region between the circulator C and the lid shown in Figures 1(a) and (b). Furthermore this was the region in which maximum coupling could be achieved with a given probe penetration for the two lowest frequency resonances. Maximum coupling to the highest frequency resonance occurred in the region between the septum marked B in Figure 1(a) and the inside wall projection designed to accommodate the bias supplies and control signals connector clearly seen in Figure 1(c). All of these swept frequency tests were conducted on an empty housing with a metal disc of approximately the same shape as the circulator shell in position C. The results are shown in Figures 14 (a) and (b).

On the basis of these exploratory measurements a series of seventeen probe scan paths were selected as shown in Figure 15 for recording power absorption characteristics at each resonant frequency as a function of probe position. The paths were selected subject to the need for resolution of detail in the two-dimensional distribution and the practical limitation of completing a long sequence of manually operated micrometer positioning steps without error. The internal walls or septa, present particular difficulties because they are not along a single line parallel to the centreline of the housing. To avoid proximity effects and possible damage

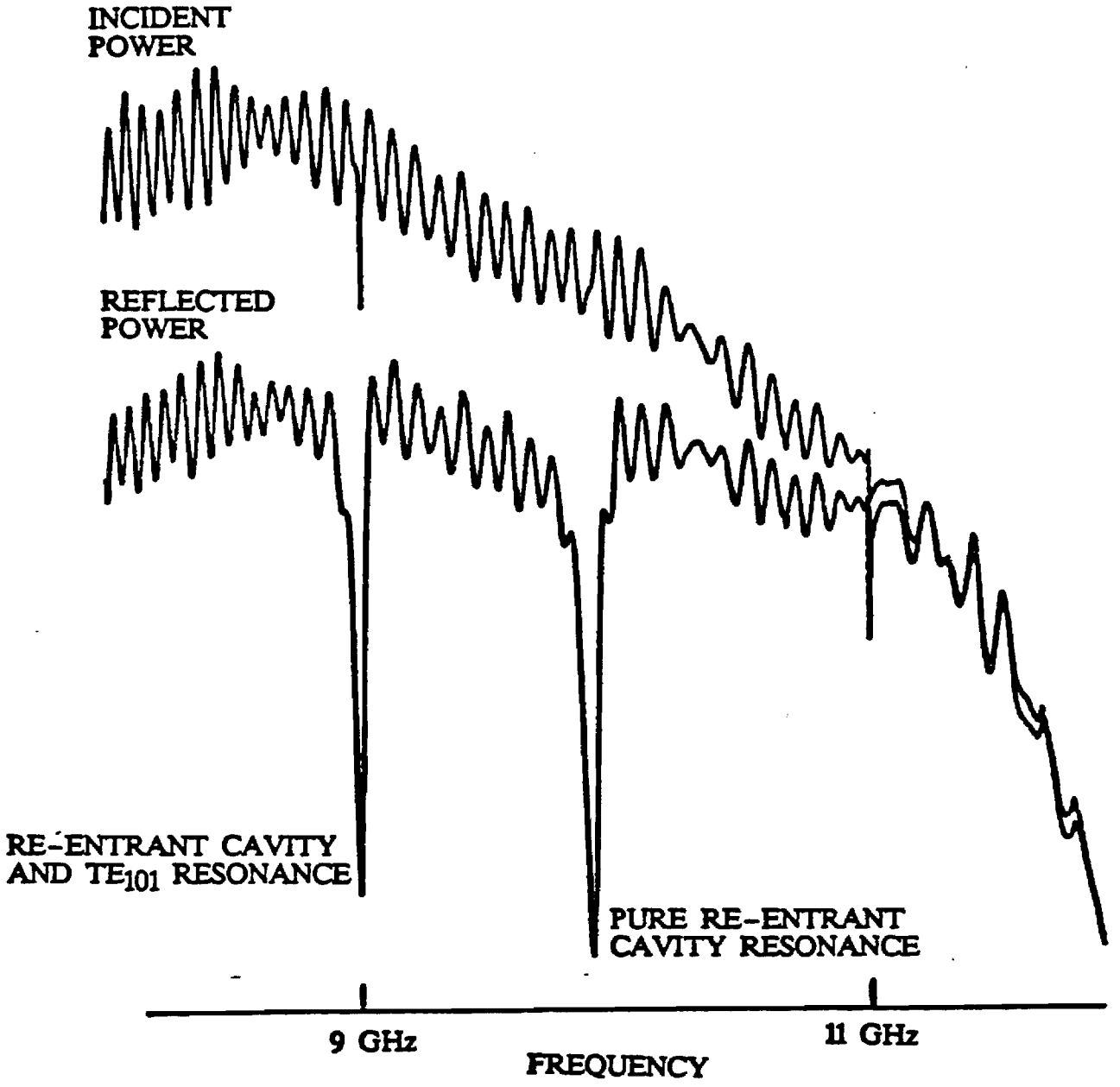

Figure 14(a) Swept frequency incident and reflected power characteristics showing cavity resonances within an empty T/R module housing. E-field probe near simulated circulator shell.

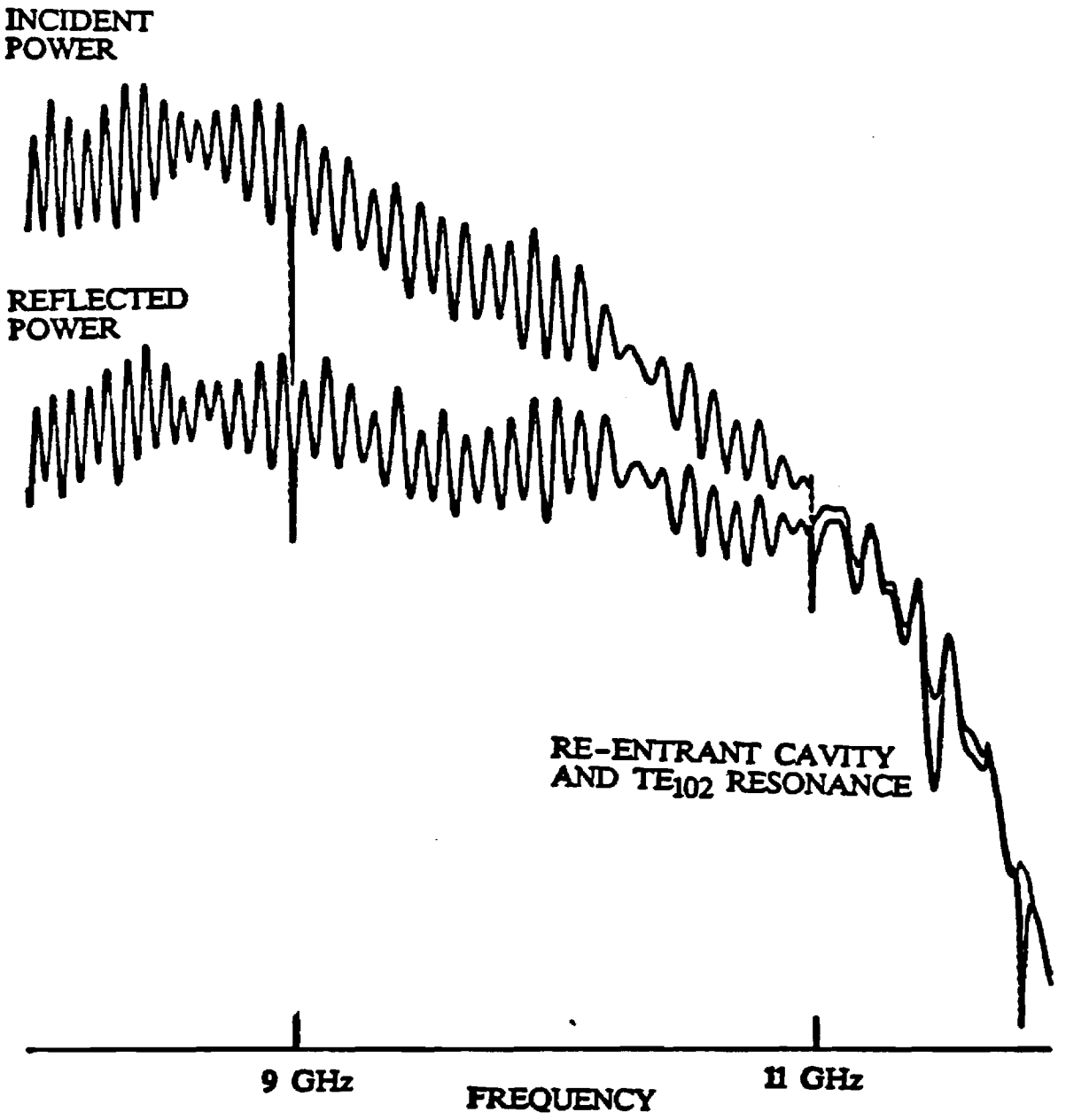

Figure 14(b) Swept frequency incident and reflected power characteristics showing TE_{102} resonance (modified by re-entrant cavity coupling in the region of the simulated circulator shell).

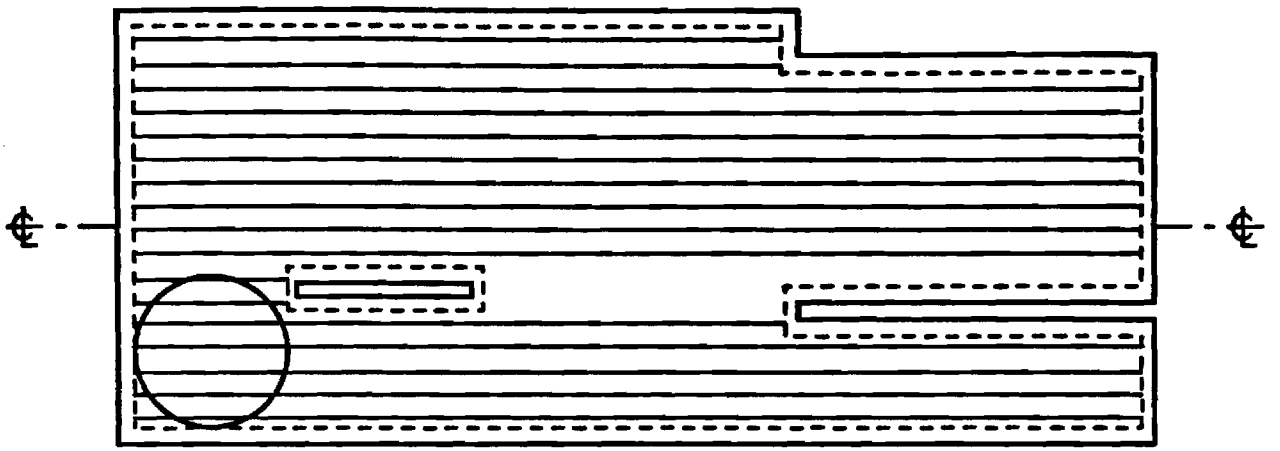

- Field distribution is mounted by moving an electric field probe along 17 parallel paths spaced 0.050 inches apart some of reduced length to avoid septa and a wall.

- A brass disc 0.420 inches diameter by 0.127 inches thick simulates a circulator housing in the lower corner.

Figure 15 Plan view of housing for a microwave phased array radar transmit-receive (T/R) module, taken from Figure 1 detail, and showing the paths scanned by the coupling probe for relative electric field distribution measurements.

to the probe three scan paths are somewhat shortened as is clear from Figure 15.

7.2 Recordings of the relative field distribution associated with each in-band eletromagnetic cavity resonance in the housing.

The three resonances identified in swept frequency recordings of Figures 14(a) and (b) occur at 8.996 GHz, 9.833 GHz and 11.775 GHz. In each case the probe was positioned for maximum absorption and the penetration at that position was adjusted for critical coupling. Then with the excitation frequency held constant the power absorption was recorded for each of the seventeen scan paths shown in Figure 15. The start point for each recording was displaced along a line at 27° to the scan direction, so that, rather than having recordings superimposed on each other, they might give a three-dimensional impression of the electric field distribution normal to the inside surface of the housing lid.

The results for each of the three resonances are shown in Figures 16(a) to (c).

A common feature of all three sets of recordings are the relatively intense fields between the housing lid and the circulator shell, or in this case the brass disc used to simulate it. Of course these recordings are an exaggerated version of the true field distributions for all of the reasons discussed in chapter 6 and one additional reason. The distance from the tip of the E-field probe to the opposite wall of the resonator is smaller at the circulator shell than elsewhere in the module housing. Referring to section 4.5, page 57, expression (10), the probe capacitance C_q will be increased if the distance to the opposite wall is decreased and this will have the effect of increasing the coupling, the power absorption and the apparent relative electric field. Thus analytical interpretation of the measurable quantity, obtained with this instrument is more complicated than ever if the resonant cavity has variable depth. There maybe a simple inverse relationship but measurements on standard resonators with different depths and known field distributions appear necessary to test such a law.

As well as the common feature each set of recordings has a

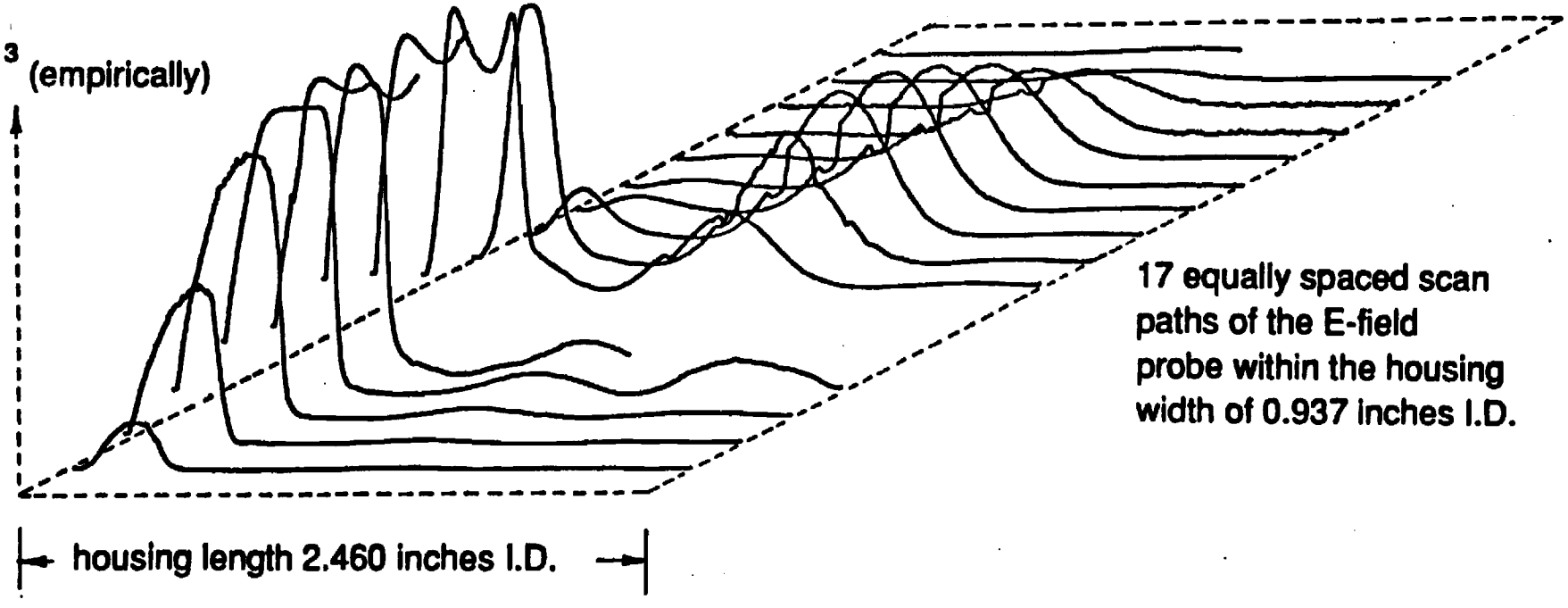

Figure 16(a) Relative distribution of the E-field for a resonance within a T/R module housing. Housing dimensions shown in Figure 1(c). Housing empty except for dummy circulator. Resonant frequency for these measurement 8.996 GHz.

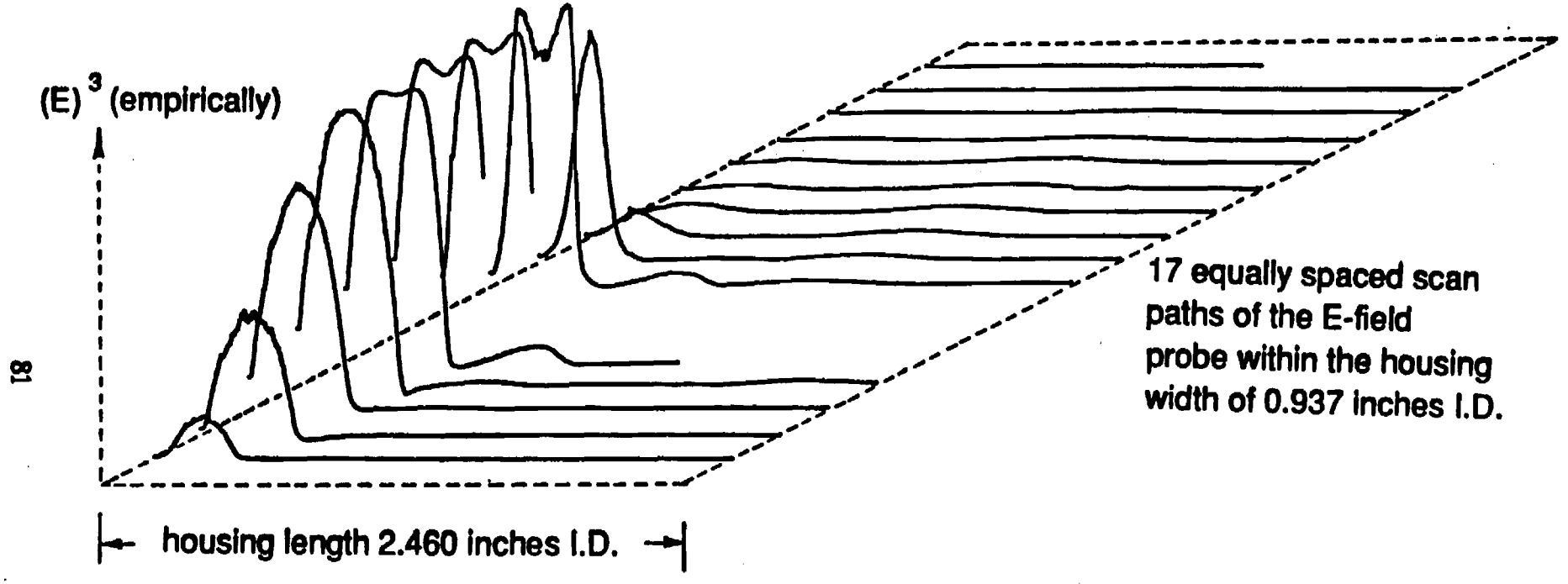

Figure 16(b) Relative distribution of the E-field for a resonance within a T/R module housing. Housing dimensions shown in Figure 1(c). Housing empty except for dummy circulator. Resonant frequency for these measurement 9.833 GHz.

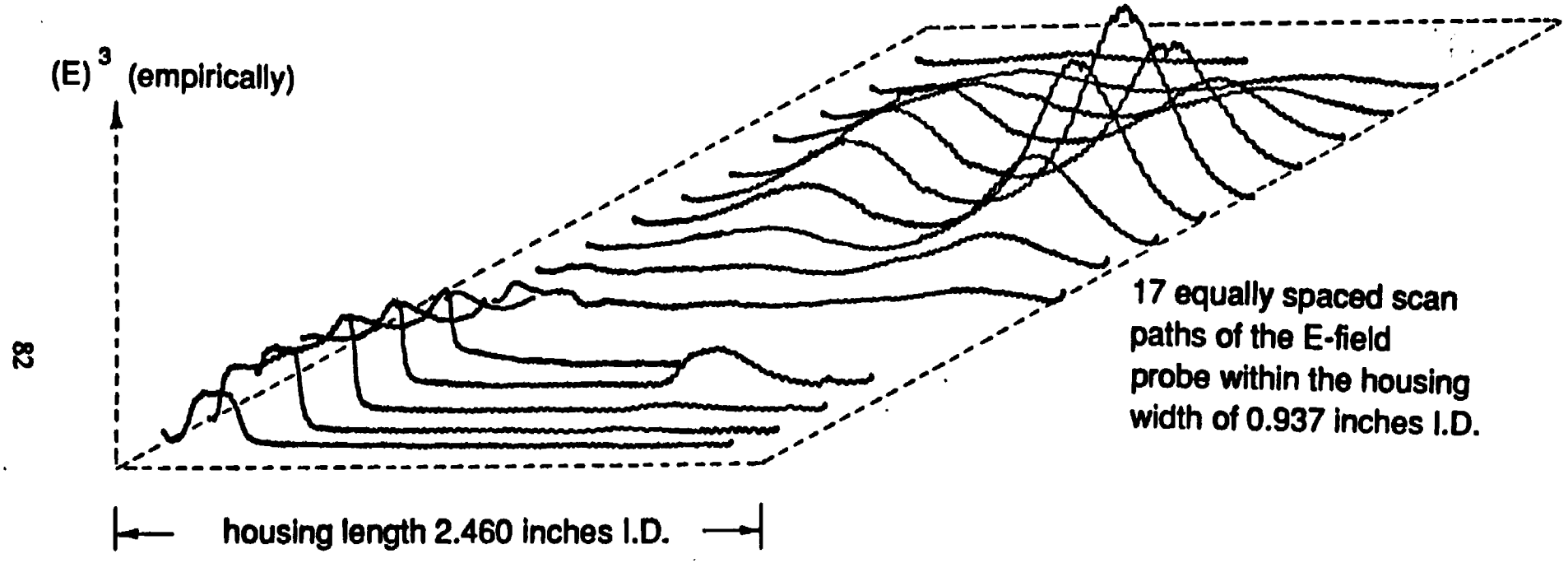

Figure 16(c) Relative distribution of the E-field for a resonance within a T/R module housing. Housing dimensions shown in Figure 1(c). Housing empty except for dummy circulator. Resonant frequency for these measurement 11.775 GHz.

distinctive feature in the wider uniform depth region between the septa and the further of the side walls. At the lowest resonant frequency Figure 16(a) shows the presence of a half-wavelength long standing wave pattern. If the septa were intended to place this part of the housing below cutoff at this frequency then that attempt has not been successful. A contributing reason could be that the circulator shell has provided reactance that is tightly coupled to the larger part of the housing and yields resonance at a lower frequency. The distinctive feature of the fields associated with the second resonance in Figure 16(b) is that they are relatively small except near the circulator shell. Thus, being quite concentrated, this resonance can be regarded as similar to that in a re-entrant cavity where the electric energy is stored between the circulator shell and the housing lid and the magnetic energy is stored circumferential to the shell. Microwave currents will flow on the cylindrical surface of the shell. The field distribution associated with the third resonance shown in Figure 16(c) exhibits two half-wavelengths of standing wave pattern in the larger part of the housing which is also coupled to and tuned by the re-entrant structure. That structure should present capacitive reactance at the lowest resonant frequency and inductive reactance at the highest. The resonances do not overlap in the frequency sweep characteristics and as a result will not be coupled to each other to any significant degree at any frequency.

7.3 The probable reason for malfunction in the T/R module.

The re-entrant cavity behaviour, observed between the circulator shell and the housing lid as relatively intense electric fields at each of three resonant frequencies, probably causes the isolation of the circulator to be much lower than expected at those frequencies. This comes about in the following way. At each of the resonances a relatively intense magnetic field will also be produced. That field will pass in part between each of the three microstrip conductors and the floor of the module housing below those conductors. Thus there are three inductive loops coupled via common circumferential magnetic flux at each of the housing resonant frequencies. Such coupling is absent if a circulator is tested on a simple flat ground plane or for that matter inside the module housing with the lid removed.

The output of the MMIC power power amplifier is connected to one port of the circulator and the MMIC low noise receiver, possibly via transmit-receive switching, is connected to another port. Oscillation due to feedback is supposed to be prevented by providing adequate isolation in the combination of circulator and transmit-receive switches. However the energy for exciting the resonance and causing oscillation would be provided by the MMIC power amplifier and coupled into the resonant fields via the loop formed between the microstrip connection to the circulator and the floor of the housing.

The resonant fields associated with the lowest and highest frequencies, as seen in Figures 16(a) and (c), extend to other parts of the housing. However the most vulnerable components, so far as being coupled to the resonances is concerned, are those that do not have a high degree of field confinement associated with their structure. Leads from relatively large lumped components such as the circulator and coaxial connectors are most vulnerable, followed by microstrip components on ceramic substrate. Least vulnerable are MMIC components on GaAs substrate because of the high dielectric constant of the semi-insulating form of that semiconductor.

7.4 A note on the sensitivity of the measuring apparatus.

Close inspection of Figure 16(a) reveals a dip on the eighth through to the fifteenth scan trace. That dip corresponds to a scratch like blemish in the thin insulating layer on the test platform. It is for reasons such as this that an improved, low friction, wear resistant insulating layer needs to be developed.

7.5 Tests on a complete T/R module.

Figure 1(c) is an indication of the components that are normally mounted within the module housing. A complete module became available and was tested at the end of the laboratory program. Even though the MMICs have a large dielectric constant they have limited effect on the resonant characteristics of the housing because they are thin and occupy a small percentage of the volume. Of greater consequence are the relatively bulky capacitors associated with the bias supplies and placed adjacent to the

bias and control signal input connector. These components contribute re-entrant cavity-type effects on the fields due, in the main, to the relatively large metal end connections. These effects probably result in a disproportionately large microwave loss being added to the total internal losses of the assembled housing.

These observations are consistent with the resonances revealed in the swept frequency recording shown in Figure 17. The lowest frequency resonance is well below the 9 GHz marker and the pure re-entrant cavity resonance has also been reduced in frequency probably because of the difference in shape of the actual circulator compared with the metal disc substitute used for the tests of Figures 16(a) to (c).

The losses associated with all of the resonances are larger corresponding to the broader absorption dips in Figure 17. Relative field distribution plots at each of the three resonant frequencies in Figure 17 that correspond to those in Figures 14(a) and (b) gave results similar in all respects to those presented in Figures 16(a) to (c). This leads to the conclusion that the metal boundaries of a housing will be the dominant factor determining resonant frequencies if the contents occupy only a small fraction of the enclosed volume. They will also be the dominant factor in determining resonant field distributions. The contents may have a large influence on microwave losses and hence the bandwidth of each resonance.

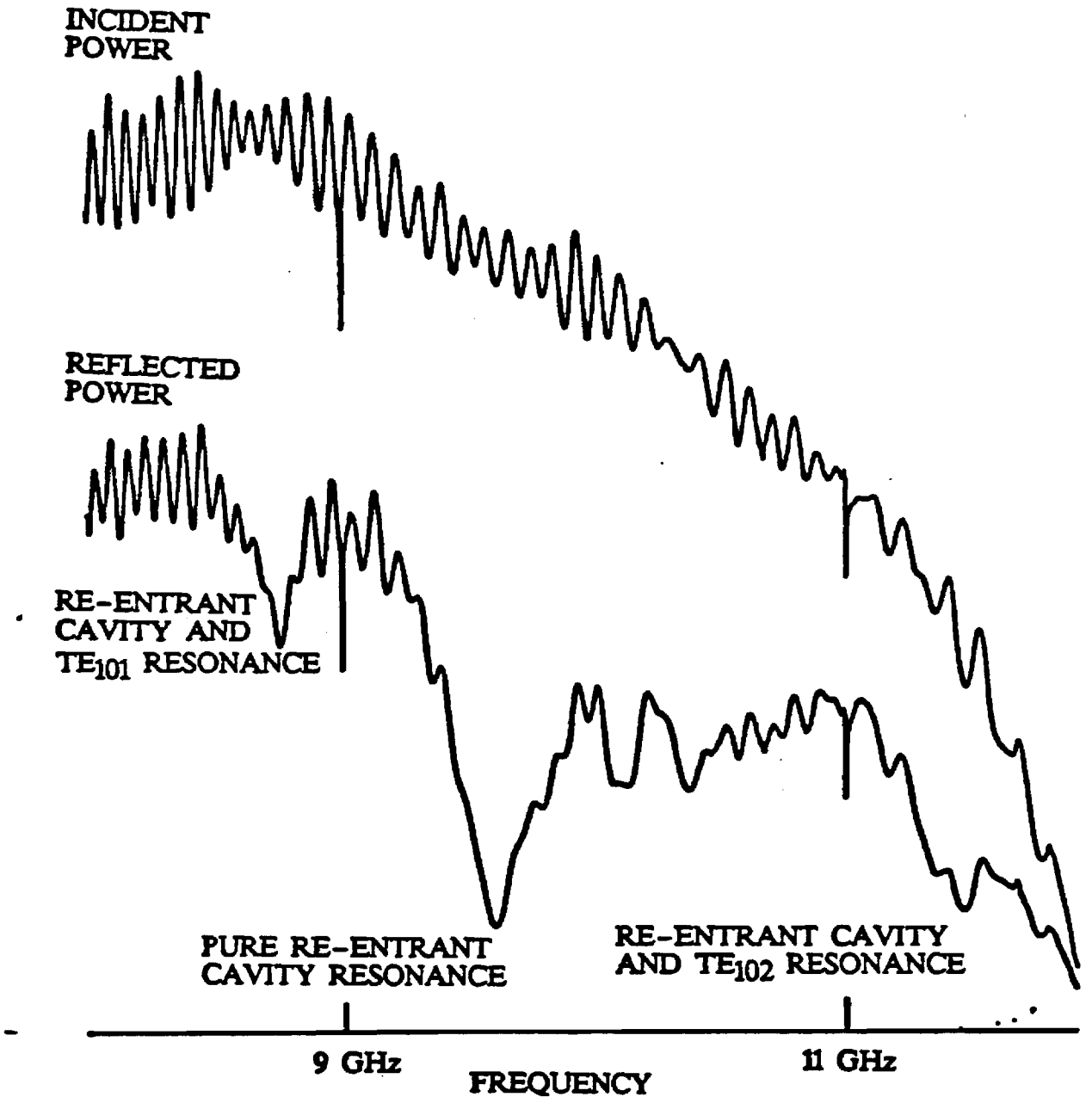

Figure 17 Swept frequency incident and reflected power characteristics showing cavity resonances within a complete MMIC T/R module.

8. CONCLUSIONS AND RECOMMENDATIONS

8.1 Conclusions

C.1. This study and its findings are relevant to microwave module housings and MMIC chip packages that have relatively broad base dimensions, low profile side walls and flat lids, with high conductivity metal providing the major part of the interior surface of what is essentially an electromagnetic cavity resonator. It is also assumed that resonances may not be suppressed simply by loading the cavity with microwave absorbent material.

C.2. The study concentrates on identifying the most likely cause of malfunction observed to occur in some modules when the lid of the housing is put in place. It is concluded that the most likely cause is electromagnetic cavity resonance within what becomes an enclosed volume and that such a resonance is the means whereby unwanted feedback occurs leading to instability, oscillation, etc. For the typical housing and package shapes in use the lowest frequency resonances are TE mode types with electric field normal to the inside surface of the lid.

C.3. A new, special purpose, two-dimensional standing wave detector has been developed to provide a method of detecting the existence of cavity resonances. It can be used to measure the frequencies at which they occur and to determine a qualitative two-dimensional measure of the field distribution associated with each resonance, without interfering with the normal operation of a microwave module within the housing under test.

C.4. It has been conclusively demonstrated that a measuring instrument can be created and that it will provide the detailed information on resonances listed in the previous paragraph. It has also been demonstrated how this diagnostic information may be used to deduce details of other field components that in turn allow the specific mechanism leading to microwave malfunction to be identified.

C.5. A simple equivalent circuit explanation of the operation of this special purpose two-dimensional standing wave detector leads to identification of the engineering development problems that must be solved to yield an accurate instrument that gives repeatable results. That analysis also identifies the complications that lie in the way of deriving an analytical relationship between the quantities that are measurable and the actual electric field distribution associated with a cavity resonance. This as yet unsolved problem does not prevent the instrument that has been demonstrated from being used as an effective diagnostic tool in testing designs and developing effective housings in which problems due to resonances are avoided.

C.6. The demonstration assembly operates in the 8 to 12 GHz frequency range and uses first generation microwave components developed 30 or more years ago except for the special test platform. This work does not indicate any particular test frequency limit although scaling of all critical dimensions for operation of an instrument at millimetre wave frequencies would reveal the main limiting factors. In principle a well designed test platform and E-field probe unit could be operated over decade bandwidths, the lowest frequency being determined by the diameter of the platform (or size of housing) and the highest frequency by the diameter of the hole in the centre of that plate and the finest practical probe wire.

C.7. Unwanted coupling between otherwise isolated parts of a module assembly, by means of cavity resonances within the housing, focusses attention on the degree of field confinement associated with individual components. Where fields are closely confined, as for example in MMICs on GaAs substrates, coupling with electromagnetic fields that occupy the volume of the housing is likely to be small compared with the coupling that may exist with larger air-spaced microwave wire bonds and microstrip lines.

8.2 Recommendations

R.1. It is recommended that a survey of microwave module housings and MMIC chip packages be undertaken to see if there are any exceptions to the rule that in general they are broad based, low side wall, rectangular boxes with flat lids. The most likely deviations from this general rule will be in the plan view of a housing where combinations of different rectangular and possibly triangular or part circular areas may be used to accommodate particular component assemblies that include MMICs. It is anticipated that all housings and packages that are predominantly metal boxes will have flat or slightly recessed flat lids in which case the instrument that has been described could be used universally.

R.2. It is recommended that the effect of the proximity of a flat metal lid on components within MMICs be investigated to test the proposal adopted in this study that it is negligible in all housings and packages in practical use, because of the confinement of fields within the high dielectric constant GaAs substrate.

R.3. It is recommended that development work proceed on improved versions of the special purpose two-dimensional standing wave detector for use in developing microwave housings and packages.

R.4 It is recommended that detailed experimental studies of the effectiveness of common features such as dividing walls, and components, such as circulators, used in housings and packages be conducted with the aim of developing design rules to replace what may be features of design based on "intuition and experience".

R.5. It is recommended that a more detailed and rigorous analysis of the method of measurement be made and tested with standard cavities within which resonances and associated field distribution are known accurately, the aim being to derive analytically the actual field distribution from measured quantities.

R.6. It is recommended that development of assemblies to operate to as high a test frequency as practical proceed, in anticipation of problems to be solved in the design of housings and packages for use in the millimetre wave bands.

R.7. It is recommended that studies of the effect of the proximity of metal walls, the field confinement of various microwave component structures, etc., on the coupling that may occur via electromagnetic resonant cavity modes be made and that rules be developed that effectively minimise such coupling. Such a study would focus on the effect that the walls of metal housing would have on the behaviour and characteristics of microwave components, circuits and sub-assemblies that form the assemblies to be packaged.

9. REFERENCES

[1] MONTGOMERY, Carol G. (ed.), "Technique of microwave measurements", McGraw-Hill, New York, 1947.

[2] GINZTON, Edward L., "Microwave measurements", McGraw-Hill, New York, 1957.

[3] RAMO, Simon, WHINNERY, John R. and VAN DUZER, Theodore, "Fields and waves in communication electronics", John Wiley, New York, 1965.